



**UCGE Reports
Number 20334**

Department of Geomatics Engineering

**Remote Sensing-Based Determination of Boreal Spring
Phenology in Alberta**

(URL: <http://www.geomatics.ucalgary.ca/graduatetheses>)

by

Navdeep S. Sekhon

August 2011



UNIVERSITY OF CALGARY

Remote Sensing-Based Determination of Boreal Spring Phenology in Alberta

by

Navdeep S. Sekhon

A THESIS

SUBMITTED TO THE FACULTY OF GRADUATE STUDIES
IN PARTIAL FULFILMENT OF THE REQUIREMENTS FOR THE
DEGREE OF MASTER OF SCIENCE

DEPARTMENT OF GEOMATICS ENGINEERING

CALGARY, ALBERTA

AUGUST 2011

© Navdeep S. Sekhon 2011

Abstract

Vegetation phenology is vital in understanding various forestry related activities. Here, the objectives were to determine the spatial dynamics of two phenological stages during spring season [*i.e.* snow gone (SGN), and coniferous needle flushing (CNF)] in the Canadian province of Alberta for years 2006-08. In the first phase, the potential of MODerate-resolution Imaging Spectroradiometer (MODIS)-based indices [*i.e.*, enhanced vegetation index (EVI), normalized difference water index (NDWI), and normalized difference snow index (NDSI)] were evaluated in determining the SGN stages. It revealed that NDWI at 2.13 μ m demonstrated best prediction capabilities (*i.e.*, on an average ~65.6% of the cases fell within ± 1 period or ± 8 days of deviation). In the second phase of delineating CNF, the logical 'OR' combination between the thresholds of NDWI at 2.13 μ m (*i.e.*, 0.525) and accumulated growing degree days (AGDD of 200 degree days) were found to be generating the best results (*i.e.*, on an average ~68.7% of the cases fell within ± 1 period of deviation). Overall, the outcomes of this research demonstrated its effectiveness in delineating the phenological stages of interest by use of remote sensing-based methods at a spatial resolution of 500m.

Preface

The outcomes of this research have been published and/or presented in a regular fashion, and listed as follows:

Journal Articles

1. Sekhon, N. S., Hassan, Q. K., & Sleep, R. W. (2010). Evaluating Potential of MODIS-based Indices in Determining “Snow Gone” Stage over Forest-dominant Regions in Alberta, Canada. *Remote Sensing*, 2, 1348-1363.
2. Sekhon, N. S. and Hassan, Q. K. Remote sensing-based determination of conifer needle flushing over boreal-dominant regions. *IEEE Journal of Selected Topics in Applied Earth Observations & Remote Sensing*, [In review].

Conference Proceedings

3. Sekhon, N.S., & Hassan, Q. K. (2010). Understanding of Spring Phenology over Forest-dominant Regions: Remote Sensing Perspective. *Proceedings of The Prairie Summit, June 1-5, 2010, Regina SK, Canada*, 381-384.
4. Sekhon, N. S., Hassan, Q. K., & Sleep, R. W. (2010). Use of Remote Sensing in Understanding Spring Phenology over the Forest Dominant Natural Subregions of Alberta. *Canadian Geomatics Conference, June 14-18, 2010, Calgary AB, Canada*, 10-05-Paper-115, 5 pp.

Abstract Presentations

5. Sekhon, N. S., & Hassan, Q. K. (2010). Determining conifer needle flushing stage in Alberta. *PCAG 2010, Sep. 24-26, 2010, North Battleford SK, Canada.*

6. Sekhon, N. S., Hassan, Q. K., & Rahman, K. M. (2011). Conifer needle flushing stage determination over boreal-dominant stands in Alberta: A remote sensing approach. *CGU-CSAFM 2011 Scientific Meeting, May 15-18, Banff AB, Canada.*

Acknowledgements

First of all, I am grateful to my supervisor Dr. Quazi K. Hassan for giving me an opportunity of being part of his research group and also for his continuous untiring guidance and support. Second, I am thankful to Robert Sleep of Alberta Sustainable Resources Development, for providing the ground records of phenology and also for his critical comments and suggestions at the various steps of this research.

For funding, I am obliged to (i) Dr. Hassan and Dept. of Geomatics Engineering for assistantships; (ii) Faculty of Graduate Studies for scholarships as of QE II Awards, FGS Awards, and FGS Travel Award; and (iii) Alberta Government for the Alberta Graduate Scholarship.

I am thankful to my group mates at “Earth Observation for Environment” laboratory for providing helping hand to develop various datasets. Additionally, I am obliged to all of the people at ‘*Trailer-H*’ for providing a joyful environment around me and always being open to my questions.

Also, I wish to extend my gratitude to the courteous staff at Geomatics Engineering; especially to Ms. Lu-Anne Markland and Ms. Janelle McConnell, for their help with various procedures and deadlines.

Last but not least, I will always be indebted to my parents for believing in my endeavours. I am also obliged to Veera & Bhabi for their enormous support and

understanding. Above all, I am beholden to *Nimrit & Vaaris* for their affection, distraction, and instruction.

Dedication

To my elder brother “Ravdeep S. Sekhon”

for

his enormous support & inspiration.

Table of Contents

Abstract.....	ii
Preface.....	iii
Acknowledgements.....	v
Dedication.....	vii
Table of Contents.....	viii
List of Tables.....	x
List of Figures and Illustrations.....	xi
List of Symbols, Abbreviations and Nomenclature.....	xiii
CHAPTER 1: INTRODUCTION.....	1
1.1 Background.....	1
1.2 Vegetation Phenology.....	3
1.3 Objectives.....	6
1.4 Thesis Structure.....	6
CHAPTER 2: LITERATURE REVIEW.....	8
2.1 Spring Phenology.....	8
2.1.1 Importance of SGN.....	10
2.1.2 Importance of CNF.....	11
2.2 Methods of Spring Phenology Determination.....	12
2.2.1 Ground Based Phenological Observations.....	12
2.2.2 Phenological Modelling.....	13
2.2.3 Remote Sensing-based Methods.....	16
2.2.3.1 Spring Onset Determination.....	19
2.2.3.2 Bud Phenology Determination.....	23
2.3 MODIS Characteristics.....	25
2.4 Summary.....	27
CHAPTER 3: STUDY AREA & DATASETS.....	28
3.1 Study Area.....	28
3.2 Datasets Used.....	31
CHAPTER 4: METHODS.....	35
4.1 Data Pre-processing.....	35
4.2 SGN Determination.....	36
4.2.1 Indices Computation.....	37
4.2.2 Qualitative Evaluation of the Indices.....	38
4.2.3 Quantitative Evaluation of the Indices.....	40
4.2.4 Mapping of SGN Using Best Predictor.....	40
4.3 CNF Determination.....	41
4.3.1 Generation of GDD maps.....	41
4.3.2 CNF Delineation from GDD and NDWI-values.....	45
4.3.3 Integration of Both GDD and NDWI-values.....	46
4.3.4 Mapping of CNF Using Best Prediction Criteria.....	46

CHAPTER 5: RESULTS & DISCUSSION	48
5.1 Delineation of SGN	48
5.1.1 Qualitative Evaluation of the Indices	48
5.1.2. Determining the Best Index in Predicting SGN Periods	52
5.1.3 SGN Maps and Spatial Dynamics	57
5.2 Delineation of CNF.....	63
5.2.1 GDD Mapping.....	63
5.2.2 Determination of GDD Threshold for CNF Occurrence.....	67
5.2.3 Determination of NDWI _{2.13µm} Threshold for CNF Occurrence	69
5.2.4 Integration of Both GDD and NDWI _{2.13µm} Thresholds	74
5.2.5 CNF Maps and Spatial Dynamics	76
 CHAPTER 6: CONCLUSIONS	 82
6.1 Summary	82
6.2 Contribution to Science	83
6.3 Recommendations for Future Work	84
 REFERENCES	 86
Web-References.....	98
 APPENDIX.....	 99
A.1 Copyright Permissions	99
A.1.1 Certificate from a Co-author.....	100
A.1.2 Certificate for Published Journal Articles	101
A.1.3 Certificate for a Book Chapter.....	104
A.1.4 Certificate from Publication	105

List of Tables

Table 2.1: Brief Description of the characteristics of MODIS bands.....	27
Table 3.1: Brief Description of the characteristics of forest-dominant natural sub- regions in Alberta.....	30
Table 3.2: Brief description of the datasets used in this study.....	34
Table 5.1: Relation between NDWI _{1.64μm} -based prediction and ground-based SGN observation period.....	54
Table 5.2: Relation between NDWI _{2.13μm} -based prediction and ground-based CNF observation period.....	56
Table 5.3: Relation between AGDD-based prediction and ground-based CNF observation period.....	69
Table 5.4: Relation between NDWI-based prediction and ground-based CNF observation period.....	72
Table 5.5: Relation between the combination of AGDD- and NDWI-based prediction and ground-based CNF observation period	75

List of Figures and Illustrations

Figure 1.1: Extent of the Boreal biome across the northern hemisphere.....	2
Figure 1.2: Extent of the Boreal biome across the landscape of Canada.....	3
Figure 1.3: Boreal phenological cycle	4
Figure 2.1: Spectral signature of different canopies	17
Figure 2.2: Methods of identifying phenology from vegetation indices temporal trend;. 18	
Figure 2.3: Spectral reflectance modeled at various levels of canopy moisture.....	23
Figure 3.1: Study area.....	29
Figure 3.2: Look-out tower sites recording phenological observations in the study area	32
Figure 3.3: Environment Canada Weather station sites locations in the study area	33
Figure 4.1: Schematic diagram showing the method followed for delineating “snow gone” (SGN) stage occurrence.....	39
Figure 4.2: Schematic diagram showing the method followed for delineating “coniferous needle flush” (CNF) stage occurrence.....	44
Figure 5.1: Temporal dynamics of averaged values from all of the lookout tower sites for EVI, NDWI _{1.64µm} , NDWI _{2.13µm} , and NDSI for the natural sub-region of <i>central mixedwood</i>	49
Figure 5.2: Temporal dynamics of averaged values from all of the lookout tower sites for EVI, NDWI _{1.64µm} , NDWI _{2.13µm} , and NDSI for the natural sub-region of <i>lower boreal highlands</i>	50
Figure 5.3: Comparison between the SGN periods from ground-based observations and predicted using NDWI _{1.64µm}	53
Figure 5.4: Comparison between the SGN periods from ground-based observations and predicted using NDWI _{2.13µm}	55
Figure 5.5: SGN Map for 2006.....	59
Figure 5.6: SGN Map for 2007	60
Figure 5.7: SGN Map for 2008.....	61
Figure 5.8: The moving average of 10 consecutive pixels of SGN period occurrence	62

Figure 5.9: Trends of seasonal bias between the satellite-based surface and ground-based air temperatures at 8-day resolution.....	64
Figure 5.10: Relation between the MODIS-based 8-day instantaneous surface temperature and 8-day average air temperature.....	66
Figure 5.11: Determination of GDD threshold for CNF occurrence.....	68
Figure 5.12: Determination of NDWI threshold for CNF occurrence.....	71
Figure 5.13: CNF Map 2006.....	77
Figure 5.14: CNF Map 2007.....	78
Figure 5.15: CNF Map 2008.....	79
Figure 5.16: The moving average of 10 consecutive pixels of CNF period occurrence ..	80

List of Symbols, Abbreviations and Nomenclature

<u>Abbreviation</u>	<u>Definition</u>
AGDD	<i>Accumulated Growing Degree Days</i>
AVHRR	<i>Advanced Very High Resolution Radiometer</i>
CCB	<i>Coniferous Closed Bud</i>
CCFM	<i>Canadian Council of Forest Ministries</i>
CFFDRS	<i>Canadian Forest Fire Danger Rating System</i>
CGS	<i>Cured Grass Stage</i>
CNF	<i>Coniferous Needle Flush</i>
COB	<i>Coniferous Open Bud</i>
DCB	<i>Deciduous Closed Bud</i>
DLO	<i>Deciduous Leaf Out</i>
DOB	<i>Deciduous Open Bud</i>
DOY	<i>Day Of Year</i>
EOSDIS	<i>Earth Observing System Data and Information System</i>
EVI	<i>Enhanced Vegetation Index</i>
FBP	<i>Fire Behaviour Prediction</i>
FFMT	<i>Forest Fire Management Terms</i>
GDD	<i>Growing Degree Days</i>
GGs	<i>Green Grass Stage</i>
LAI	<i>Leaf Area Index</i>
LANDSAT	<i>LAND-use SATellite</i>
LSP	<i>Land Surface Phenology</i>
LWIR	<i>Long Wave Infra Red</i>
MCV	<i>Maximum Composite Value</i>
MODIS	<i>MODerate-resolution Imaging Spectroradiometer</i>
MRT	<i>MODIS Reprojection Tool</i>
NAD 83	<i>North American Datum 1983</i>
NASA	<i>National Aeronautics and Space Administration</i>
NDSI	<i>Normalised Difference Snow Index</i>
NDVI	<i>Normalised Difference Vegetation Index</i>
NDWI	<i>Normalised Difference Water Index</i>
NIR	<i>Near Infra-Red</i>
NOAA	<i>National Oceanic and Atmospheric Administration</i>
NRCAN	<i>Natural Resources CANada</i>
NSR	<i>Natural Sub-Region</i>
SGN	<i>Snow GoNe</i>
SIN	<i>Sinusoidal</i>
SOG	<i>Snow On Ground</i>

SPG	<i>Snow Patches on Ground</i>
SPOT	<i>Système Probatoire d'Observation de la Terre</i>
SWIR	<i>Short-Wave Infra-Red</i>
TGS	<i>Transition Grass Stage</i>
UTM	<i>Universal Transverse Mercator (Projection)</i>
URL	<i>Uniform Resource Locator (Online Web)</i>
VI	<i>Vegetation Index</i>

Symbol

Definition

I_{UL}	<i>Interval Upper Limit</i>
I_{LL}	<i>Interval Lower Limit</i>
<i>i.e.</i>	<i>that is</i>
K	<i>Kelvin (Temperature)</i>
$^{\circ}N$	<i>Degrees North (Latitude)</i>
$^{\circ}W$	<i>Degrees West (Longitude)</i>
$NDWI_{1.64 \mu m}$	<i>NDWI with SWIR band centred at 1.64 μm</i>
$NDWI_{2.13 \mu m}$	<i>NDWI with SWIR band centred at 2.13 μm</i>
P	<i>Period of MODIS 8-day epoch</i>
Q_n	<i>n^{th} Quartile</i>
r^2	<i>Coefficient of determination (Pearson's)</i>
T_s	<i>Surface Temperature (MODIS –based)</i>
ρ_y	<i>Surface reflectance of band 'y'</i>
μm	<i>Micro Meter (Micron)</i>
\bar{T}_a	<i>Average Air Temperature</i>

CHAPTER 1: INTRODUCTION

If Spring came but once a century instead of once a year, or burst forth with the sound of an earthquake and not in silence, What wonder and expectation there would be in all hearts to behold the miraculous change.

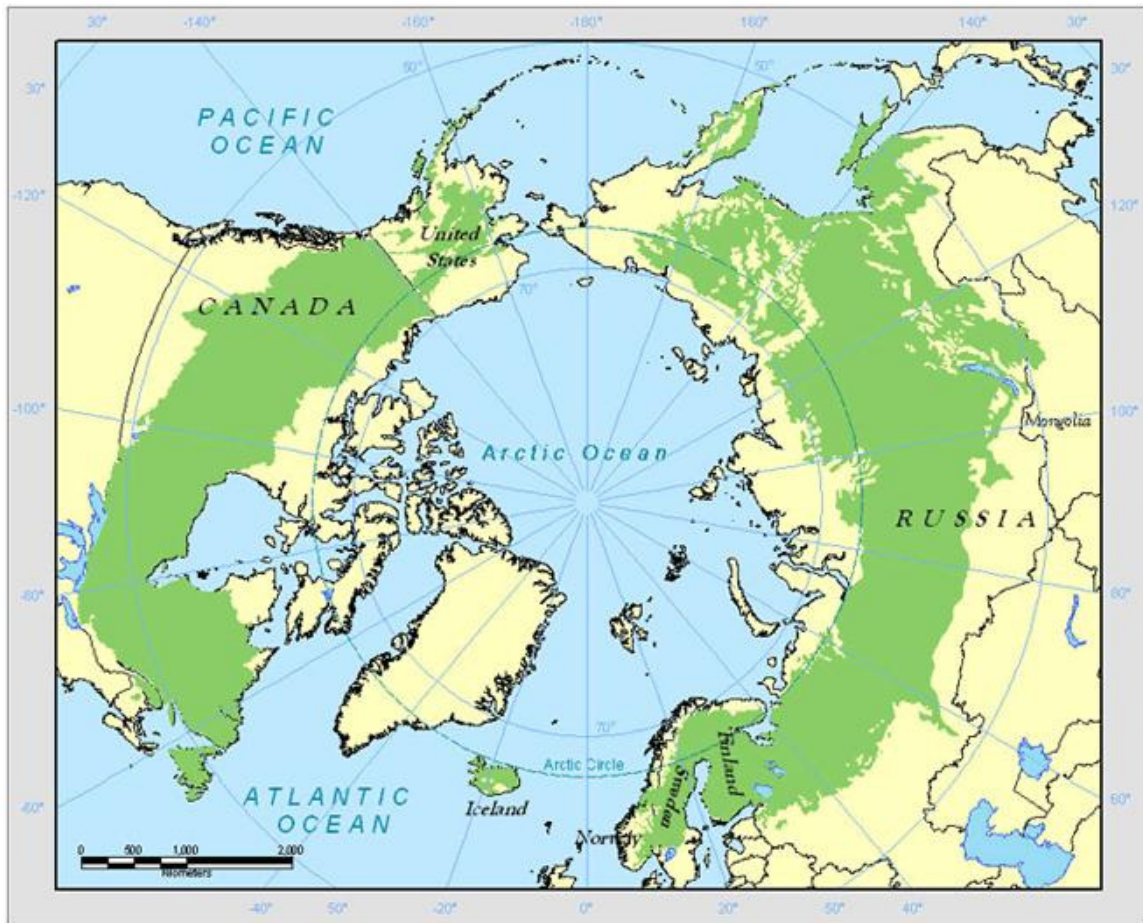
: Henry Wadsworth Longfellow (1807-1882).

1.1 Background

Boreal forests are the largest biome in the world and have circumpolar extents at sub-arctic latitudes in the northern hemisphere (see Figure 1.1; Hart and Chen, 2006). At global level, it is accounted for one-third portion of all of the forested regions (Simpson et al., 2011), whereas the Canadian boreal forest is ~8% of the global forest (Hassan et al., 2006).

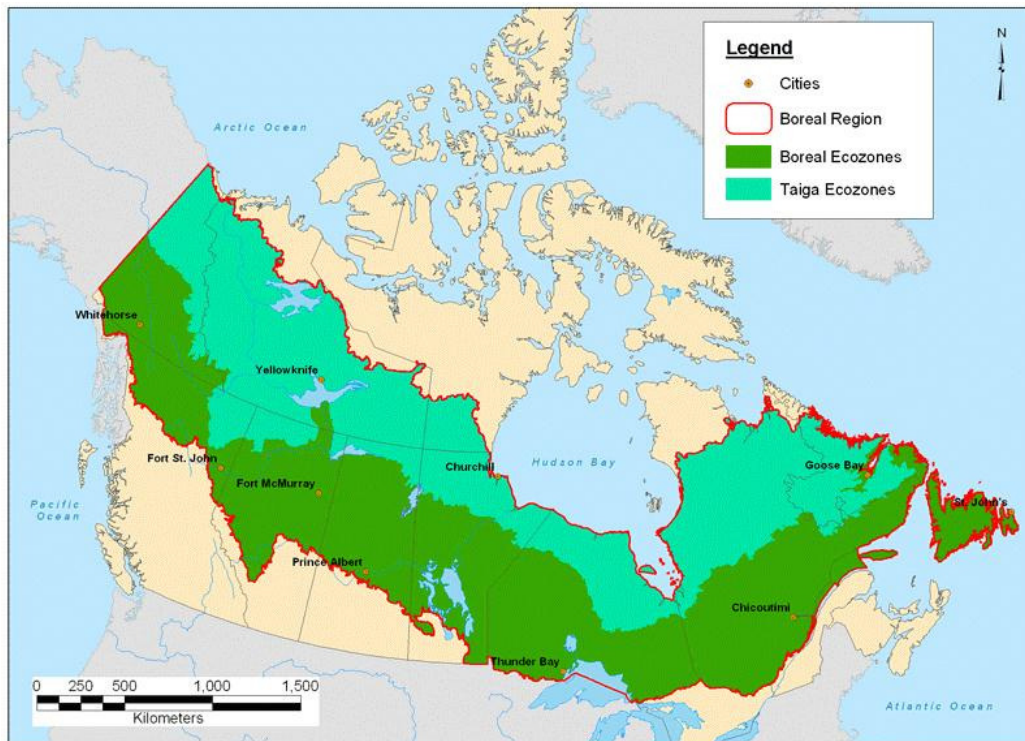
In Canadian context, boreal forest covers uninterrupted band of landmass from east coast to west coast (see Figure 1.2; Weber and Stocks, 1998); where northern limits defined by the tree line extent and southern boundaries coinciding to prairie and temperate forests (CCFM, 2011). The 34% of the Canada's total landmass is forested; with boreal forests amounting to 77% of this forested landscapes (Power and Gillis, 2006). It is storage of ~71.4 billion tonnes of carbon, with an additional of ~136.7 billion tonnes of carbon in the boreal peat lands (Carlson et al., 2009). Thus it is important for us to study the boreal forest dynamics in particular to understand the impact of climate on the vegetation (i.e., vegetation phenology).

Figure 1.1: Extent of the Boreal biome across the northern hemisphere.



Source: <http://www.borealcanada.ca/popup.html?images/maps/global-boreal.gif>

Figure 1.2: Extent of the Boreal biome across the landscape of Canada



Source: <http://www.borealcanada.ca/popup.html?images/maps/canadas-boreal-2007.gif>

1.2 Vegetation Phenology

Vegetation phenology is the study of understanding the occurrence and timing of the recurring responses of the plants (White et al., 2009; McCloy, 2010; Liang et al., 2011). It is important in describing various forestry related functionalities; such as vegetation growth, rate of carbon sequestration, hydrological cycle, insect outbreak, forest fire, and effects of natural disturbances among many other (Westerling, 2006; Julien and Sobriono, 2007; Jönsson et al., 2010).

In most of the instances, the climatic variables are primarily responsible for seasonal and inter-annual variability observed in the phenological events at local, regional, and global scales (Cleland et al., 2007; Dufour and Morin, 2010). In particular to boreal forested regions, the phenological stages can broadly be classified/categorized into the following categories: (i) snow stages; (ii) spring onset; (iii) greening-up stages; (iv) bud developmental stages; and (v) peak growing season (Delbart et al., 2008; White et al., 2009; Gu et al., 2010). These classes can be further sub-classified on the basis of the type of vegetation, e.g., understory, grass, deciduous, and coniferous phenology.

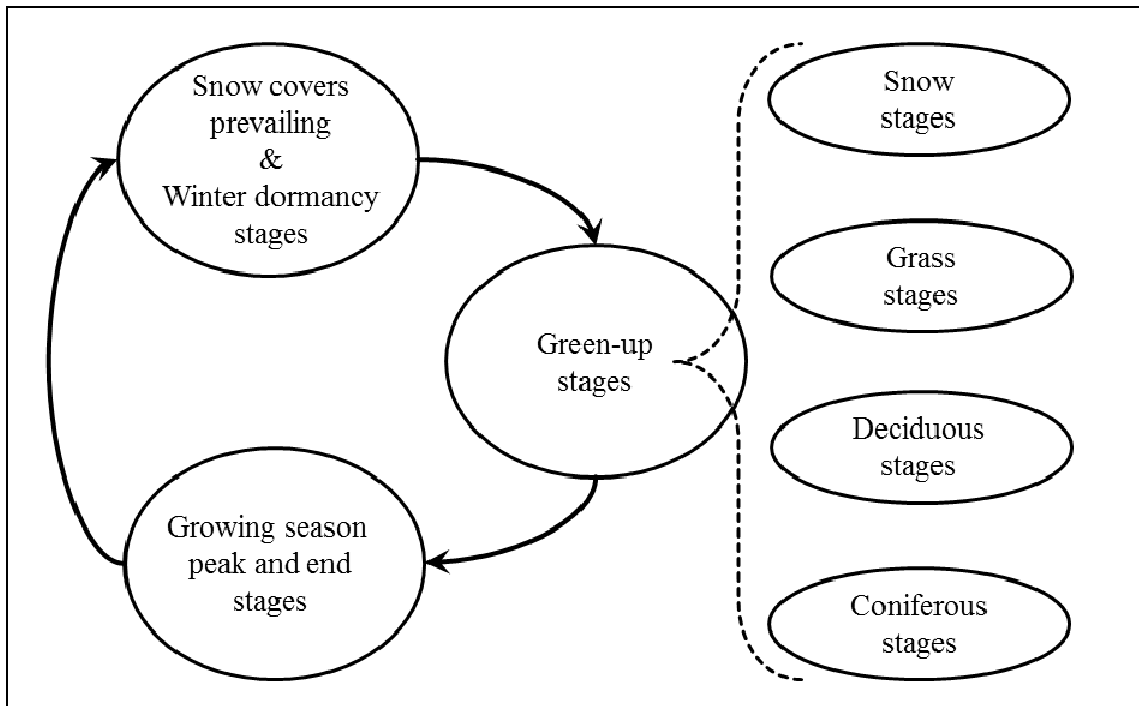
In general, phenological cycle is divided into three major classes recurring after each other as shown in Figure 1.3. For example: (i) the beginning of year falls under winter dormancy stage with prevailing snow cover; (ii) spring dynamics referred as 'green-up'; (iii) finally, the season transects into the peak growing season stages, and ends up again at the onset of winter season.

Among the various stages, the spring phenological events have been considered in the scope of this Thesis. Generally, the spring phenology, *i.e.* 'green-up', spans from the stages of snow melt to the beginning of peak growing season. Based on the type of vegetation and the associated phenomenon the stages of green-up are further subdivided into four categories (FFMT, 1999). These are:

- (i) Snow stages;
- (ii) Grass stages;
- (iii) Deciduous stages; and

(iv) Coniferous stages.

Figure 1.3: Boreal phenological cycle



In this study, the two particular green-up stages are of interest; namely “snow gone” (SGN) and “conifer needle flushing” (CNF). The SGN is the last phenological stage recorded of the melting snow covers (FFMT, 1999). The melting snow covers induce a green-up by exposing the vegetation; especially over the evergreen stands. The SGN stage marks the end of the snowmelt and may coincide to the beginning of green-up through the vegetation vigour (Delbart et al., 2005). The CNF stage, on the other hand, is the last phenological stage recorded of the bud development during the green-up phase

(FFMT, 1999). After the needle flushing the major spring activity of the conifers, *i.e.* physiological processes prominently aiming generation of new foliar, would potentially cease (Hannerz, 1999). In other words CNF may mark the end of further green-up of vegetation. Hence, the two stages of interest are important in determining the actual length of the vegetation activity during the spring.

1.3 Objectives

In the scope of the Thesis, the overall goal is to develop methods in determining the spring phenological stages of interest over the boreal forest-dominant regions in the Canadian Province of Alberta using primarily remote sensing data. The developed methods should be able to define the spatial dynamics of the vegetation phenological stages, thus the outcomes may potentially be useful in understanding various widespread landscape dynamics. Those include forest fire management, climate change, carbon budgets, Ecohydrology, among others. The specific research objectives of this Thesis are to:

- (i) develop methods for determining SGN, and implement over Alberta in generating the spatial dynamics; and
- (ii) develop methods for determining CNF, and implement over the conifer dominant boreal forest stands in Alberta

1.4 Thesis Structure

This Thesis consists of five (5) chapters. *Chapter one* (this one) provides background information about boreal forest and vegetation phenology. It also provides objectives of

this research. *Chapter two* presents literature review regarding the works related to the delineation of the phenological stages and their importance. It also provides a brief description of the remote sensing platform used in the study. *Chapter three* provides a brief description of the study area and required datasets.

Chapter four describes the proposed methods used in this study in achieving the research objectives. *Chapter five* presents the outcomes of the research and discussion on the results. *Chapter six* provides concluding remarks by summarizing the entire work, its contribution and further possibilities of the research.

CHAPTER 2: LITERATURE REVIEW

This chapter is divided into 4 sections. The first section (*i.e.*, 2.1) describes various phenological stages associated with spring season and their importances. Second section (*i.e.*, 2.2) provides review on the methods in determining the phenological stages of interest. Third section (*i.e.*, 2.3) presents the characteristics of widely employed remote sensing sensor in phenological studies, which is MODerate-resolution Imaging Spectroradiometer (MODIS). Finally, section 2.4 provides a summary for the entire chapter.

2.1 Spring Phenology

Spring phenology in boreal forested regions is the stages corresponding to the green-up, which are potentially caused by exposure of vegetation with the melting of snow covers and/or by the growth of vegetation biomass after end of the winter dormancy. Over the boreal forest stands of Canada, the phenology of spring time is recorded as a set of the following stages (FFMT, 1999):

- (i) Snow stages:
 - (a) *Snow on Ground* (SOG: defined as the date when at least 75% of the surrounding area is covered by snow);
 - (b) *Snow Patches on Ground* (SPG: defined as the date when 25 to 75% of the surrounding area is covered by snow); and
 - (c) *Snow Gone* (SGN: defined as the date when less than 25% of the surrounding area is covered by snow).

(ii) Grass stages:

- (a) *Cured Grass Stage* (CGS: defined as the date when at least 75% of the surrounding area grass is ‘cured’);
- (b) *Transition Grass Stage* (TGS: defined as the date when 50-75% of the surrounding area grass is ‘cured’); and
- (c) *Green Grass Stage* (GGS: defined as the date when less than 50% of the surrounding area grass is ‘cured’).

(iii) Deciduous Stages:

- (a) *Deciduous Closed Bud* (DCB: defined as the date when at least 75% buds of the trembling aspen (*Populus tremuloidies*) in the surrounding area are still closed);
- (b) *Deciduous Open Bud* (DOB: defined as the date when at least 75% buds of the trembling aspen (*Populus tremuloidies*) in the surrounding area have swollen, such that leaf are visible but still not opened); and
- (c) *Deciduous leaf-out* (DLO: defined as the date when at least 75% new leaves of the trembling aspen (*Populus tremuloidies*) in the surrounding area have opened and attained diameter of at least 1.25cm).

(iv) Coniferous Stages:

- (a) *Coniferous Closed Bud* (CCB: defined as the date when at least 75% buds on the white spruce (*Picea glauca*) and/or black spruce (*Picea mariana*) have swollen but the bud “sheath” or “cap” has remained intact;

- (b) *Coniferous Open Buds* (COB: defined as the date when at least 75% buds on the white spruce (*Picea glauca*) and/or black spruce (*Picea mariana*) have swollen to the point such that the bud “sheath” or “cap” has fallen off); and
- (c) *Coniferous Needle Flush* (CNF: defined as the date when the tips of at least 75% fresh buds of white spruce (*Picea glauca*) and/or black spruce (*Picea mariana*) in the surrounding area have reached to a minimum of 2 cm new growth since the start of the growing season).

Currently, these phenological observations are used by forest fire management agencies to develop maps in defining ‘fuel types’, which is an important component of the Fire Behaviour Prediction (FBP) module of the Canadian Forest Fire Danger Rating System (CFFDRS) (Burgan, 1979; FFMT, 1999; Lawson and Armitage, 2008). As, the intent of this study is to develop methods for mapping SGN and CNF, thus their importance are briefly described prior to reviewing the existing methods in determining them.

2.1.1 Importance of SGN

In practice, the SGN stage marks the end of snow covers on the ground; hence it is critical for:

- (i) determining the onset of the forest fire season as conditions tend to dry out after snowmelt (Westerling et al., 2006; Lawson and Armitage, 2008);
- (ii) determining the end of snow-melt effects on the remote sensing-based phenological identifications (Delbart et al., 2005), see section 2.2.3 for details;

- (iii) determining the surface energy fluxes, as snow has high albedo values (Dozier and Painter, 2004);
- (iv) determining the spatial and temporal controls over hydrological fluxes of the watersheds (Molotch and Margulis, 2008).

2.1.2 Importance of CNF

The CNF is the last bud-developmental stage of brandishing new needles on conifers; after the stages of closed bud (*i.e.*, appearance of new buds) and open buds (*i.e.*, shedding of scales from the buds) (FFMT, 1999). It is worthwhile to study the CNF because:

- (i) it defines the transition between spring developmental phases and the peak growing season (Hannerz, 1999);
- (ii) it indicates the end to proneness of bud damages due to late spring frost (Agren et al., 1991; Jones and Cregg, 2006; Man et al., 2009);
- (iii) it relates to the carbon exchange aspect, as conifers show a transition from source to sink near to the completion of bud developmental stages (Leinonen and Kramer, 2002; Richardson et al., 2009); and
- (iv) it is related to the foliage moisture content and thus has potential in predicting forest fire danger (Van Wagner, 1977; Johnson, 1992; Wang and Zwiazek, 1999; Agee et al., 2002).

2.2 Methods of Spring Phenology Determination

The methods of determining phenological stages can be broadly classified into three classes, *i.e.*:

- (i) *in-situ* ground based observations;
- (ii) phenological modeling from the climatic variables; and
- (iii) remote sensing-based methods.

2.2.1 Ground Based Phenological Observations

The ground based observations are the most accurate and historic one among other methods. The historic records of plant phenology are available for European regions and other eastern continents; dating back to 5,000 years in China for example (Cleland et al., 2007). In Canada, such records are also available in particular to western regions dating back to late 1800's (Beaubien and Freeland, 2000). In Alberta, the phenological look-out tower (approximately 120 sites currently in use) records of phenology (mainly, spring to growing season end) are available since the early 1970's. In USA the individual phenological records are available from mid of the 20th century (Cleland et al., 2007).

Recently, scientists established a national phenological network, in USA, on realizing the need for collecting and sharing proper record of phenology at the continental scale (Betancourt et al., 2005). Similar other numerous volunteer-based networks (e.g., Plant watch, Operation Budburst, AMC's Mountain Watch) acquire and share data on various phenological events.

However, ground based observations are subjective in approach, thus potentially differ from person to person. Even the scientific observations may be unable to describe the trends over the natural vegetation, as mostly they are over vegetation grown under controlled/laboratory environments (Cleland et al., 2007). Besides, the response of same species may potentially differ across the landscape due to the variations in climatic variables (Liang and Schwartz, 2009; Gu et al., 2010). Thus, we require techniques to address the spatial variability in relation to phenology (Hassan and Bourque, 2009; Morisette et al., 2009).

2.2.2 Phenological Modelling

The key issue behind these modelling approaches is to understand which climate variables play a critical role in triggering the phenological stages of interest and their requirements. In general, a phenological stage of interest is to be declared when the magnitude of the required climatic variables reaches to a certain threshold (Penuelas et al., 2004; Man and Lu, 2010).

If the nutrient supply and other biotic factors (e.g., intra and inter-species competition) are not limiting; the major climatic variables which control the phenological stages are:

- (i) incident photosynthetically active radiation or available photoperiod,
- (ii) water regime, and
- (iii) temperature regimes (Campbell and Sugano, 1979; Agren et al., 1991; Leinonen and Kramer, 2002; Hassan and Bourque, 2009).

Various studies have used these variables to model the phenology over different biomes of the globe. For example:

- (i) Bailey and Harrington (2006) modeled phenology of Douglas-fir (*Pseudotsuga menziesii*) from temperature regimes;
- (ii) Chiang and Brown (2007) used temperature driven phenology model for a cool-temperate forest;
- (iii) Gunter et al. (2008) employed phenology models based on water regimes, solar radiation, and photoperiod in a tropical montane rain forest; and
- (iv) Penulas et al. (2004) considered the water (precipitation) and temperature regimes to model phenology of a Mediterranean forest.

In natural forest conditions the regimes of incident photosynthetically active radiation (in other words, available photoperiod) and temperature are strongly related with some time lag in-between the two at both diurnal and seasonal scales (Prescott and Collins, 1951). For example, the maximum solar radiation incidents around solar noon-period while the temperature reach its maximum later in the afternoon. Thus, modelling the phenology in relation to temperature alone can potentially mimic both of the temperature and incident photosynthetically active radiation regimes.

If water availability for the plant growth is sufficient in a region, the regime of favorable temperatures can be considered as the most critical variable. In general, this is the case over boreal ecozones; where the snow-melting during the spring period is often fulfilling the water requirements (Jones and Cregg, 2006).

Yet, another consideration of climatic control on phenology is to figure out the “chilling requirements” (*i.e.*, unfavorable cold temperatures enough for causing cold hardiness) (Leinonen and Kramer, 2002); however over boreal forests in northern latitudes (*i.e.* our region of interest), such requirements are fulfilled as a result of severe cold temperature regimes during the winter period (Beaubien and Freeland et al., 2000).

Hence, often a simple spring warming model, *i.e.*, considering temperature controls only, is mostly better in performance with comparison to the complex phenological models, *i.e.*, considering many or all of the controlling factors (Jönsson et al., 2010).

The temperature controls in spring warming models are usually modeled at point locations; as a function of air temperature measurements termed as growing degree days [GDD: defined as the difference between daily mean air temperature and a base temperature (Hassan and Bourque, 2009; Akther and Hassan, 2011)]. The ‘base temperature’ is assumed to be the lower limit of air temperature above which vegetation is active for the physiological processes rendering the phenological stage of interest (Weilgolaski, 1999; Dufour and Morin, 2010; Man and Lu, 2010).

Despite the effectiveness of GDD-based methods in phenological studies, its applicability is limited in addressing the spatial context as GDD is usually computed at point locations. To address this issue, it is possible to employ the remote sensing-based GDD-mapping methods developed over the past several years (Hassan et al., 2007a; Hassan et al., 2007b; Akther and Hassan, 2011), that primarily uses remote sensing-based surface

temperature (T_s). These methods already have demonstrated potential over temperate and boreal-dominant regions in Canada; as:

- (i) Hassan et al. (2007a) used the MODIS –based surface temperature and flux tower long wave radiation data to generate the GDD over the temperate forest of New Brunswick, Canada; and
- (ii) Akhter and Hassan (2011) used MODIS-based surface temperature and weather station based air temperature to generate GDD over the parts of boreal forest in northern Alberta, Canada.

2.2.3 Remote Sensing-based Methods

In order to address the spatial dynamics of boreal vegetation phenology, remote sensing-based methods have also been experimented over various geographic regions (Reed et al., 2009, White et al., 2009; Liang et al., 2011). These methods mainly rely on detecting the changes in surface reflectance (induced by changes of biophysical and/or biochemical characteristics influenced by the climatic variables, see Figure 2.1); by exploiting the temporal trends observed in various remote sensing-derived vegetation indices (VI) (Xiao et al., 2009; McCloy, 2010).

The occurrence of phenological stage may be associated to one of the following phase in explored temporal trends:

- (i) when it hits a pattern, *i.e.*, minimum, maximum, beginning of platform, sharp drop/rise etc. (e.g., Delbart et al., 2005) [see Figure 2.2(a)];

- (ii) when it crosses a threshold of response (e.g., Delbart et al., 2006) [see Figure 2.2(b)]; or
- (iii) when the logistic curve fitted into it register a sharp change in curvature (e.g., Zhang et al., 2003; Zhang et al., 2004) [see Figure 2.2(c)].

Figure 2.1: Spectral signature of different canopies [modified after Clark (1999)].

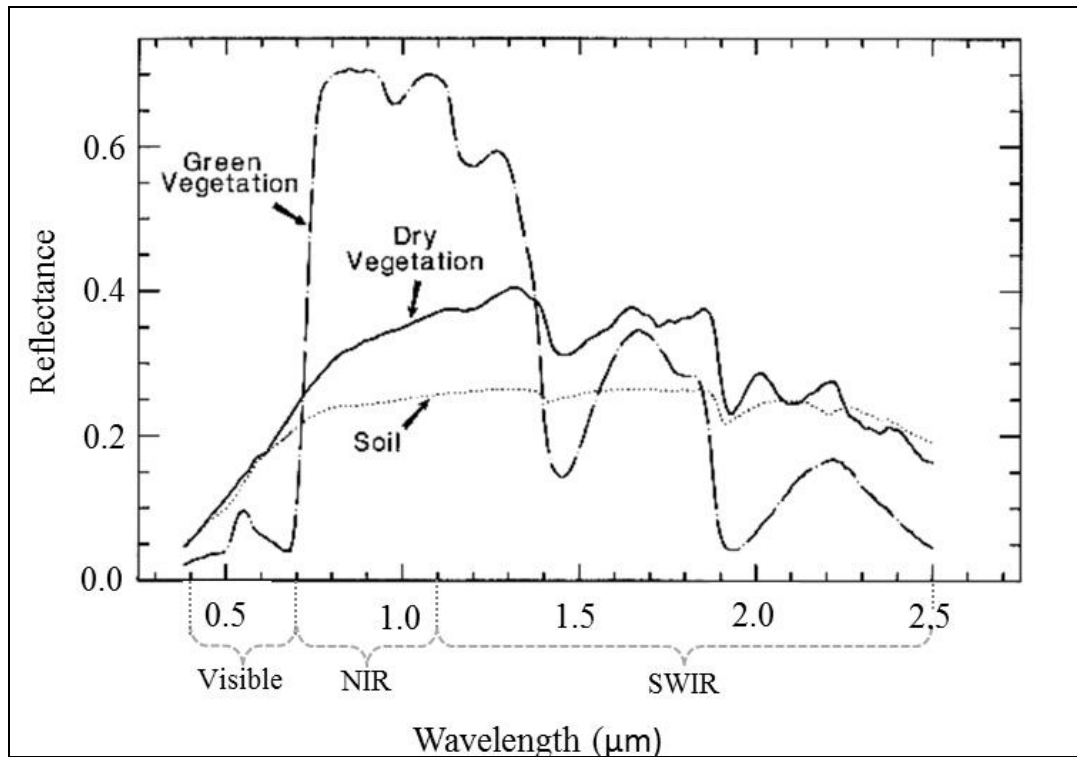
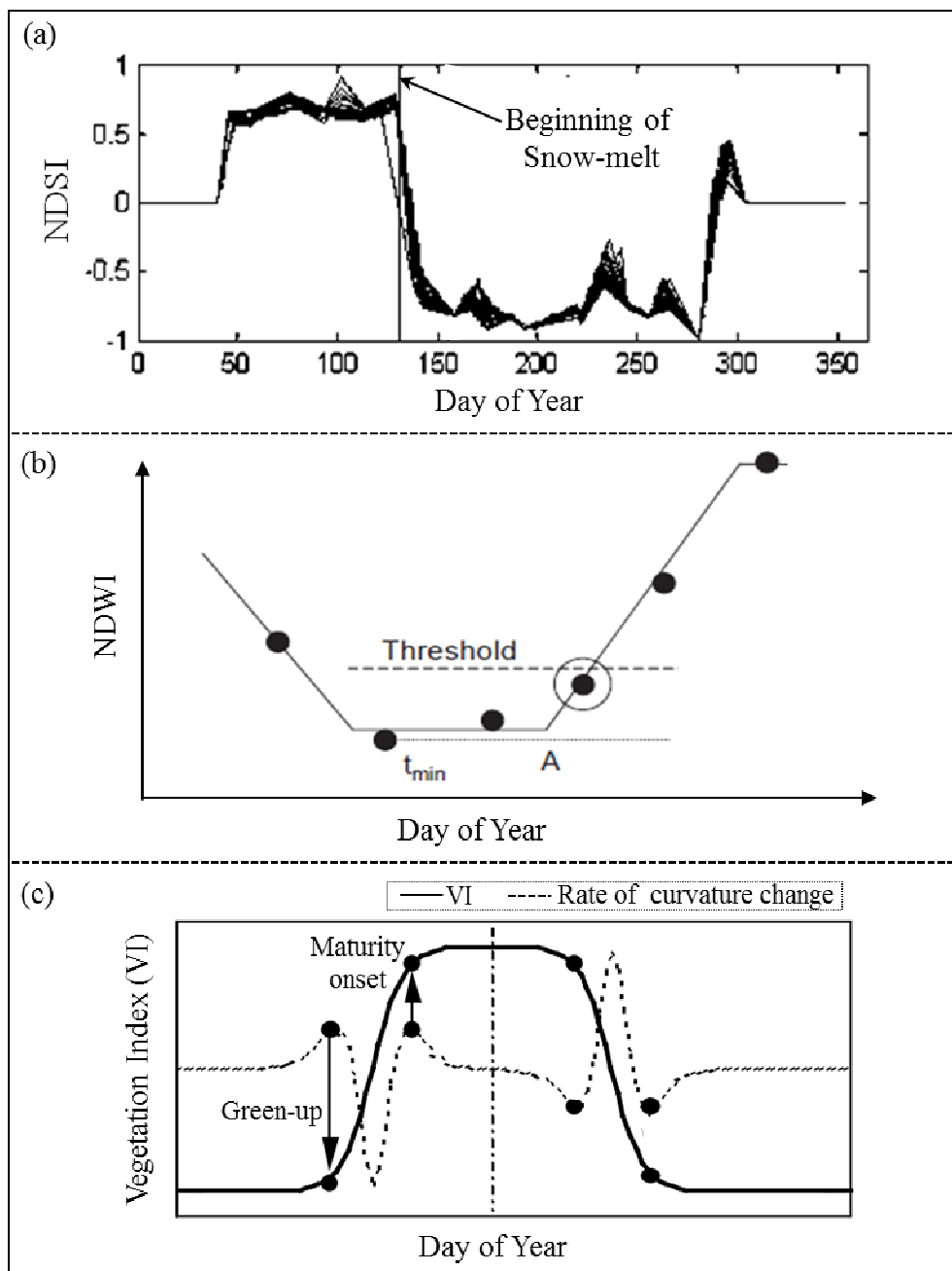


Figure 2.2: Methods of identifying phenology from vegetation indices temporal trend; (a) by identifying a pattern; (b) by using a threshold; and (c) by rate of curvature change.



Source: (a) & (b) modified after Delbart et al. (2005)

Source: (c) modified after Zhang et al. (2003)

The commonly used vegetation indices in phenological studies are as follows:

- (i) normalized difference vegetation index [NDVI: based on surface reflectance (*i.e.*, in red and near infrared (NIR) spectral bands) and with values ranging from 0 to 1; e.g. White et al., (2009)];
- (ii) enhanced vegetation index [EVI: based on surface reflectance (*i.e.*, in red, blue and NIR spectral bands) and with values ranging from 0 to 1; e.g. Zhang et al., (2003)];
- (iii) normalized difference water index [NDWI: based on surface reflectance (*i.e.*, in NIR and short wave infrared (SWIR) spectral bands) and with values ranging from -1 to +1; e.g. Delbart et al., (2005)];
- (iv) normalized difference snow index [NDSI: based on surface reflectance (*i.e.*, in green and SWIR spectral bands) and with values ranging from -1 to +1; e.g. Rinne et al., (2009)]; and
- (v) leaf area index [LAI: vertical integration of the leaf area; e.g. Fisher et al., (2007)].

2.2.3.1 Spring Onset Determination

The most commonly used remote sensing-based indices for determining the onset of the spring and/or growing season are the NDVI and enhanced EVI; For example:

- (i) Moulin et al.(1997) used derivatives of the NOAA/AVHRR –based NDVI trends to determine the begin date of growing cycle (*i.e.* spring onset) for various biomes at the global scale;

- (ii) Jenkins et al. (2002) used AVHRR –based NDVI threshold values in the trends to determine season onset dates for temperate forests in US;
- (iii) Zhang et al. (2004) used changes in curvature of the logistic curve fitted in MODIS –based EVI temporal trends for detections of season onsets, over entire biomes of the northern latitudes (i.e. 35°-70°N);
- (iv) Ahl et al. (2006) used changes in curvature of the logistic curve fitted in MODIS –based NDVI, EVI & LAI temporal trends for detections of season onsets over a study site in northern Wisconsin, USA.
- (v) Thayne and Price (2008) used changes in curvature of the logistic curve fitted in MODIS –based NDVI trends for greenness onset date determinations, over the prairies and shrublands of Kansas, USA.

In general, NDVI and EVI are quite capable of determining the general seasonal patterns (e.g., spring onset, peak of the growing season, and end of the growing season) over temperate and tropical zones (Reed et al., 2009; Xiao et al., 2009). However, the use of NDVI might have larger uncertainty over the boreal forest-dominant regions (where snow accumulation is very common) to determine the onset of the growing season (Delbart et al., 2005; Delbart et al., 2006). As EVI exhibits similar responses as NDVI at the onset of growing season (Hassan et al., 2007a), we could also assume that EVI might respond similar in the presence of snow. However, this requires further investigation.

Another index NDWI (a measure of moisture content in canopy) has been implemented successfully in various vegetation and phenological studies. For example:

- (i) Xiao et al.(2002) used SPOT-4 VEGETATION-derived NDWI in connecting phenology to classify the landscape over Northeastern China;
- (ii) Jackson et al. (2004) used Landsat –based NDWI temporal trends to estimate the vegetation water content over the growing season over croplands in state of Iowa, USA;
- (iii) Picard et al. (2005) calibrated a spring warming model for bud burst predictions using the threshold based estimates from SPOT-4 VEGETATION –based NDWI temporal trends over Russian boreal ecosystem;
- (iv) Delbart et al.(2005,2006, and 2008) modeled the spring phenology over boreal Eurasia using the threshold based estimates from NDWI temporal trends obtained from various remote sensing platforms,; and
- (v) Trombetti et al. (2008) incorporated MODIS –based NDWI, along with various other VI, into an artificial neural network to estimate vegetation water content dynamics during the entire year for USA.

On contrary to NDVI & EVI, temporal trends of NDWI reflect vegetation development stages independently from the snow melting phases (Delbart et al., 2005; Delbart et al., 2006; Reed et al., 2009). Because, the NDWI decreases during the snow melting period; and starts to increase at the onset of the real vegetation growth (Delbart et al., 2005). Hence, separation of snow phases increases the potential of NDWI in the understanding of the later phenological events as well (Reed et al., 2009).

In the formulation of NDWI, however, various wavelengths within the SWIR spectral ranges can be employed, such as:

- (i) centered at 1.24 μm (e.g., Gao, 1996);
- (ii) centered at 1.64 μm (Wilson and Sader, 2002; Frensholt and Sandholt, 2003; Yilmaz et al., 2008); and
- (iii) centered at 2.13 μm (Chen and Jackson, 2005; Gu et al., 2007; Yi et al., 2008).

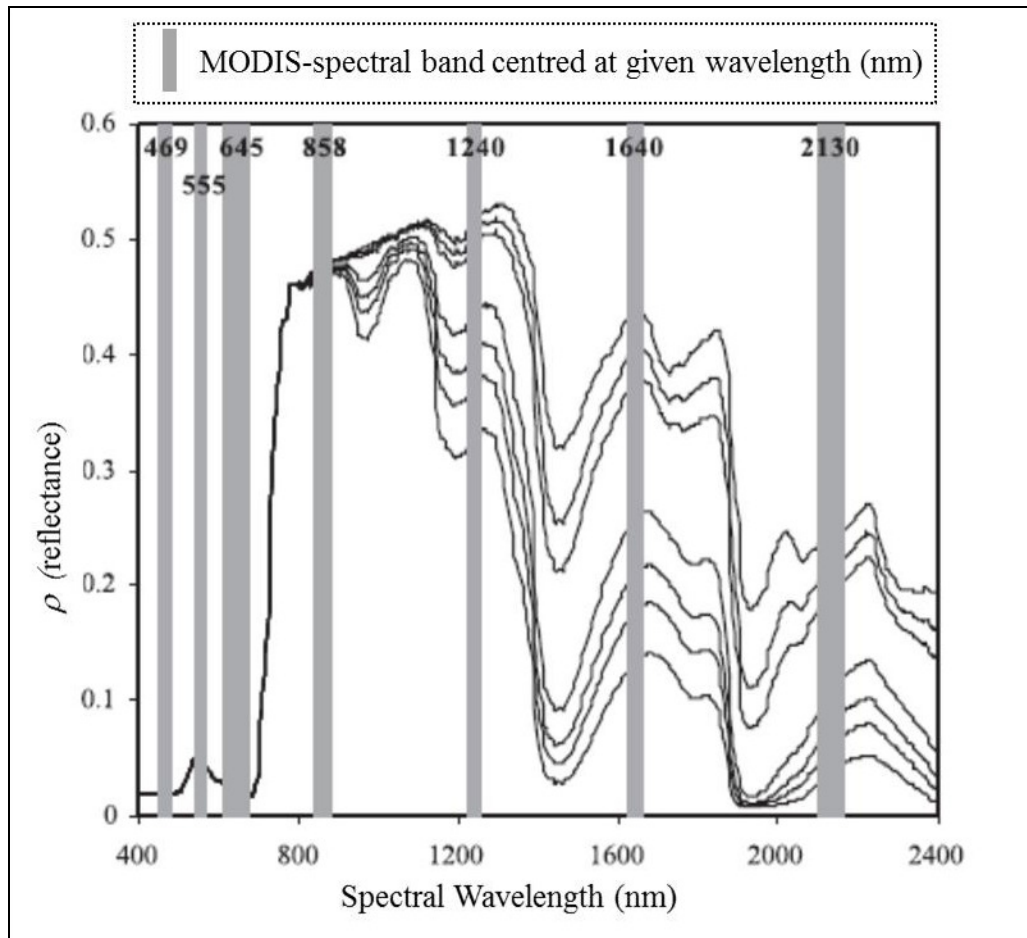
The reflectance dynamics over vegetation within SWIR ranges are also shown in Figure 2.3. It reveals that the reflectance of SWIR centred at 1.24 μm does not largely deviates from the reference band in calculating the NDWI (*i.e.*, NIR band centred at 0.858 μm). However, the other two SWIR bands seem to be more useful. Thus, the intention is to use two SWIR bands from MODIS, *i.e.*, band 6 (1.628–1.652 μm) and band 7 (2.105–2.155 μm) in the formulation of NDWI. This can be useful to quantify the appropriate band in calculating NDWI in determining the SGN stages.

Additionally it is also possible to determine the snow dynamics by using NDSI. For example:

- (i) Klien et al. (1998) mapped snow covers through the use of NDSI and NDVI;
- (ii) Rinne et al. (2009) used NDSI in conjunction with surface albedo to quantify SGN;
- (iii) Delbart et al. (2005) used NDSI to determine the onset of the snow melting time and to characterize the temporal dynamics of NDWI; and
- (iv) Dankers and De Jong (2004) used NDSI alone to determine the SGN stages.

However, it is required to evaluate the performance NDSI in our study area.

Figure 2.3: Spectral reflectance modeled at various levels of canopy moisture [modified after Zarco-Tejada et al. (2003)].



2.2.3.2 Bud Phenology Determination

The application of any of the remote sensing-derived indices in determining the bud phenological stage of our interest (*i.e.*, CNF) has not been reported so far in the literature to the best of our knowledge.

The trends of LAI may be used to study the phenological stages associated to the leaf development (Fisher et al., 2006). However, this approach may be limited in the boreal ecosystem with coniferous forest stands which does not shed needles and having interference with the conditions of the forest floor.

However, the combination of land surface temperature with vegetation index [either NDVI/EVI (e.g., Jenkins et al., 2002; Zhang et al., 2004) or NDWI (e.g., Delbart et al., 2008)] has been employed to predict various bud phenological stages. The addition of temperature enhances the overall prediction capacity because temperature has a major influence on the plant activities (Gyllenstrand et al., 2007). Thus, the incorporation of temperature will be important when predicting bud phenology (Jenkins et al., 2002; Zhang et al., 2004; Delbart et al., 2008).

In this research, the intention is to explore the potential of delineating CNF stage using two variables; namely of GDD and NDWI. It is worthwhile to mention that the GDD-based prediction is to be considered as the cause of the occurrence for CNF; on the contrary, NDWI represents the response of the CNF stage occurrence in terms of canopy moisture dynamics. The performance of NDWI's in delineating SGN would determine the formulation of NDWI to be used in this phase. Note that the predictions from these methods require ground-based observations in order to validate the findings.

2.3 MODIS Characteristics

During the last decade, the most widely used remote sensing sensor is MODIS in determining phenological stages across the world. Among the other multispectral remote sensing sensors/platforms used in phenological studies (namely: NOAA-AVHRR, LANDSAT, SPOT-VGT) MODIS is preferable due to its following aspects:

- (i) MODIS provides coverage of earth surface dynamics at almost global levels.
- (ii) It provides reflectance datasets which are geo-referenced and corrected for atmospheric interactions. While similar datasets from other platforms require such prior data pre-processing steps.
- (iii) MODIS recordings of reflectance are most detailed and are available in 36 spectral bands, covering the spectrum from 0.45 μ m to 14.385 μ m. While, SPOT-VGT has just four spectral bands; with coverage of only visible and NIR bands. On other hand, NOAA-AVHRR has six spectral bands with coverage of visible, SWIR, and Long wave (for surface temperature); LANDSAT has seven bands with coverage of visible, NIR, SWIR, and long wave (for surface temperature).
- (iv) MODIS provides datasets at better spatial resolution, ranging from 250m to 1Km (depending on the spectral band). While for NOAA-AVHRR it ranges from 1.1 Km at nadir to 5 Km off-nadir for each spectral band. In case of SPOT-VGT it is 1km for entire field of view in each spectral band.
- (v) MODIS provides efficient daily temporal coverage; *i.e.*, 1-day temporal resolution(similar with SPOT-VGT). While temporal resolution for the LANDSAT is of 16-days. However, note that LANDSAT datasets are preferable to MODIS datasets in terms of the spatial (27m) resolution.

The MODIS is onboard with two remote sensing platforms (i.e., Terra and Aqua) of National Aeronautics and Space Administration (NASA). Both of the platforms are near-polar, sun synchronous, and having circular orbit at an elevation of 705 Km above the earth surface. Terra acquires data in descending node (i.e., north to south) about local time of 10:30 am while Aqua acquires data around local time of 1:30 pm in ascending node (i.e., south to north). Together the platforms provide the cross track scans (with 20.3 rpm) of the earth surface at almost daily level. Each swath of data covers area of 2330 Km (cross track) by 10 Km (along track) (NASA, 2011).

MODIS provides various datasets based on the 36 spectral bands. These data are free and available through online application of *Earth Observing System Data and Information System* (EOSDIS 2009). MODIS-based datasets used in this study (refer section 3.2) are based on band 1 to band 7 (i.e., surface reflectance product for computing EVI, NDSI, and NDWI) and band 31 to band 32 (i.e., emissivity used to develop land surface temperature product). A brief description of these MODIS bands is provided in Table 2.1.

Table 2.1: Brief Description of the characteristics for MODIS bands of interest.
 [modified after NASA (2011)]

Band #	Spectral Wavelength		Name	Spatial Resolution (m)
	Central Band (μm)	Bandwidth (μm)		
1	0.645	0.620 - 0.670	Red	250
2	0.8585	0.841 - 0.876	NIR	250
3	0.469	0.459 - 0.479	Blue	500
4	0.555	0.545 - 0.565	Green	500
5	1.24	1.230 - 1.250	SWIR	500
6	1.64	1.628 - 1.652	SWIR	500
7	2.13	2.105 - 2.155	SWIR	500
31	11.03	10.780 – 11.280	LWIR	1000
32	12.02	11.770 – 12.270	LWIR	1000

2.4 Summary

The literature review reveals that the integration of all of the three methods (*i.e.*, ground-based observations, phenological modelling, and remote sensing-based methods) of determining phenology are essential to predict the various phenological stages. Among various remote sensing-based methods, it seems that the use of NDWI in conjunction with the satellite based temperatures (*i.e.*, GDD accumulations) may produce the desired results.

CHAPTER 3: STUDY AREA & DATASETS

3.1 Study Area

Figure 3.1 shows the extent of the study area, i.e., the province of Alberta.

Geographically, Alberta falls in between parallels of 49-60 °N latitudes, and 110-120 °W longitudes. It experiences a continental climatic regime with cold winters and relatively short and moderately warm summers with the following characteristics (Dowing and Pettapiece, 2006):

- (i) average annual temperatures vary in the range $-3.6\text{ }^{\circ}\text{C}$ to $+4.4\text{ }^{\circ}\text{C}$;
- (ii) summer average temperatures vary in the range $8.7\text{ }^{\circ}\text{C}$ to $18.5\text{ }^{\circ}\text{C}$;
- (iii) winter average temperatures vary in the range $-25.1\text{ }^{\circ}\text{C}$ to $-9.6\text{ }^{\circ}\text{C}$; and
- (iv) average annual precipitation is in between 333-989 mm.

On the basis of climatic regimes, soil type, topography, and vegetation, Alberta is classified into the 21 natural sub-regions (Dowing and Pettapiece, 2006). Fourteen out of 21 natural sub-regions located in the northern and south-western regions of Alberta are mostly forest-dominant areas; and their characteristics are briefly described in Table 3.1. These forest-dominant natural sub-regions occupy ~76% of the total land area in the province where all of the lookout towers are located (see Figure 3.1 and Table 3.1 for more details).

Figure 3.1: Study area: (a) its geographical extent in Canadian extent; (b) its constituting 21 natural sub-regions and “%” of provincial area covered.

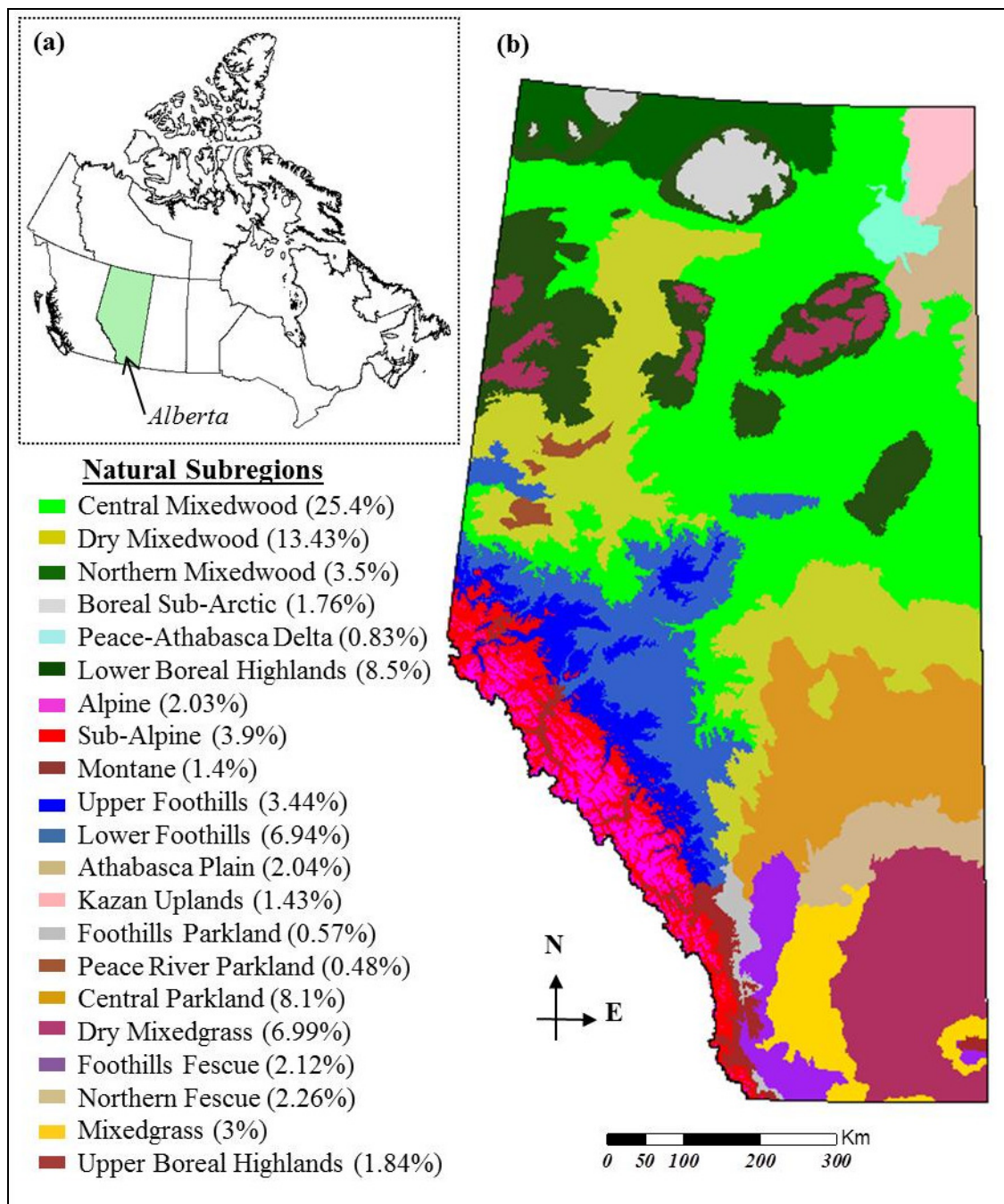


Table 3.1: Brief Description of the characteristics of forest-dominant natural sub-regions in Alberta. [modified after Dowling and Pettapiece (2006)]

Name	Area (Sq. Km.)	Mean annual Temp. (°C)	Mean annual precip. (mm)	Ecoclimatic zone	Dominant vegetation	No. of lookout towers [#]
Central Mixedwood*	167,856	0.2	478	Boreal	Deciduous-mixedwood	25
Dry Mixedwood*	85,321	1.1	461	Boreal	Deciduous-mixedwood	1
Northern Mixedwood*	29,513	-2.5	387	Boreal	Conifer (<i>Picea mariana</i>)	2
Boreal Subarctic*	11,823	-3.6	512	Boreal	Conifer (<i>Picea mariana</i>)	4
Peace Athabasca Delta*	5,535	-1.4	377	Boreal	Shrubs, pockets of <i>Populus balsamifera</i> , <i>Betula pendula</i> , <i>Picea glauca</i>	0
Lower Boreal Highlands*	55,615	-1.0	495	Boreal	Early to mid-seral pure or mixed forests hybrids	23
Alpine	15,084	-2.4	989	Cordilleran	Largely non-vegetated, shrublands	3
Sub-Alpine	25,218	-0.1	755	Cordilleran	Mixed Conifer (<i>Pinus and Picea</i>)	21
Montane	8,768	2.3	589	Cordilleran	Conifer-mixedwood	3
Upper Foothills	21,537	1.3	632	Boreal-Cordilleran transition	Conifer (<i>Pinus and Picea</i>)	17
Lower Foothills	44,899	1.8	588	Boreal-Cordilleran transition	Conifer-mixedwood	17
Athabasca Plain*	13,525	-1.2	428	Boreal	<i>Pinus banksiana</i> , dunes largely unvegetated	2
Kazan Uplands*	9,719	-2.6	380	Boreal	Mainly rock barrens, pockets of <i>Pinus banksiana</i>	1
Upper Boreal Highlands*	11,858	-1.5	535	Boreal	Conifer (<i>Pinus and Picea</i>)	11

[#] Note that, the records for all towers for each phenological stage were not available for every year.

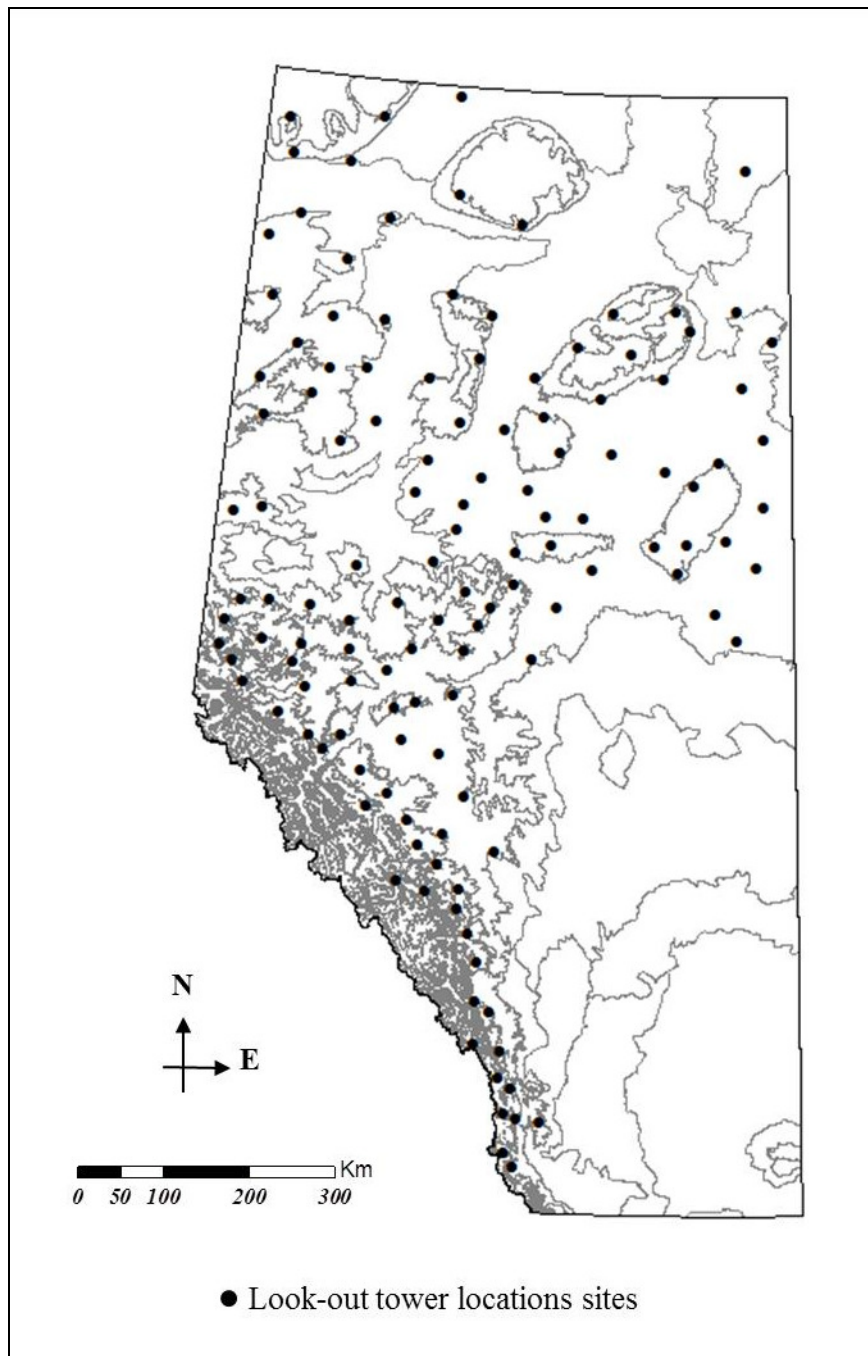
3.2 Datasets Used

In fulfilment of the research objectives the datasets available from various platforms were used; namely as:

- (i) NASA's freely available MODIS-based products of surface reflectance, T_s , and land cover maps for entire province of Alberta;
- (ii) Environment Canada's freely available ground-based observations for the variable of daily mean air temperature (locations shown in Figure 3.2) across entire province of Alberta; and
- (iii) Alberta Department of Sustainable Resources Development's ground-based records of phenology (locations shown in Figure 3.3) across boreal regions of the province of Alberta.

More detailed descriptions of these datasets are provided in Table 3.2.

Figure 3.2: Look-out tower sites recording phenological observations in the study area; total 130* in number.



** Note that, the records for all towers for each phenological stage were not available for every year.*

Figure 3.3: Environment Canada Weather station sites locations in the study area; total 182 in number.

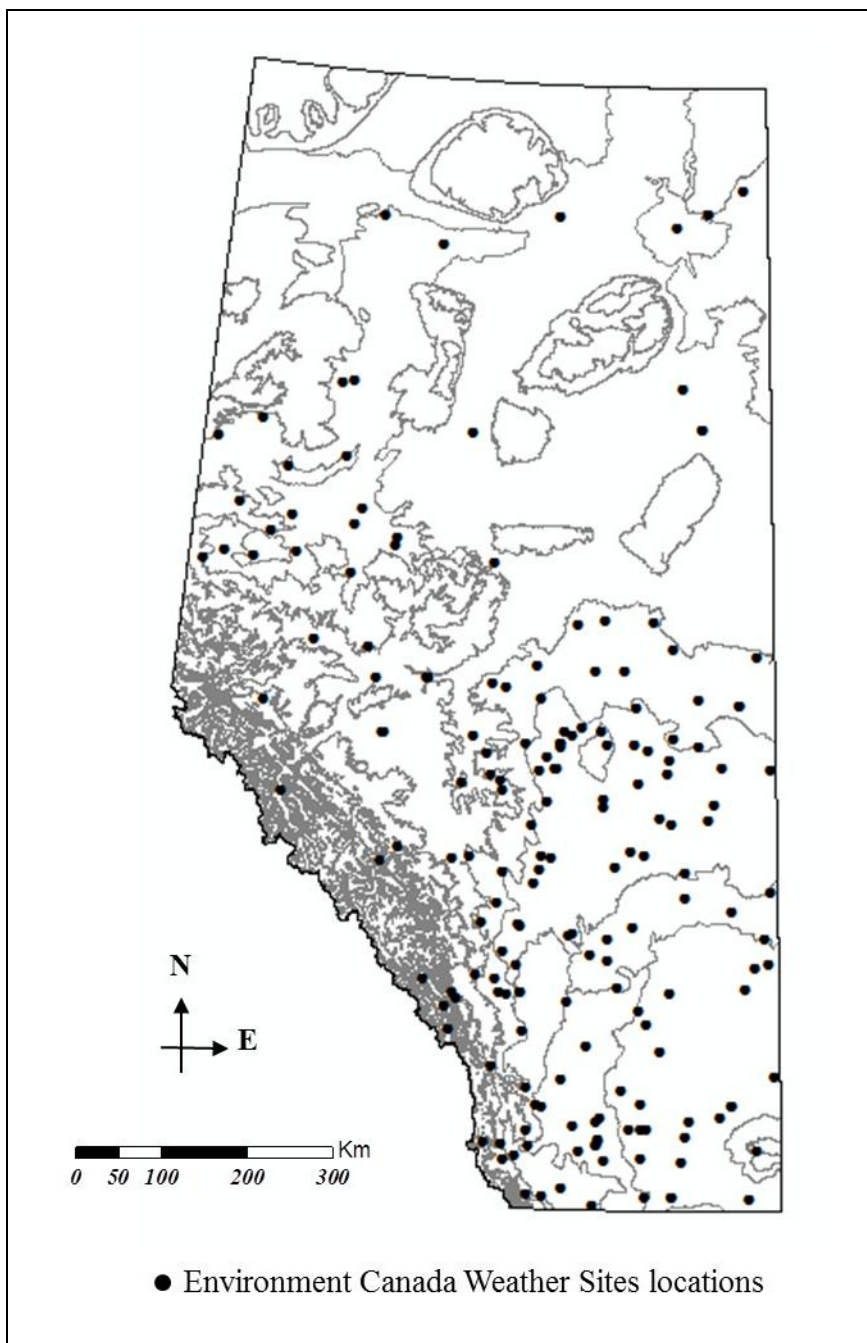


Table 3.2: Brief description of the datasets used in this study

Dataset	Description
MODIS-based T_s (<i>i.e.</i> , MOD11A2 v.005)	8-day composites of instantaneous T_s at 1Km spatial resolution. The acquired 4 adjacent scenes were mosaicked together to generate each of the image covering the full extent of Alberta. For each of year, 27 images were generated (<i>i.e.</i> , 81 images in total for the period 2006-2008) spanning between 30 March to 31 October for 2006-2007, and 29 March to 30 October 2008.
MODIS based land cover map (<i>i.e.</i> , MCD12Q1 v.004)	Annual composite of land cover map at 500m spatial resolution during 2007, with the following land cover classes: (i) water; (ii) grasses/cereal crops; (iii) shrubs; (iv) broadleaf crops; (v) savannah; (vi) broadleaf forest; (vii) needle leaf (<i>i.e.</i> , conifer-dominant) forest; (viii) unvegetated; (ix) urban; and (x) unclassified.
MODIS-based surface reflectance (<i>i.e.</i> , MOD09A1 v.005)	8-day composites of surface reflectance at 500m spatial resolution. The acquired 4 adjacent scenes were mosaicked together to generate each of the image covering the full extent of Alberta. For each of the year, there were 46 images (<i>i.e.</i> , 138 images over 3 years) spanning from 1 January to 31 December.
Daily mean air temperature	Daily mean of air temperature acquired at 1.2-2m above the surface at the first order weather stations operated by Environment Canada at ~182 sites across Alberta (see Figure 3.3 for location information) during the period 2006-08.
CNF stage	The ground-based CNF Observations for white and/or black spruce at ~118 lookout tower sites operated by Alberta Department of Sustainable Resources Development across Alberta (see Figure 3.2 for location information) for the period 2006-2008 were acquired. Around each of the lookout tower sites, 20 to 100 trees were sampled to declare the CNF stage (Dylan Heerema: a veteran lookout tower operator, Personal Communication).
SGN stage	The ground-based SGN Observations for ~115 lookout tower sites operated by Alberta Department of Sustainable Resources Development across Alberta (see Figure 3.2 for location information) for the period 2006-2008 were acquired..

CHAPTER 4: METHODS

4.1 Data Pre-processing

For the two MODIS products four swaths were required to produce the entire extent of the study area. Each of MODIS-based swath images was reprojected from their original SIN projection to UTM Zone 12 NAD 83 using MODIS Reprojection Tool (MRT, 2008). Then next step was to mosaick together the four adjacent scenes to create images that covered the entire extent of the study area.

So that five hundred fifty two scenes of the MODIS-based 8-day composites of surface reflectance data (i.e., MOD09A1 v.005) were acquired at 500 m resolution for the years 2006–2008; eventually to generate one hundred thirty eight 8-day periodical images. For each of the years, there were forty six 8-day periodical images spanning from January 1 to December 31. At this point, the cloud contaminated pixels using the “500 m state flags” information (another available layer within the MOD09A1 dataset) were excluded from further analysis.

While, three twenty four scenes of the MODIS-based 8-day aggregates of surface temperature (T_s), i.e., MOD11A2 v.005, were acquired; eventually to generate eighty one 8-day periodical images of the study area. For each of the years, there were twenty seven 8-day periodical images spanning from 30 March to 31 October for 2006-2007, and 29 March to 30 October 2008.

In order for all of the datasets to have the same temporal resolution (i.e., 8-day intervals like T_s and surface reflectance datasets), the daily mean air temperature data were averaged for the same 8-day imaging periods of the MODIS data. Also as, ground-based phenology data (i.e., SGN and CNF) were recorded in the form of day of year (DOY = 1 to 365 or 366), it required conversion to the equivalent period of MODIS data (i.e., 8-day imaging epochs) for comparison with MODIS-derived CNF stages. For this purpose, the following expression was employed:

$$P = \left[\left(\frac{DOY - 1}{8} \right) + 1 \right] \quad (4.1)$$

where, P (=1 to 46) is the corresponding equivalent imaging period of MODIS.

The value of P is always integer even if the calculated values is a floating number, e.g., P=20 if Eq 4.1 produces values in between 20 to 20.875.

4.2 SGN Determination

Figure 4.1 illustrates the steps involved in processing both of the MODIS and ground-based observations for this phase of SGN determination. In this phase, the major steps were to:

- (i) compute four MODIS-based indices (i.e., EVI, $NDWI_{1.64\mu m}$, $NDWI_{2.13\mu m}$, and NDSI);
- (ii) perform a qualitative evaluation of four MODIS-based indices in predicting the SGN stages;

- (iii) compare the SGN values predicted by the efficient indices as determined in step (ii) with the observations available at lookout tower sites across the landscape (as shown in Figure 3.2 by black circles); and
- (iv) generate a SGN map using the best predictor as determined in step (iii) to discuss the spatial variability over the entire Province of Alberta.

4.2.1 Indices Computation

MODIS-based indices of EVI (Huete et al., 2002), $NDWI_{1.64\mu m}$ (Wilson and Sader, 2002), $NDWI_{2.13\mu m}$ (Chen et al., 2005) and NDSI (Hall et al., 2002) were calculated as follows:

$$EVI = 2.5 \frac{\rho_{NIR} - \rho_{Red}}{\rho_{NIR} + 6\rho_{Red} - 7.5\rho_{Blue} + 1} \quad (4.2)$$

$$NDWI_{1.64\mu m} = \frac{\rho_{NIR} - \rho_{SWIR \text{ at } 1.64\mu m}}{\rho_{NIR} + \rho_{SWIR \text{ at } 1.64\mu m}} \quad (4.3)$$

$$NDWI_{2.13\mu m} = \frac{\rho_{NIR} - \rho_{SWIR \text{ at } 2.13\mu m}}{\rho_{NIR} + \rho_{SWIR \text{ at } 2.13\mu m}} \quad (4.4)$$

$$NDSI = \frac{\rho_{Green} - \rho_{SWIR \text{ at } 1.64\mu m}}{\rho_{Green} + \rho_{SWIR \text{ at } 1.64\mu m}} \quad (4.5)$$

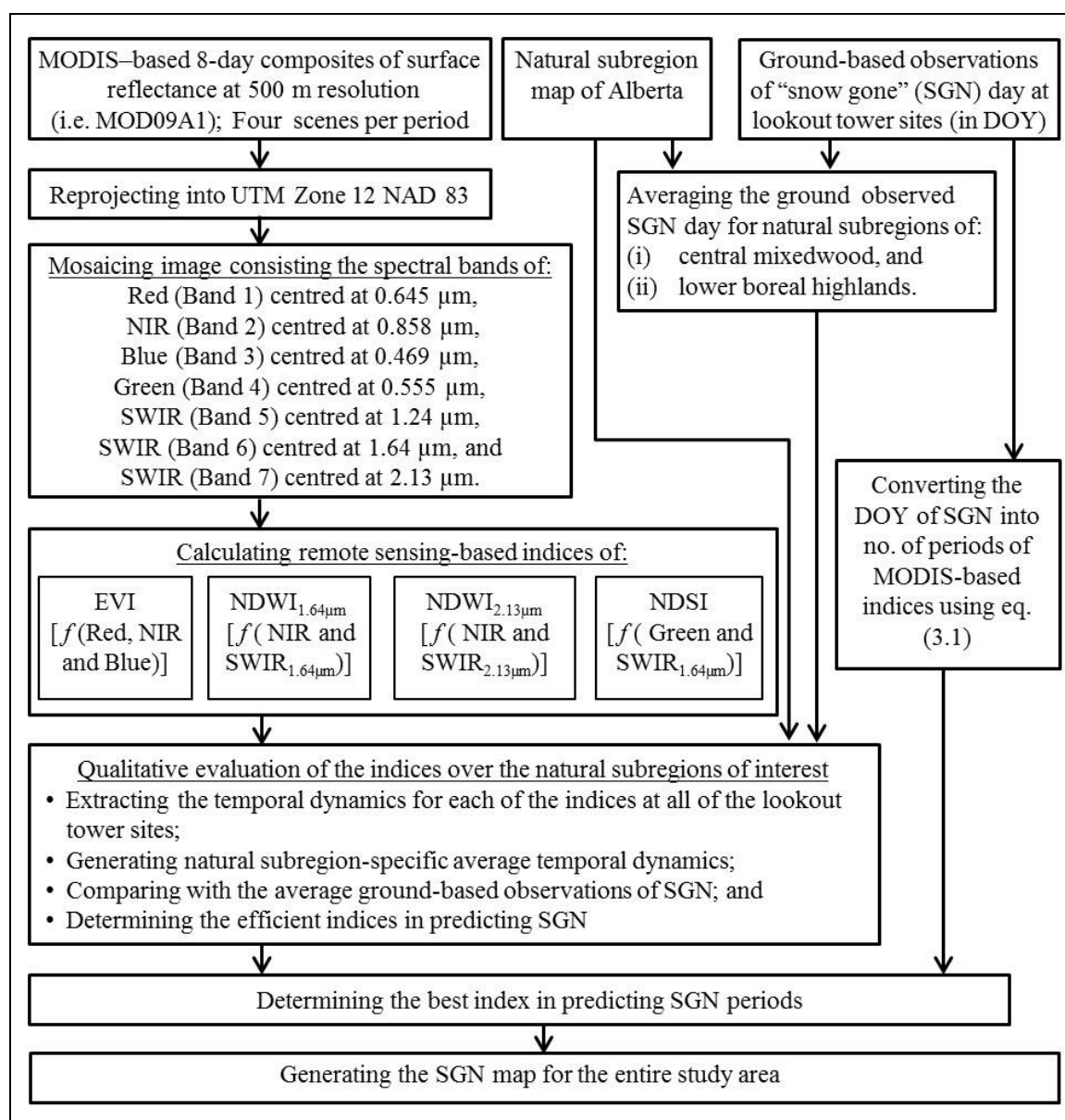
where, ρ is the surface reflectance for the blue, green, red, NIR, and SWIR spectral bands.

4.2.2 Qualitative Evaluation of the Indices

After computing all of the indices, a qualitative evaluation to determine the efficient indices in predicting SGN stages was performed. For this, two of the forest-dominant natural sub-regions (*i.e.*, central mixedwood and lower boreal highlands, where there were approximately 45 lookout towers; and also these are more vulnerable to forest fire (Dowing and Pettapiece, 2006) were considered; and executed the following steps:

- (i) extracted the temporal dynamics of each of the indices at all of the lookout tower sites; and then generated sub-region-specific average temporal dynamics for each of the indices;
- (ii) calculated the natural sub-region-specific average SGN day using the ground-based observations; and
- (iii) compared the values obtained from steps (i) and (ii), qualitatively by overlaying each other in the graphical form.

Figure 4.1: Schematic diagram showing the method followed for delineating “snow gone” (SGN) stage occurrence over the study area.



4.2.3 Quantitative Evaluation of the Indices

The qualitative evaluation demonstrated that the indices of $NDWI_{1.64\mu m}$, $NDWI_{2.13\mu m}$ were better in comparison to others (see Section 5.1. for more details). The minimum values of these two indices during the spring period (*i.e.*, 65–200 DOY or 06 March–19 July) were coincided with the observed SGN stage. Thus, it was required to execute the following steps:

- (i) extraction of the temporal dynamics for these two indices at all of the lookout tower sites across the entire study area (see Figure 3.2 for the lookout tower sites);
- (ii) declaration of the minimum values during the spring period as the indices-based SGN period;
- (iii) then comparison of the predicted SGN with the ground-based observations of SGN periods; and
- (iv) computation of the overall deviations between the predicted and observed SGN periods, and determined the best index in determining the SGN.

4.2.4 Mapping of SGN Using Best Predictor

The mapping was performed using the best predictor index in generating the SGN maps. The results of previous steps established the concept of associating a pattern (*i.e.*, minimum value) in the temporal trend of best predictor index to the phenological stage of SGN. For mapping, the temporal dynamics of the best index during the spring season at each pixel were analysed and the corresponding period of the minimum-value of the index was determined as the period of “SGN”.

4.3 CNF Determination

Figure 4.2 shows a schematic diagram describing the methods involved in CNF determination from GDD and NDWI. Note that, NDWI to be used (*i.e.*, NDWI_{1.64 μ m} or NDWI_{2.13 μ m}) in this phase was the best predictor in determining the SGN. Thus, it would have lower uncertainties induced by snow melt into its temporal trends. The major components of this phase were to:

- (i) generate GDD maps for the period 2006-08;
- (ii) determine thresholds of cause (*i.e.* GDD) and response (*i.e.* NDWI) for predicting CNF during 2006 using ground-based CNF observations;
- (iii) compare CNF predictions (*i.e.* based on the determined thresholds for GDD, NDWI, and both combined together logically) with the ground-based observations for the period 2007-2008; and
- (iv) generate CNF occurrence map using best predictor (determined in objective (iii)); to discuss the spatial dynamics.

All of these components are described in the following sub-sections.

4.3.1 Generation of GDD maps

Before generating the GDD maps, the bias between 8-day T_s and average air temperature (\bar{T}_a) at ~182 weather station sites (see Figure 3.3 for the weather station sites) were examined to understand the inter- and intra-seasonal coincidence between them. During each of the 8-day periods, the values of T_s and \bar{T}_a at all of the weather station sites were averaged, and the bias was calculated using the following expression:

$$Bias(i) = \frac{\sum_{j=1}^n (T_s - \bar{T}_a)}{n} \quad (4.6)$$

where, i is the 8-day period of interest, and n is the total number of weather station sites during the i^{th} period.

In generating GDD maps at 1 km spatial resolution, the method described in Akther and Hassan (2011) was adopted. It consisted of the following two steps:

- i. Establishing relation between 8-day composites of MODIS-based instantaneous T_s (i.e., acquired between 10:30 am - 12:00 pm) with \bar{T}_a acquired at ~182 weather stations across Alberta (see Figure 3.3 for location information) during the period 2006. Then this observed relation was used to predict \bar{T}_a during 2007 and 2008. The predictions were then cross-validated with the corresponding ground-based observation of \bar{T}_a using linear regression analysis. In this analysis, some outliers were declared on the basis of the residual values (i.e., difference between predicted and ground observed \bar{T}_a) beyond the permissible limits. These limits were defined on the basis of quartile ranges of the residual values as follows:

$$\begin{aligned} I_{UL} &= Q_3 + 2.5(Q_3 - Q_1) \\ I_{LL} &= Q_1 - 2.5(Q_3 - Q_1) \end{aligned} \quad (4.7)$$

where, I_{UL} and I_{LL} are the upper and lower limits respectively;
and Q_3 and Q_1 are the third and first quartile values of the
residuals.

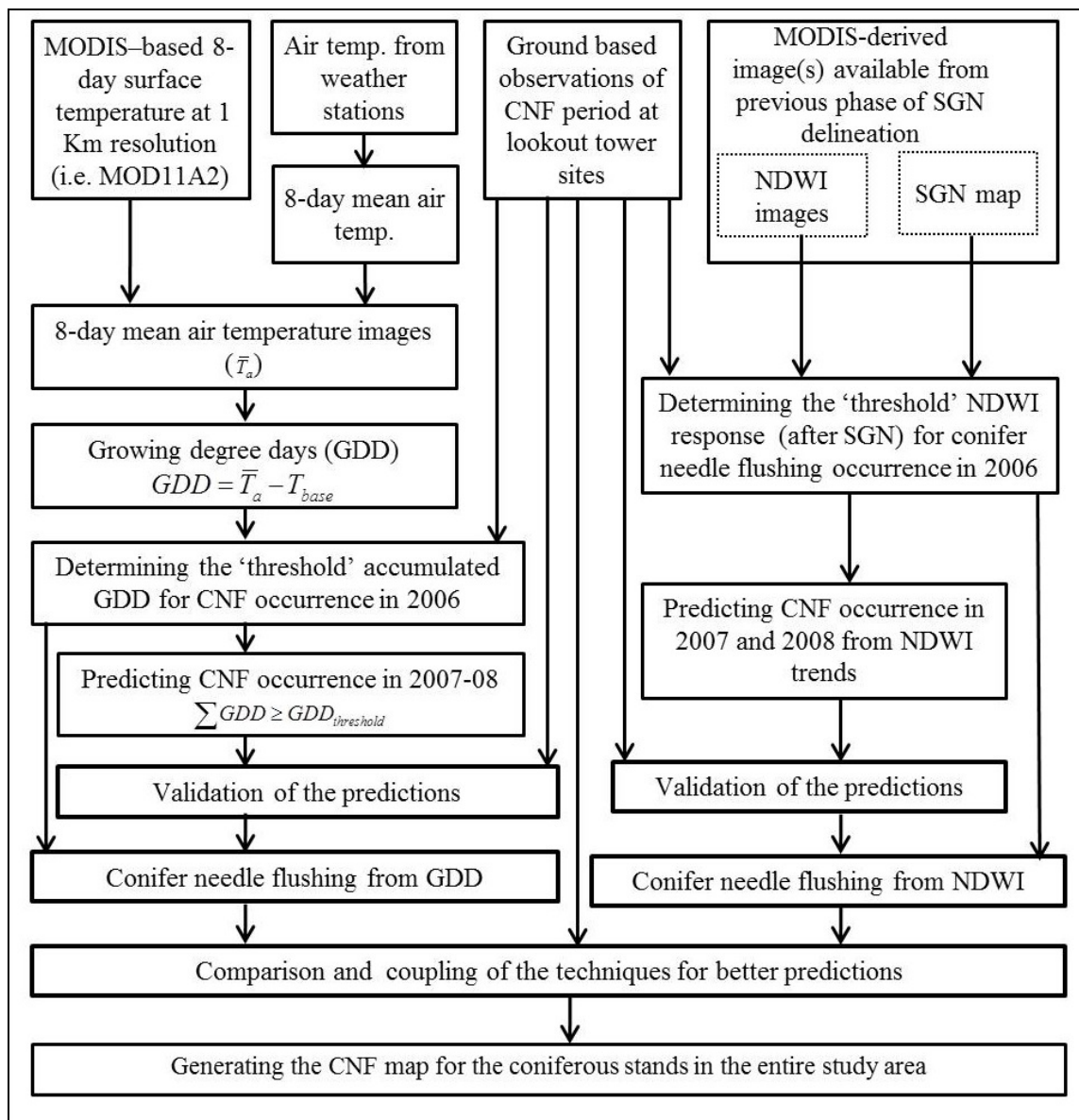
- ii. The obtained relation from step (i) was then applied in converting the MODIS-based instantaneous T_s into equivalent 8-day \bar{T}_a ; and then calculated GDD-values using the following expression:

$$GDD = \begin{cases} \bar{T}_a - T_{base} & \text{if } \bar{T}_a > T_{base} \\ 0 & \text{otherwise} \end{cases} \quad (4.8)$$

where, T_{base} is base temperature with a magnitude of 5 °C (=278.15 K), because the assumption is that the trees require this minimum air temperature to initiate growing conditions (Rossi et al., 2007; Hassan and Bourque 2009).

The selection of T_{base} may require optimization in some studies in order to address the species and site variability (Weilgolaski, 1999). However, in this study the selection of our T_{base} may not be critical as our objective is to predict CNF from very similar temperature regimes, as that of the model calibration/development phase (Man and Lu, 2010).

Figure 4.2: Schematic diagram showing the method followed for delineating “coniferous needle flush” (CNF) stage occurrence over the study area.



4.3.2 CNF Delineation from GDD and NDWI-values

As a first step, the temporal trends of both GDD and NDWI along with SGN periods were extracted during the years of 2006-08 at the lookout tower sites where the ground-based CNF records were available. These datasets were then divided into two groups:

- (i) calibration dataset consisting of ~34% data points (i.e., data from 2006); and
- (ii) validation dataset consisting of ~66% data points (i.e. data from the years 2007-08).

The calibration phase consisted of the following steps:

- (i) calculated the accumulated GDD (AGDD) and observed NDWI-values during the CNF ground- based observation period at each of the lookout tower sites;
- (ii) calculated an average and standard deviation AGDD and NDWI-values during the CNF ground-based observation periods; and these were considered to be the predictor-specific initial “threshold-values” for CNF determination; and
- (iii) evaluated the sensitivity of the initial threshold-values for both of the AGDD and NDWI-values in determining the CNF stage upon varying in the bound “initial threshold \pm 1 standard deviation” as most of the data were found to be in this range. Within the bound, the thresholds were then evaluated at each “1/3 standard deviation” intervals. The best thresholds were then identified when the deviations between the predicted and observed CNF period were the least.

In validation phase, the CNF periods were predicted during the years 2007-2008 using the best thresholds for AGDD and NDWI obtained in the calibration phase. Then next

step was to calculate the deviations between the predicted and observed CNF periods to determine the suitability of the proposed method.

4.3.3 Integration of Both GDD and NDWI-values

In this step, it was evaluated how the integration of the causal (i.e., AGDD) and response (i.e., NDWI)-based predictors could enhance the determination of the CNF stage. In the process of integrating both GDD and NDWI-values in determining the CNF stage, the best thresholds of AGDD and NDWI determined in section 4.3.2 were considered. The CNF period was predicted in two ways:

- (i) if at least one of the predictors reached to the corresponding threshold-value (i.e., logical ‘OR’ condition between the predictors); and
- (ii) both of the predictors would reach to the threshold-values (i.e., logical ‘AND’ condition between the predictors);
- (iii) then compared the predicted CNF period with the ground-based CNF observations by analysing the deviations between them.

4.3.4 Mapping of CNF Using Best Prediction Criteria

Among all of the evaluated predictors (i.e., GDD and NDWI individually as described in section 4.3.2; and the integration of GDD and NDWI as described in section 4.3.3), the best predictor was implemented in mapping CNF stage over the conifer-dominant natural sub-regions. The results of previous steps established the concept of associating attainment of a threshold value in the temporal trend of the predictor(s) to the phenological stage of CNF. For mapping, the temporal dynamics of the indices during

the spring season at each pixel were analysed and the corresponding period when the indices reached to the threshold-values was determined as the period of “CNF”.

Note that the land cover map (described in Table 3.2) was used in delineation of the pixels with conifer as dominant vegetation type. In general, the conifer stands were found in the 9 natural sub-regions (i.e., marked with * symbols beside the name of the natural sub-regions in Table 3.1; all of them are located in the boreal ecoclimatic zone).

CHAPTER 5: RESULTS & DISCUSSION

The chapter presents the outcomes of the phenology delineation methodology described in previous chapter. The agreements of the predictions with the ground-based data are presented in terms of deviations, such that – and + deviations represent the early and delayed predictions respectively.

5.1 Delineation of SGN

5.1.1 *Qualitative Evaluation of the Indices*

Figures 5.1 and 5.2 show the average temporal dynamics for all of the four indices over the natural sub-regions of central mixedwood and lower boreal highlands. Such trends are shown for the period of 2006–2008. The average DOY of SGN from ground records in the central mixed wood (shown as vertical red dotted lines in Figure 5.1) was found to be 112.6 in 2006, 120.5 in 2007, and 130.5 in 2008; while for the lower boreal highlands, it was 121.9 in 2006, 125.2 in 2007, and 129.0 in 2008.

In general, EVI remained low during the winter months (approximately DOY in between 1 and 89) before it started to increase in the spring. These increasing trends might be a result of either snow melting or a combination of both snow melting and greening up (Delbart et al., 2005).

Figure 5.1: Temporal dynamics of averaged values from all of the lookout tower sites for EVI, $NDWI_{1.64\mu m}$, $NDWI_{2.13\mu m}$, and NDSI for the natural sub-region of *central mixedwood* (i.e., ~25.5% of the province) for the period of 2006-08. The average SGN day from the ground-based observations for the same natural region is shown by dotted line running vertically.

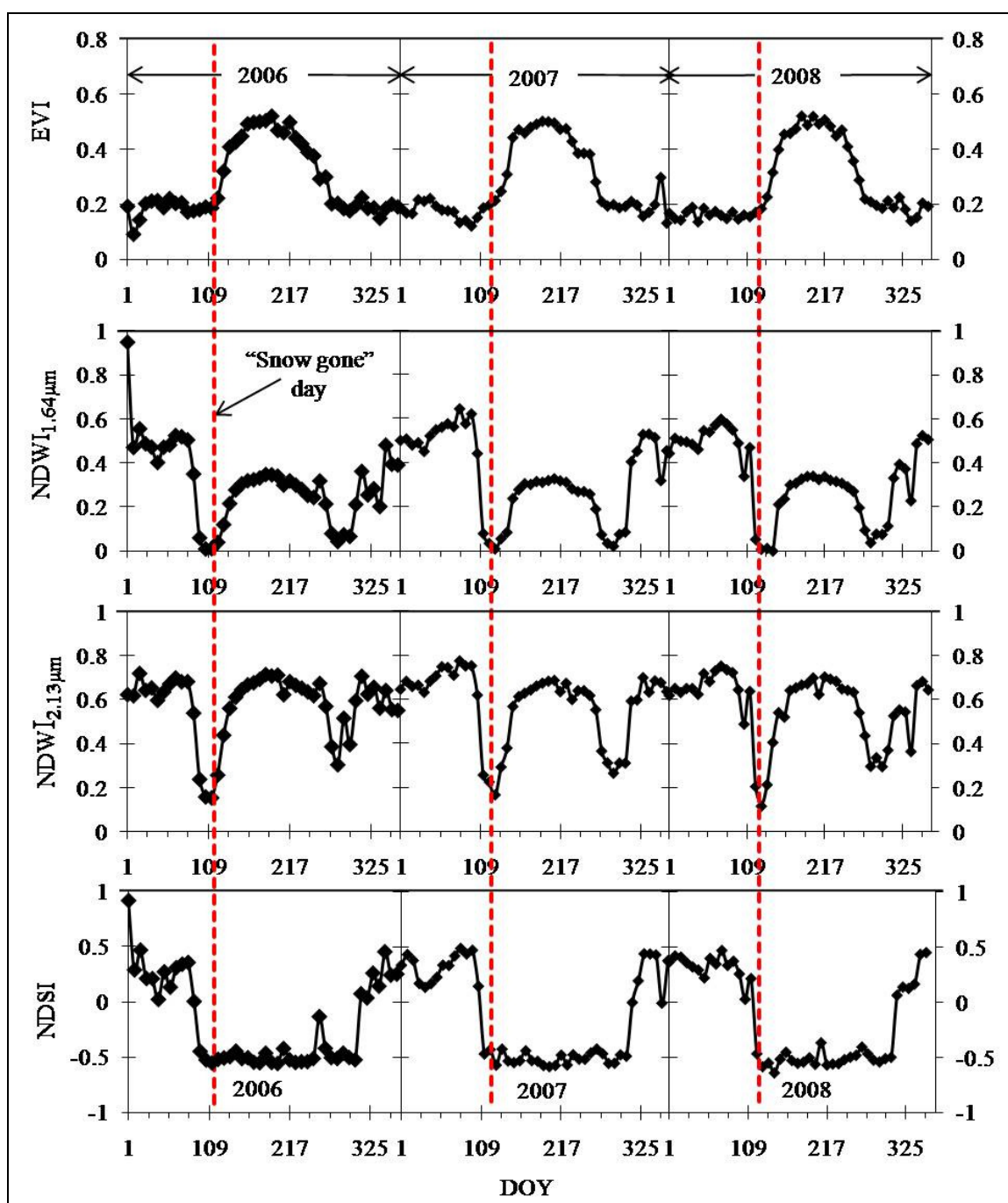
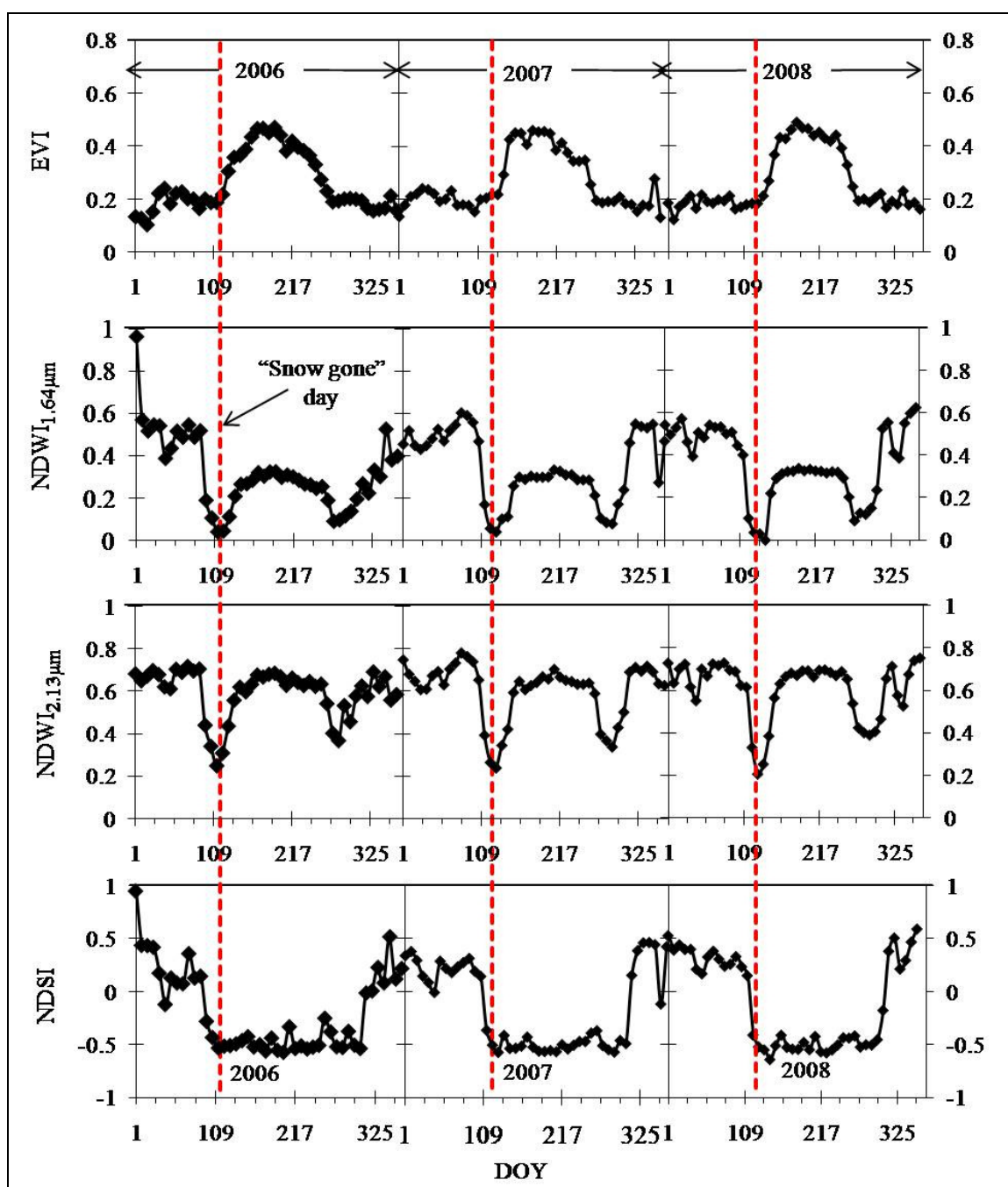


Figure 5.2: Temporal dynamics of averaged values from all of the lookout tower sites for EVI, $NDWI_{1.64\mu m}$, $NDWI_{2.13\mu m}$, and NDSI for the natural sub-region of *lower boreal highlands* (i.e., ~8.5% of the province) for the period of 2006-08. The average SGN day from the ground-based observations for the same natural region is shown by dotted line running vertically.



The NDWI's and NDSI, maintained high values during the winter (DOY in between 1 and 73 on an average) and then started to decrease (about 81 DOY). This might be due to the onset of snow melting (Delbart et al., 2005; Delbart et al., 2006).

The NDWI values were observed to reach a minimum value (about 109 to 135 DOY); and then started to increase again. Similar trends were also observed by others (Delbart et al., 2005; Delbart et al., 2006). The rises in NDWI might be associated with the SGN stage and/or greening up (Delbart et al., 2005; Delbart et al., 2006). As the NDWI depicts the snow melting and greening up in opposite directions; the stage corresponds to the minimum values of NDWI might be considered as SGN stage or onset of the growing season as well.

In general, a value of 0.4 for the NDSI corresponds to snow disappearance (Klien et al., 1998; Hall et al., 2002), however, this value might even reach to 0.1 depending on the amount and type of vegetation/forests (Hall et al., 2002). Additionally, the values of NDSI might reach below “zero” values and refer as “summer conditions” (Klien et al., 1998).

Also, some spikes were noticed in the temporal dynamics for all of the indices. These might be associated with spatial variation in atmospheric transmissivity and other extrinsic factors that affect the calculations of the MODIS-based indices (Hassan and Bourque, 2010).

Among the four indices, the temporal trends of EVI did not clearly indicate the SGN stage (see Figures 5.1 and 5.2 for more details). These results confirmed the assumption that snow might influence the predictive capability of EVI similar to NDVI (Delbart et al., 2005; Delbart et al., 2006).

In terms of NDSI, the deviation between the ground-based observations of SGN and NDSI-based estimates (when the NDSI-values first went below a threshold of 0.1 during the spring time) were found in the range of -3 to -5 periods (*i.e.*, -24 days to -40 days).

Due to the fact that both of the NDWI's showed a distinct temporal pattern (*i.e.*, the lowest values were found in the early spring as shown as Figures 5.1 and 5.2) in comparison to the ground-based SGN stages, these two were considered as the efficient indices. Thus, these indices were further analysed by assuming that these would be able to determine the period of SGN.

5.1.2 Determining the Best Index in Predicting SGN Periods

The comparisons between the predicted SGN periods using the $NDWI_{1.64\mu m}$ and with the ground-based observations at all of the individual lookout tower sites are illustrated in Figure 5.3 and Table 5.1. The similar comparisons between the predicted SGN periods using the $NDWI_{2.13\mu m}$ and with the ground-based observations are also illustrated in Figure 5.4 and Table 5.2.

In both figures (Figures 5.3 and 5.4), the right and left sides of the 1:1 line represent negative deviation (early prediction) and positive deviation (delayed prediction) respectively. And the total no. of operational lookout tower sites for each of the years is denoted by n inside the panels.

Figure 5.3: Comparison between the SGN periods at each of the lookout tower sites during 2006-2008 periods from ground-based observations and predicted using $NDWI_{1.64\mu m}$.

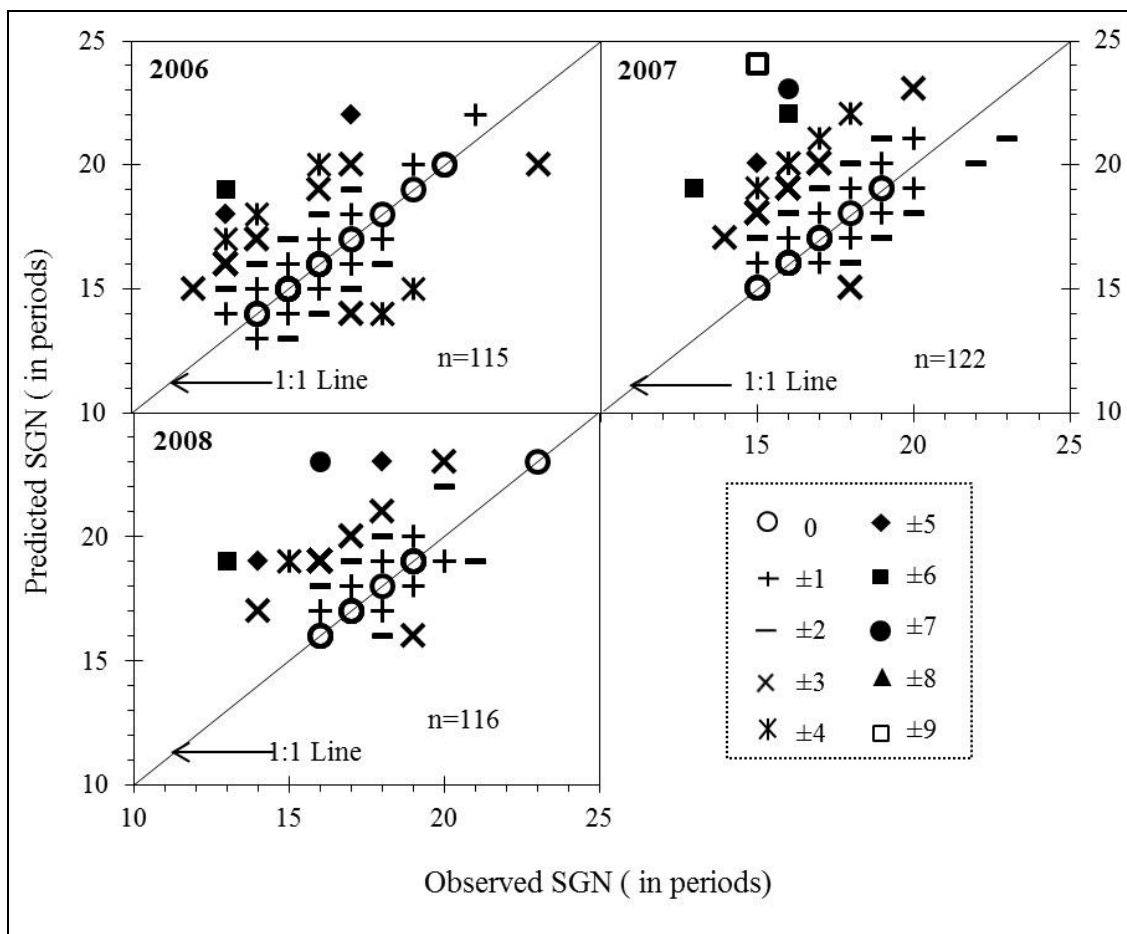
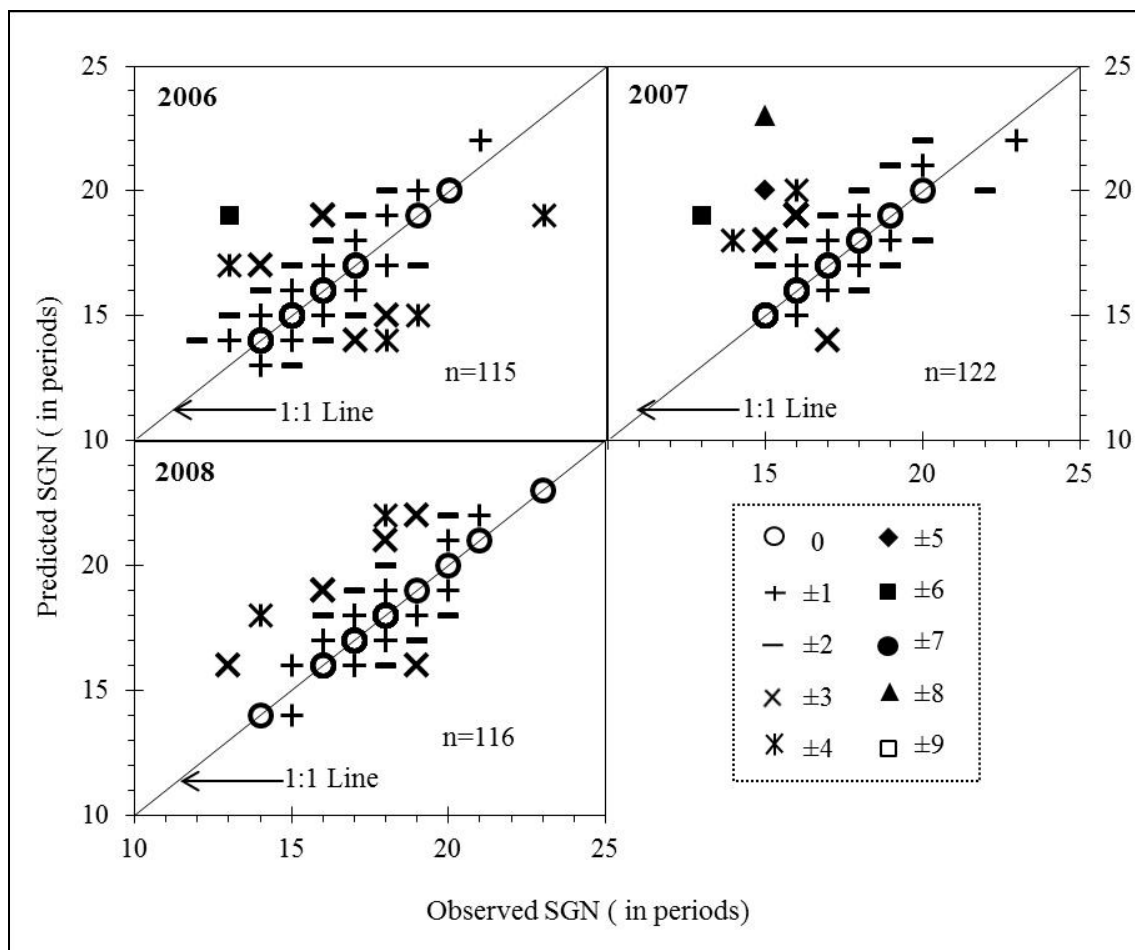


Table 5.1: Relation between NDWI_{1.64μm} -based prediction and ground-based SGN observation period at the lookout tower sites during 2006-2008.

<i>% of lookout tower sites</i>				
Deviation (in periods)	2006 (n=115)	2007 (n=122)	2008 (n=116)	2006-08 (n=353)
± 0	20.87	14.76	11.21	15.61
± 1	59.13	50	44.83	51.32
± 2	80	75.41	63.8	73.07
± 3	92.17	90.98	94.84	92.66
± 4	97.39	95.9	96.56	96.62
± 5	99.13	96.72	98.28	98.04
± 6	100	98.36	99.14	99.17
≥ ± 7	100	100	100	100

In case of NDWI_{1.64μm}, the predictions were marginally acceptable with 51.3% of the cases were within ±1 periods of deviation from the ground observed records on an average during the three years. Also, on an average approximately 73% of the observations fell within ±2 periods of deviation from the ground observed records; 93% in ±3 periods of deviation from the ground observed records; and the remaining 7% were in between ±3 and ±9 periods of deviation.

Figure 5.4: Comparison between the SGN periods at each of the lookout tower sites during 2006-2008 period from ground-based observations and predicted using $NDWI_{2.13\mu m}$.



In case of $NDWI_{2.13\mu m}$ on the other hand, demonstrated better capabilities in comparison with $NDWI_{1.64\mu m}$. The predictions were really promising with 65.6% of the cases were within ± 1 periods of deviation from the ground observed records on an average during the three years. While, on an average approximately 90% of the observations fell within

± 2 periods of deviation from the ground observed records; 96% within ± 3 periods deviation from the ground observed records; and the remaining 4% in between ± 3 and ± 9 periods of deviation.

Table 5.2: Relation between NDWI_{2.13 μ m} -based prediction and ground-based CNF observation period at the lookout tower sites during 2007-2008 using the best NDWI threshold of 0.525.

<i>% of lookout tower sites</i>				
Deviation (in periods)	2006 (n=115)	2007 (n=122)	2008 (n=116)	2006-08 (n=353)
± 0	27.82	21.31	25	24.71
± 1	65.21	59.01	72.42	65.55
± 2	91.3	86.06	93.11	90.16
± 3	95.65	95.9	98.28	96.62
± 4	99.13	97.54	100	98.9
± 5	99.13	98.36	100	99.17
± 6	100	99.18	100	99.73
$\geq \pm 7$	100	100	100	100

The relatively higher deviations (*i.e.*, $> \pm 4$ periods with relatively less probability of ~5% of the time) were, in general, observed in the high elevation areas which are located in the natural sub-regions of alpine, sub-alpine, and upper foothills.

The discrepancies between the predicted and ground-based observations of SGN periods could be attributed due to the following factors:

- (i) The ground-based observations were entirely on the basis of visual inspection, thus it highly depended on the experience of an operator to interpret the situation; and
- (ii) Spatial resolution of the NDWI's and ground-based observations might not be in agreement in some instances.

5.1.3 SGN Maps and Spatial Dynamics

Figures 5.5 to 5.7 shows the SGN map generated using $NDWI_{2.13\mu m}$ (the best predictor as per Section 5.1.2) for the years of 2006-2008. The maps also show the location of two transects; namely a-b (east to west) and c-d (north to south). The moving average of 10 consecutive pixels of SGN period of occurrence along transects and its variations over the three years of the study (*i.e.*, 2006-08) are shown in Figure 5.8.

During 2006, ~64.5% of the times SGN occurred in the range of 97-128 DOY (*i.e.*, 7th April to 8th May). In 2007, ~62.7% SGN occurrence was in range of 105-135 DOY (*i.e.* 15th April to 16th May). While, during 2008, it revealed that approximately 56% of the times the SGN stages fell in the range of 121–136 DOY (*i.e.* 30th April to 15th May).

The generalized spatial patterns are discussed as follows:

- (i) In general, temperature decreases northwards in the northern hemisphere (Hassan et al., 2007a) so that the northward increment of SGN stages in our study would be expected.
- (ii) The natural sub-regions in the high elevation areas (*i.e.*, alpine and sub-alpine as shown in polygon I; montane in the middle of polygon II; upper boreal highlands in the middle of polygon III; and sub-alpine in polygon IV) experienced relatively high SGN stages (*i.e.*, in the range of 137–200 DOY). This is reasonable as the high elevation areas experience relatively cooler temperature regime, which influences the snow to stay relatively longer period of time.

During the period 2006-2008, the periods of SGN occurrence along the two transects (see Figure 5.8), revealed that the SGN occurrence periods were variable. The moving average trends revealed that the SGN occurrence was getting late for each year; from about 14th period in 2006 to 17th period in 2008. Note that the peaks in the trends correspond to the high elevation areas. These changes might be as a function of climate change, however it requires more investigation to confirm which is beyond the scope of this Thesis.

Figure 5.5: SGN Map for 2006; (a) Spatial dynamics of $NWDI_{2.13\mu m}$ predicted SGN map for the entire study; and (b) it's relative frequency distribution. The polygons I-IV in panel (a) are outlined to have more discussion in the text. Also the location of two transects 'a-b' and 'c-d' are shown in panel (a).

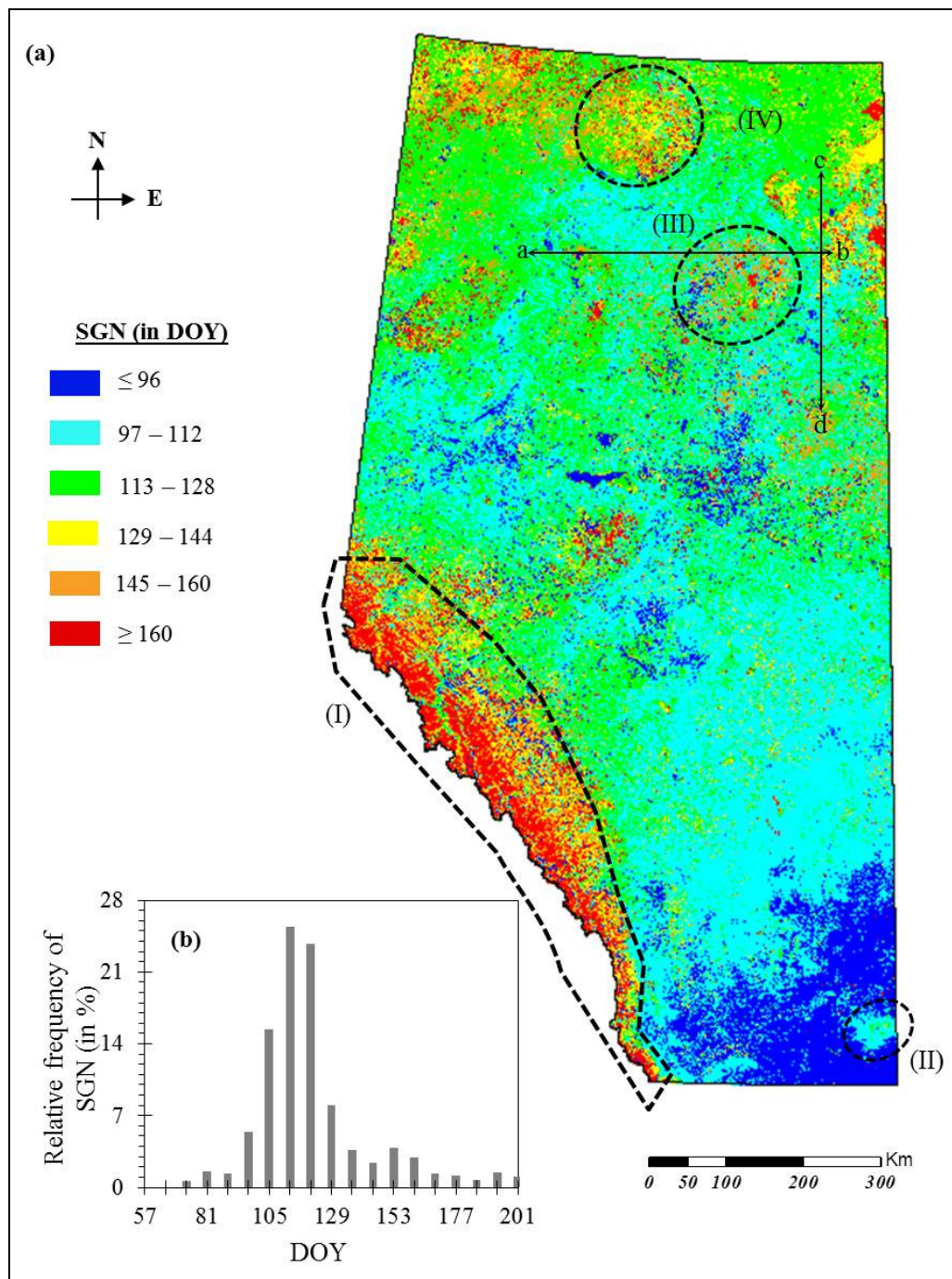


Figure 5.6: SGN Map for 2007; (a) Spatial dynamics of $NWDI_{2.13\mu m}$ predicted SGN map for the entire study; and (b) it's relative frequency distribution. The polygons I-IV in panel (a) are outlined to have more discussion in the text. Also the location of two transects 'a-b' and 'c-d' are shown in panel (a).

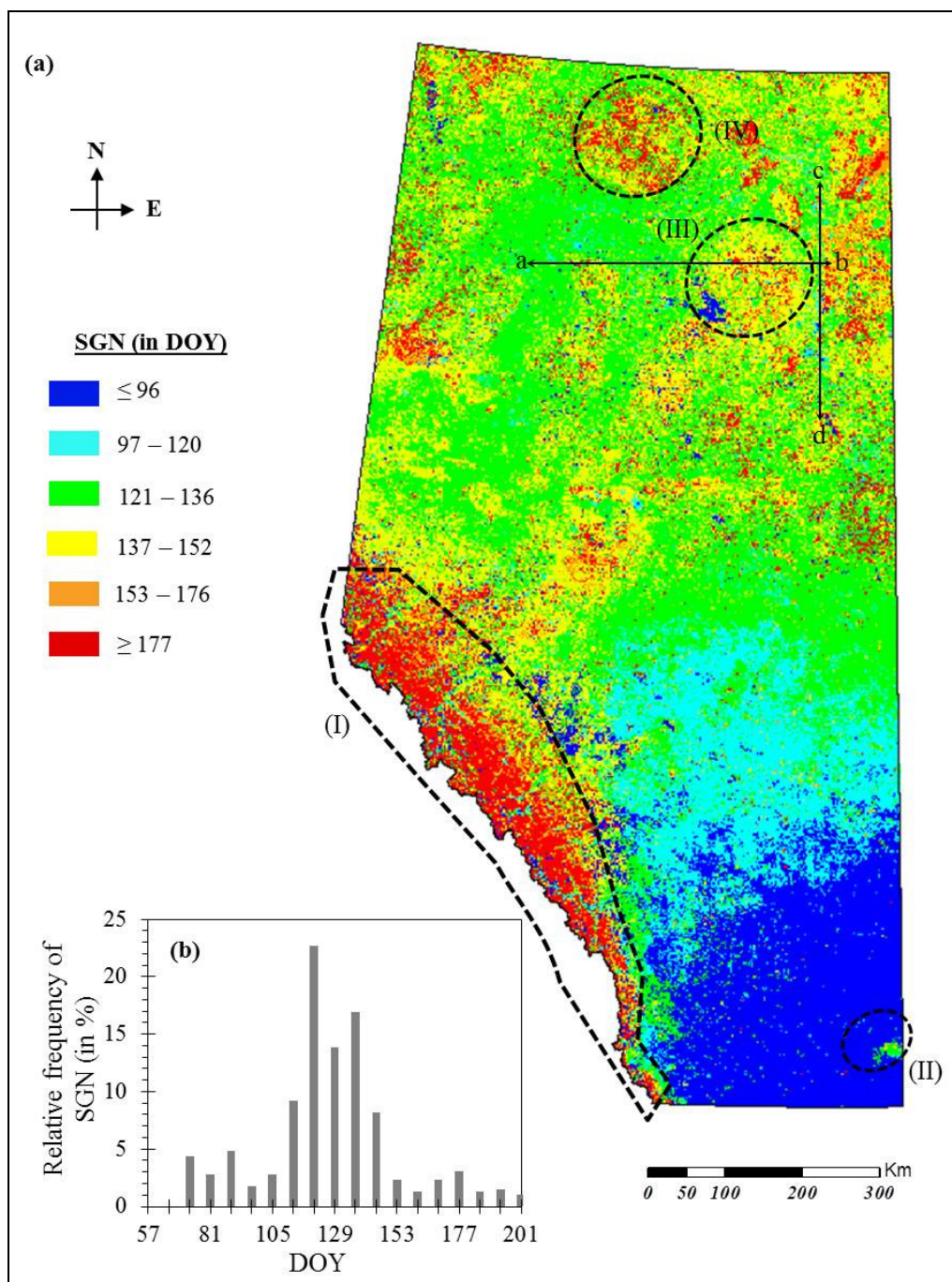


Figure 5.7: SGN Map for 2008; (a) Spatial dynamics of $NWDI_{2.13\mu m}$ predicted SGN map for the entire study; and (b) it's relative frequency distribution. The polygons I-IV in panel (a) are outlined to have more discussion in the text. Also the location of two transects 'a-b' and 'c-d' are shown in panel (a).

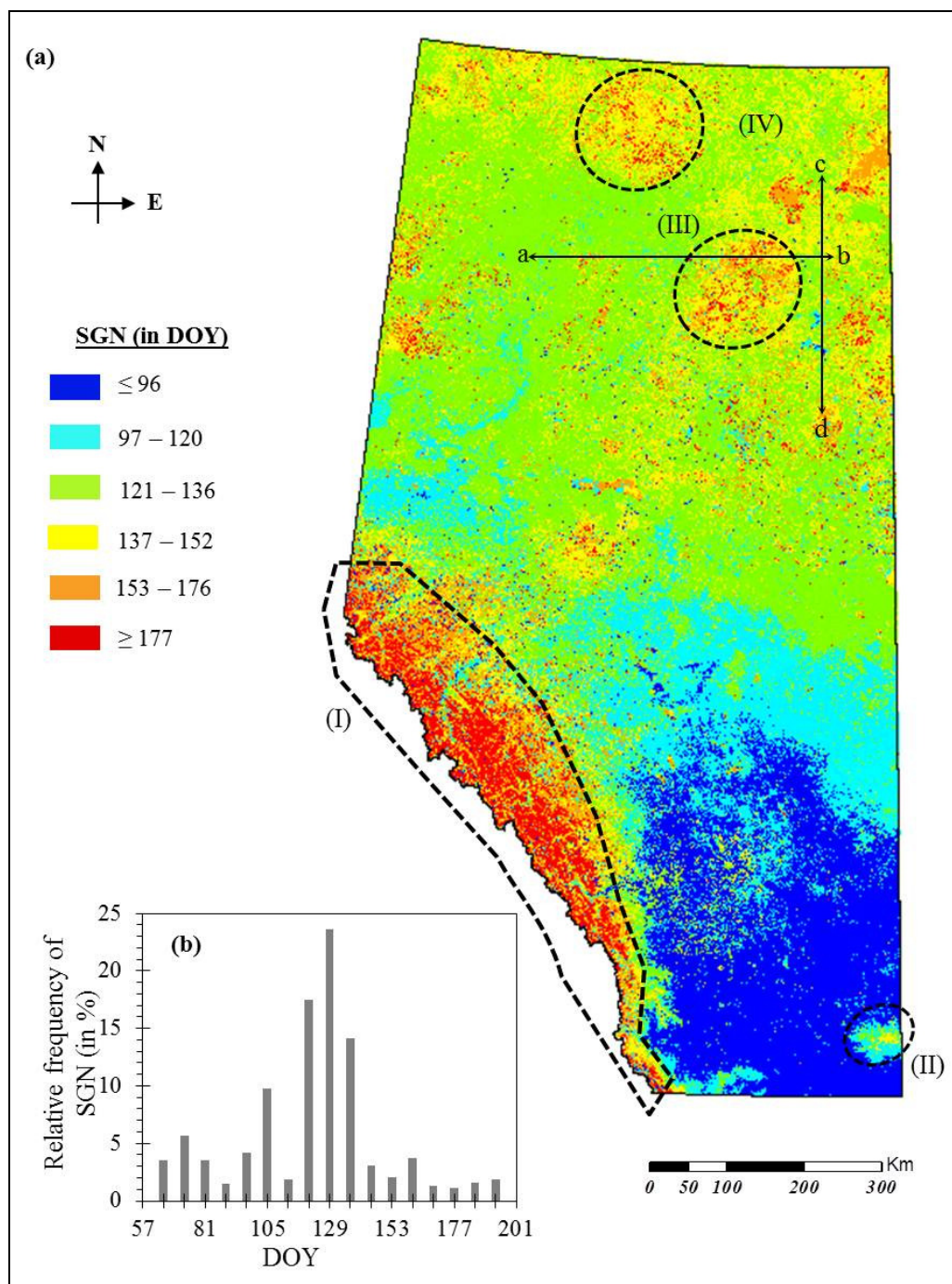
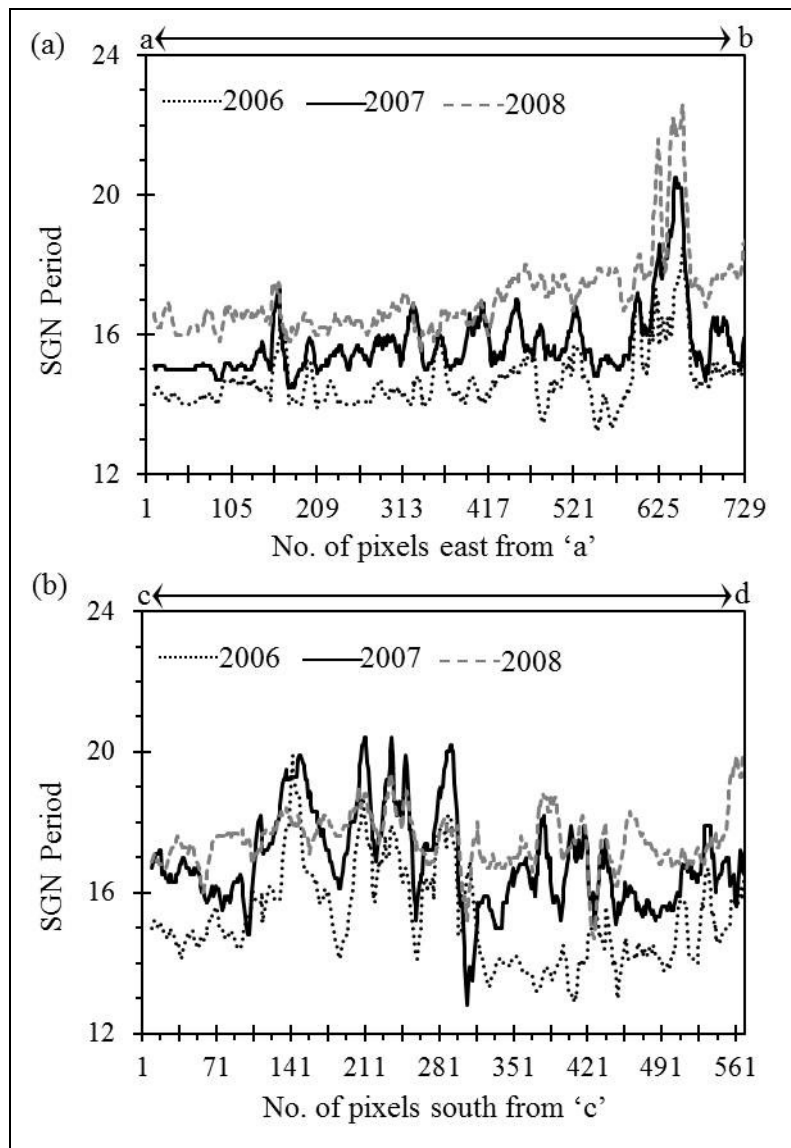


Figure 5.8: The moving average of 10 consecutive pixels of SGN period occurrence and its variations over the years of 2006-08 along the two transects: (a) a-b (east to west); and (b) c-d (north to south).



5.2 Delineation of CNF

The initial challenge of this phase was to successfully map GDD over the regions of interest. Followed by, identifying of the thresholds in GDD and NDWI, for the CNF occurrence. NDWI used in this phase was $NDWI_{2.13\mu m}$; as in previous phase it has depicted best predictions of SGN. The following subsections provide the description of the results obtained for CNF determination, in accordance to the workflow.

5.2.1 GDD Mapping

Figure 5.9 shows the bias between T_s and \bar{T}_a during the period 2006-2008. The bias was found to be:

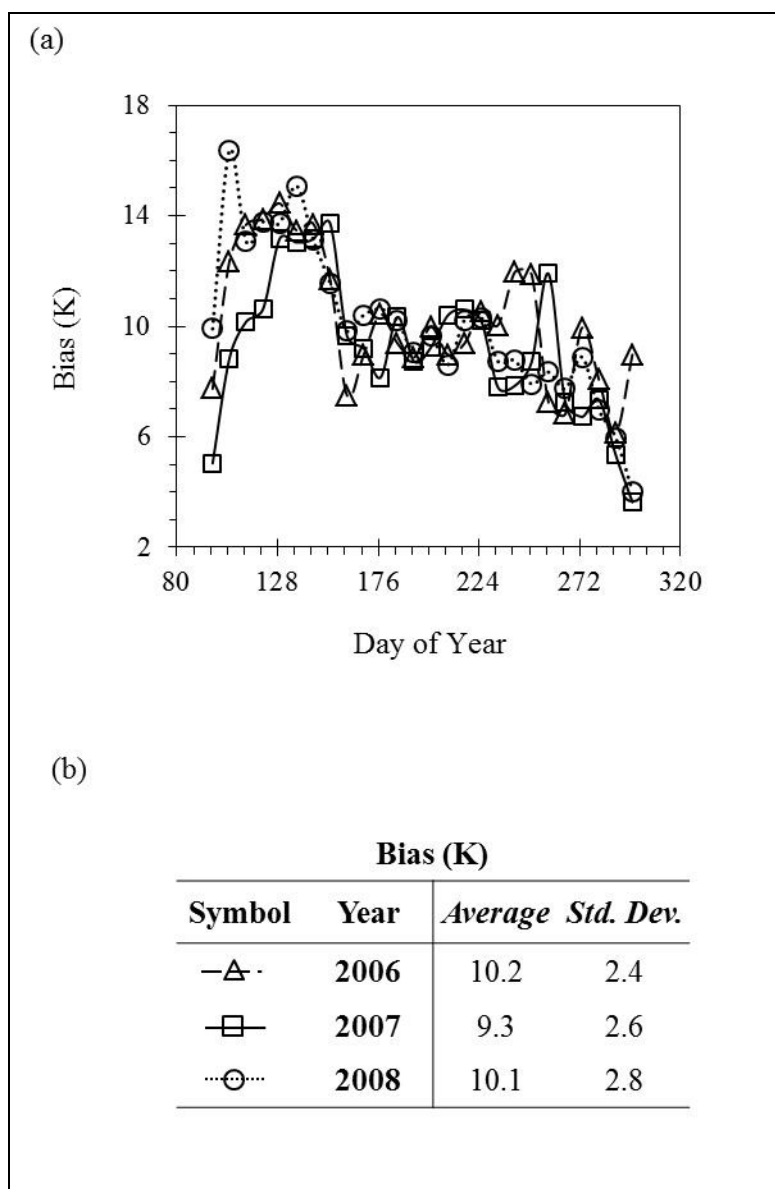
- (i) relatively high (i.e., ~13 K) during early spring;
- (ii) almost constant (~9K) for the most of the growing season (i.e., after spring); and
- (iii) relatively low (~5K) during fall and late winter.

During 2006-2008, found that the bias was having an average and standard deviation of ~10 and 2.6 K respectively.

The seasonal biases in T_s and \bar{T}_a (see Figure 5.9) might be associated with:

- (i) change in the characteristics of the surface due to snow dynamics; and
- (ii) change in the evapotranspiration rate.

Figure 5.9: (a) Trends of seasonal bias between the satellite-based surface and ground-based air temperatures in Kelvin(K) at 8-day resolution for years of 2006, 2007, & 2008; (b) table showing the values of average and standard deviation of the bias between two temperatures over the entire season for the corresponding years.

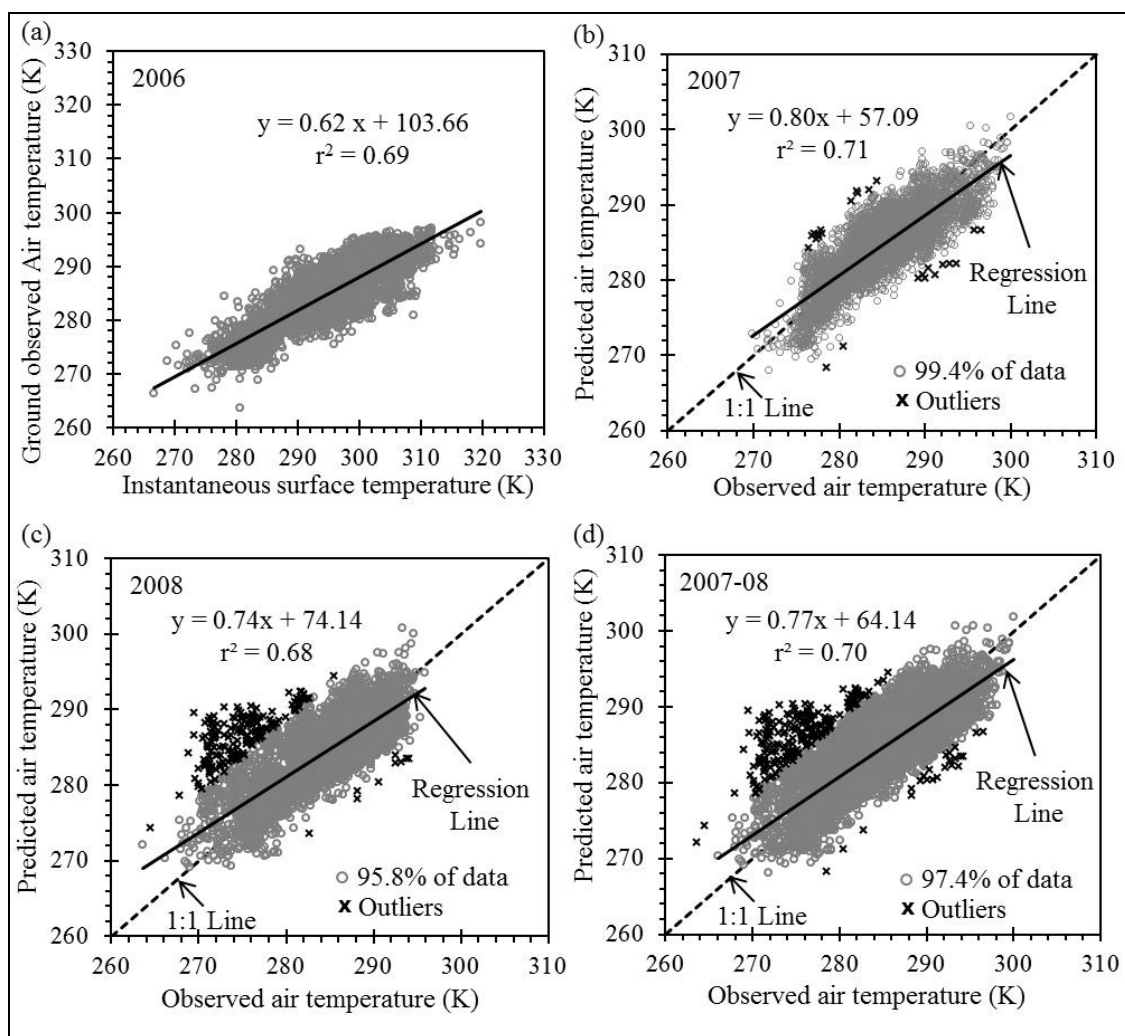


The relation between T_s and \bar{T}_a during 2006 is shown in Figure 5.10a. It was observed that a reasonably strong relation (i.e., $r^2=0.69$ with a slope and intercept of 0.62 and 103.66 respectively) existed between the variables of interest (see Figure 5.10a).

The application of this observed relation during 2007, 2008, and 2007-2008 also revealed reasonable agreement (i.e., r^2 in the range 0.68-0.71 with a slope and intercept in the range of 0.74-0.80 and 57.09-74.1489.52 respectively; see Figure 5.10b-d) for greater than ~96% of the data. Note that ~4% of data points (i.e., 26 out of 4561 in 2007, 182 out of 4287 in 2008, 234 out of 8848 in 2007-2008; see Figure 5.10b-d as shown in dark black colour) were classified as outliers as determined using Eq. 4.7.

During establishing relations between T_s and \bar{T}_a (see Figure 5.10a) and their validations (see Figure 5.11b-d), some discrepancies were observed (i.e., ~31%). These would be due to the spatial resolution differences between the MODIS-based T_s (i.e., 1 km spatial resolution) and ground-based \bar{T}_a data (i.e., at point locations representing several square meters) (Akther and Hassan, 2011; Liang et al., 2011).

Figure 5.10: (a) Relation between the MODIS-based 8-day instantaneous surface temperature and 8-day average air temperature during 2006; (b) & (c) validation of the relation observed during 2006 and its comparison with the 8-day average air temperature during 2007 & 2008 respectively; (d) validation of the observed relation over 2007-08 lumped together.



5.2.2 Determination of GDD Threshold for CNF Occurrence

Figure 5.11a shows averaged temporal trends of AGDD in 2006 upon considering all of the lookout tower sites (i.e., 114 in total).

The initial AGDD threshold, *i.e.*, average, was found to be 225 degree days with a standard deviation of ± 75 degree days during the period of ground-based CNF observations (averaged ground-based CNF observation period shown in Figure 5.11a with a dotted vertical line). The frequency distribution of the AGDD thresholds revealed that they were in between 150-300 degree days (i.e., initial threshold ± 1 standard deviation) for approximately 71% of the times (see Figure 5.11b).

Upon varying the threshold in the range of “initial threshold ± 1 standard deviation” at each 1/3 standard deviation intervals, it was found that the threshold of 200 degree days were able to produce the best overall agreements at 0 (i.e., 30.7%), and ± 1 (i.e., 68.4%) period of deviation (see Figure 5.11c for more details).

The implementation of the final AGDD threshold (i.e., 200 degree days) during the period 2007-2008 revealed that the deviations were within ± 1 period for reasonable amount of the times (i.e., 61% in 2007; 53% in 2008, and 57.1% in 2007-2008) (see Table 5.3 for more details).

Figure 5.11: Determination of GDD threshold for CNF occurrence; (a) averaged temporal trends of GDD and AGDD at all of the lookout tower sites during 2006; and the dotted vertical line shows the averaged ground-based CNF observation period; (b) relative frequency of the AGDD at all of lookout tower sites; (c) implementation of various AGDD threshold to determine the best threshold in predicting the CNF period.

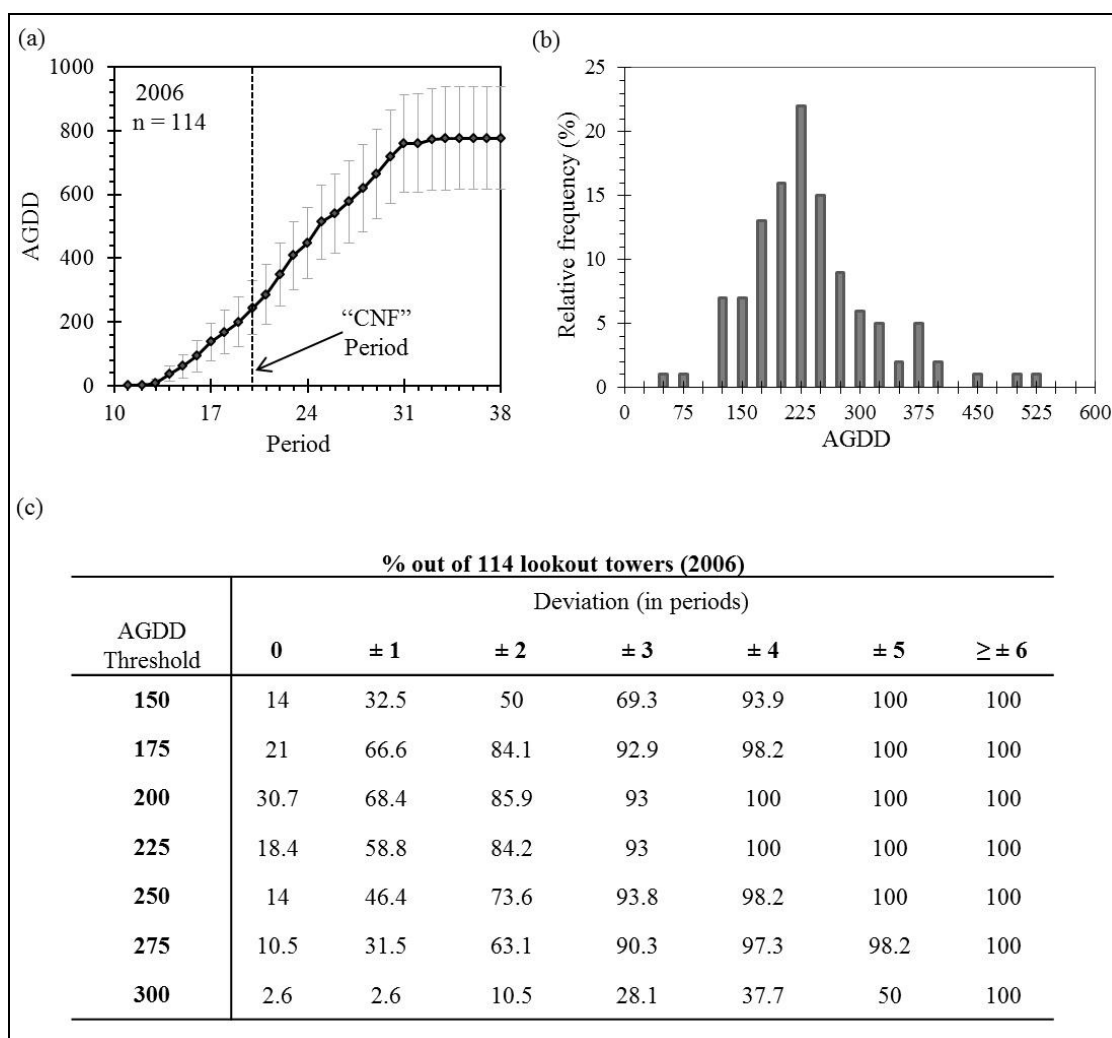


Table 5.3: Relation between AGDD-based prediction and ground-based CNF observation period at the lookout tower sites during 2007-2008 using the best AGDD threshold of 200 degree days.

<i>Deviation (in periods)</i>	<i>% of look-out towers</i>		
	2007 (n =118)	2008 (n =115)	2007-08 (n =233)
0	21.2	19.1	20.2
± 1	61	53	57.1
± 2	89.8	80.8	85.4
± 3	98.3	94.7	96.6
± 4	100	98.3	99.2
± 5	100	98.3	99.2
± 6	100	100	100
≥ ± 7	100	100	100

5.2.3 Determination of NDWI_{2.13μm} Threshold for CNF Occurrence

Figure 5.12a shows an average temporal trend of NDWI_{2.13μm} -values by extracting their values at all of the lookout tower sites (i.e., 114 in total) during 2006.

It was observed that the NDWI_{2.13μm} -values were relatively stable (i.e., maintaining an average of ~0.7) during the winter season (i.e., between 1-11 period; 1 Jan. - 29 March) due to the prevailing snow covers; and followed by a decreasing trend as a result of snow

melting and reached to a minimum value [i.e., defined as the end of snow melting (Delbart et al., 2005) or SGN stage (previous result)] before it started to increase again.

The average of $NDWI_{2.13\mu m}$ -values in comparison with the average ground-based CNF observation periods at 114 lookout tower sites (shown in Figure 5.12a using dotted vertical line) during 2006 was 0.523 with a standard deviation of 0.165. The frequency distribution of the $NDWI_{2.13\mu m}$ thresholds revealed that they were in between 0.375-0.675 (i.e., approximately initial threshold ± 1 standard deviation) for approximately 60% of the times (see Figure 5.12b).

Upon varying the threshold in the range of “initial threshold ± 1 standard deviation” at each $1/3^{rd}$ standard deviation intervals, observed that the $NDWI_{2.13\mu m}$ threshold values of 0.525, 0.550, and 0.575 were predicting the CNF with similar agreements (i.e., ~54% at ± 1 period deviation; see Figure 5.12c). These clearly indicated the insensitivity of the $NDWI_{2.13\mu m}$ threshold in this range; thus considered 0.525 as the final $NDWI_{2.13\mu m}$ threshold which was the closet to the initial threshold of 0.523.

The implementation of the final $NDWI_{2.13\mu m}$ threshold (i.e., 0.525) during the period 2007-2008 revealed that the deviations were within ± 1 period for reasonable amount of the times (i.e., 57.6% in 2007; 65.2% in 2008, and 61.4% in 2007-2008) (see Table 5.4 for more details).

Figure 5.12: Determination of NDWI threshold for CNF occurrence; (a) averaged temporal trends of NDWI at all of the lookout tower sites during 2006; and the dotted vertical line shows the averaged ground-based CNF observation period; (b) relative frequency of the NDWI at all of lookout tower sites; (c) implementation of various NDWI threshold to determine the best threshold in predicting the CNF period.

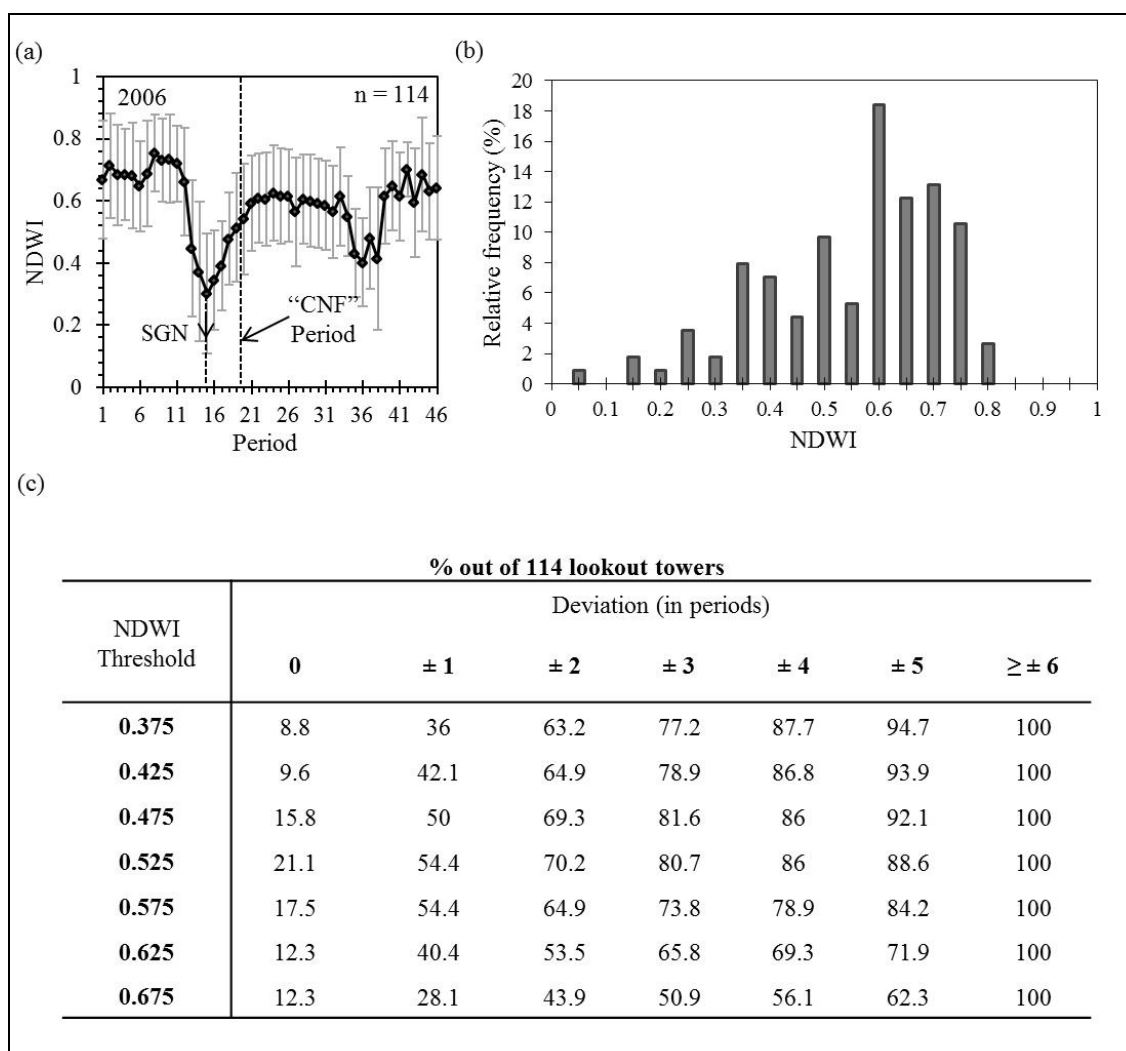


Table 5.4: Relation between NDWI-based prediction and ground-based CNF observation period at the lookout tower sites during 2007-2008 using the best NDWI threshold of 0.525.

<i>Deviation (in periods)</i>	<i>% of look-out towers</i>		
	2007 (n =118)	2008 (n =115)	2007-08 (n =233)
0	25.4	33.9	29.6
± 1	57.6	65.2	61.4
± 2	67.8	75.6	71.7
± 3	78.8	83.4	81.1
± 4	82.2	85.1	83.7
± 5	87.3	88.6	88
± 6	90.7	92.1	91.4
≥ ± 7	100	100	100

The variability observed in the values of AGDD and $NDWI_{2.13\mu m}$ during the period of ground observed CNF occurrence could be associated with one or assimilation of the following factors:

- (i) water stress (Royce and Barbour, 2001);
- (ii) climatic conditions of previous season (Gamache and Payette, 2004; Dufour and Morin, 2010); and

- (iii) genetic differences among inter and intra-species (Quiring, 1994; Weiglowski, 1999; Tanja et al., 2003), etc.

The determined AGDD threshold of 200 degree days in this study was consistent with other studies. As of:

- (i) O'Reilly and Parker (1982) found that the mean AGDD-values of 'bud flushing' (i.e., the appearance of the buds before the CNF stage) for white and black and spruce were on an average 91 and 150 degree days (with 5 °C base temperature) respectively in northern Ontario;
- (ii) Hannerz (1999) found that the AGDD requirements for needle flushing for various clones of Norway spruce (*Picea abies*) in Sweden were 150-250 degree days;
- (iii) Man & Lu (2010) reported AGDD (with base temperature 5 °C) requirements on an average to be 150 degree days with standard deviation of 56 degree days (with a median of 179 degree days) for white spruce under various controlled temperature treatments .

Note that all these studies were conducted under experimental setup; while this study represented the observations over naturally occurring stands.

On the other hand, it was not possible to compare the determined $NDWI_{2.13\mu m}$ threshold value with any other reported studies, as the implementation of $NDWI_{2.13\mu m}$ temporal dynamics in determining the CNF stages were so far not found in the literature.

According to analysis, it was found that the deviations were greater than ± 1 period for ~32% of the times. The larger deviations (i.e., $> \pm 1$ periods) might have happened due to the following reasons:

- (i) the ground-based observations were subjective, and highly dependable on the interpretation of the observer;
- (ii) spatial resolution of MODIS-based prediction might not be always at the same resolution of ground observation for all of the cases (Fisher and Mustard, 2007);
and
- (iii) the implementation of a global AGDD threshold over the entire study area might be unable to capture all of the variability (O'Reilly and Parker, 1982; Man and Lu, 2010).

5.2.4 Integration of Both GDD and NDWI_{2.13μm} Thresholds

The results from combining both of the predictors using logical 'OR' and 'AND' conditions in predicting CNF stage are shown in Table 5.5.

It revealed that the logical 'OR' produced the best results at ± 1 period deviation (i.e., ~68% of the times). It enhanced the predictability at:

- (i) 0 period deviation-level (i.e., 28.2% of the times) in comparison to GDD threshold (i.e., 20.2%);
- (ii) ± 1 period deviation-level (i.e., 68.7% of the time) in comparison to both GDD (i.e., 57.1% of the time) and NDWI_{2.13μm} thresholds (i.e., 61.4% of the time).

On the contrary, the logical 'AND' were 21%, and 49.7% of the times at 0, and ± 1 period deviation respectively.

Table 5.5: Relation between the combination of AGDD- and NDWI-based prediction and ground-based CNF observation period at the lookout tower sites during 2007-2008.

<i>Deviation (in periods)</i>	<i>% of look-out towers</i>					
	2007		2008		2007-08	
	(n=118)		(n=115)		(n=233)	
	"OR"	"AND"	"OR"	"AND"	"OR"	"AND"
0	22.9	23.7	34.8	18.3	28.8	21
± 1	63.6	55.1	73.9	44.4	68.7	49.7
± 2	83.1	74.6	87.8	68.8	85.4	71.6
± 3	94.1	83.1	93.9	84.4	94	83.6
± 4	96.7	85.7	96.5	87	96.6	86.2
± 5	97.5	89.8	96.5	90.5	97	90.1
± 6	98.3	92.5	98.2	94	98.3	93.1
$\geq \pm 7$	100	100	100	100	100	100

The best observed results upon using logical 'OR' condition between GDD and NDWI_{2.13 μ m} thresholds might be associated with the shifting of positive deviations in GDD-based predictions towards the zero deviation as a result of early prediction by

NDWI_{2.13 μ m} threshold. It would be the case where the conifer stands might respond to relatively lower AGDD for needle flushing.

5.2.5 CNF Maps and Spatial Dynamics

As the best agreements were found by using logical ‘OR’ between the predictors, this was employed in generating a CNF map over the conifer-dominant pixels during 2006-2008 as shown in Figure 5.13 to 5.15. Note that the model predictions are specific to conifer species of white and/or black spruce; while the map shows predictions for the entire conifer stands, assuming these two species are to be the dominating ones across the landscape. The maps also show the location of two transects; namely a-b (east to west) and c-d (north to south). The moving average of 10 consecutive pixels of CNF occurrence period along transects and its variations over the three years of the study (*i.e.*, 2006-08) are shown in Figure 5.16.

During 2006, ~65.2% of the times CNF occurred in the range of 137-160 DOY (*i.e.*, 17th May to 9th June). In 2007, ~74.1% SGN occurrence was in range of 145-168 DOY (*i.e.*, 25th May to 17th June). While during 2008, it was observed that the ~75% of times CNF stage occurred in between 153-176 DOY (*i.e.*, 1st June to 24th June).

Figure 5.13: CNF Map 2006; Spatial dynamics of CNF during 2008 over conifer-dominant 9 natural sub-regions using the best predictor (i.e., logical ‘OR’ between AGDD and NDWI thresholds), where the white area represents non conifer-dominant natural sub-regions in Alberta; Also the location of two transects ‘a-b’ and ‘c-d’ are shown.

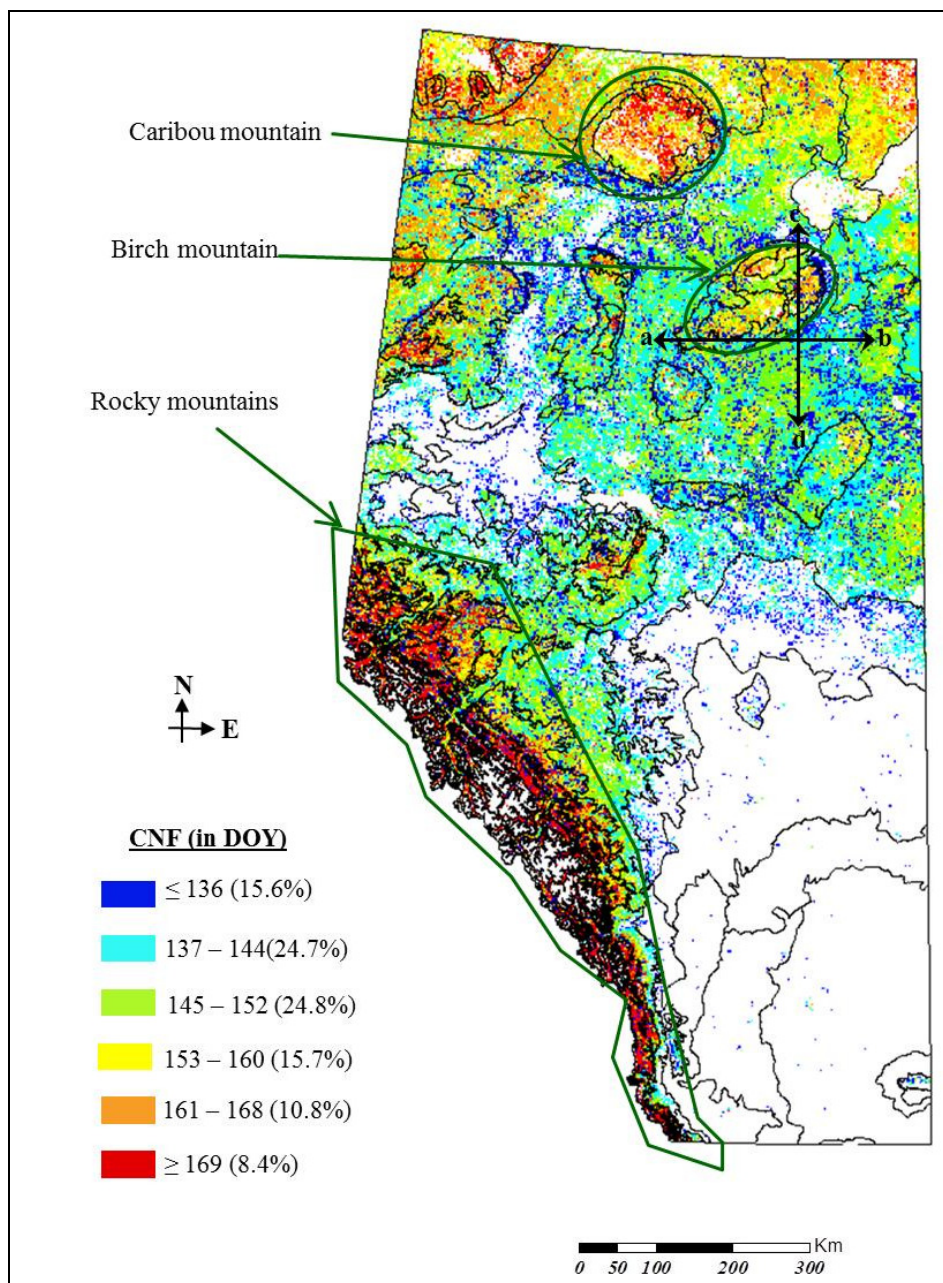


Figure 5.14: CNF Map 2007; Spatial dynamics of CNF during 2008 over conifer-dominant 9 natural sub-regions using the best predictor (i.e., logical 'OR' between AGDD and NDWI thresholds), where the white area represents non conifer-dominant natural sub-regions in Alberta; Also the location of two transects 'a-b' and 'c-d' are shown.

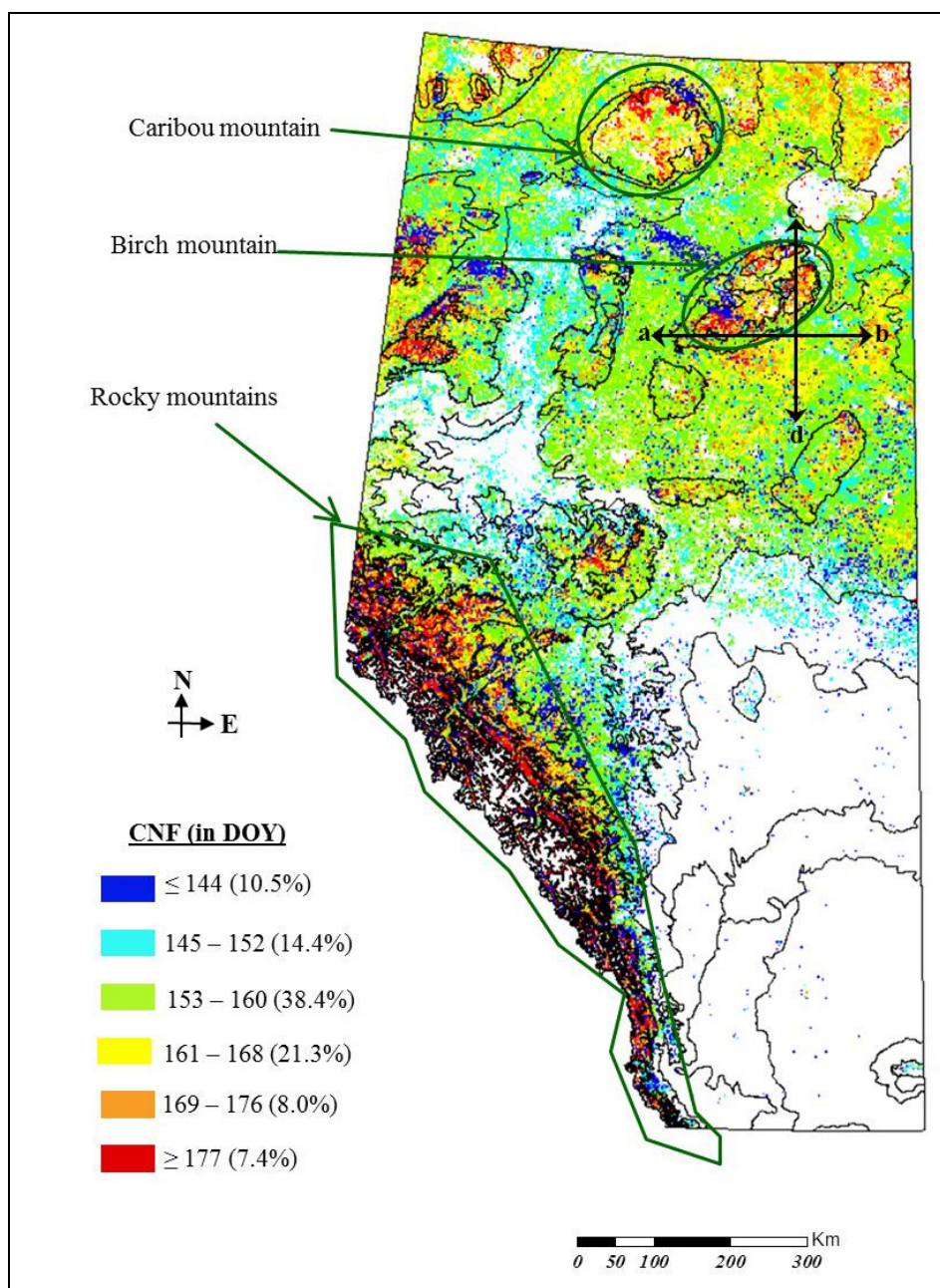


Figure 5.15: CNF Map 2008; Spatial dynamics of CNF during 2008 over conifer-dominant 9 natural sub-regions using the best predictor (i.e., logical 'OR' between AGDD and NDWI thresholds), where the white area represents non conifer-dominant natural sub-regions in Alberta; Also the location of two transects 'a-b' and 'c-d' are shown.

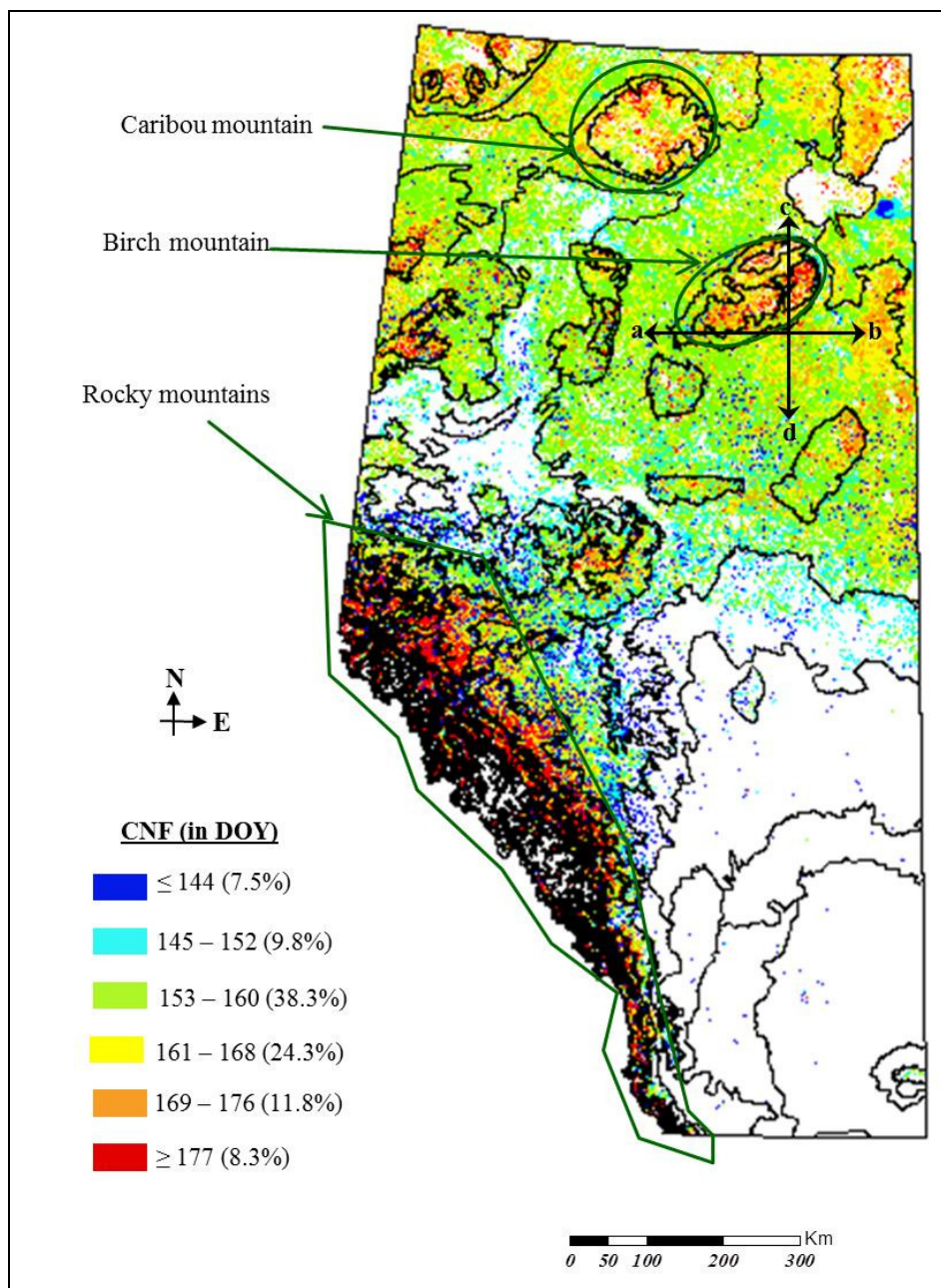
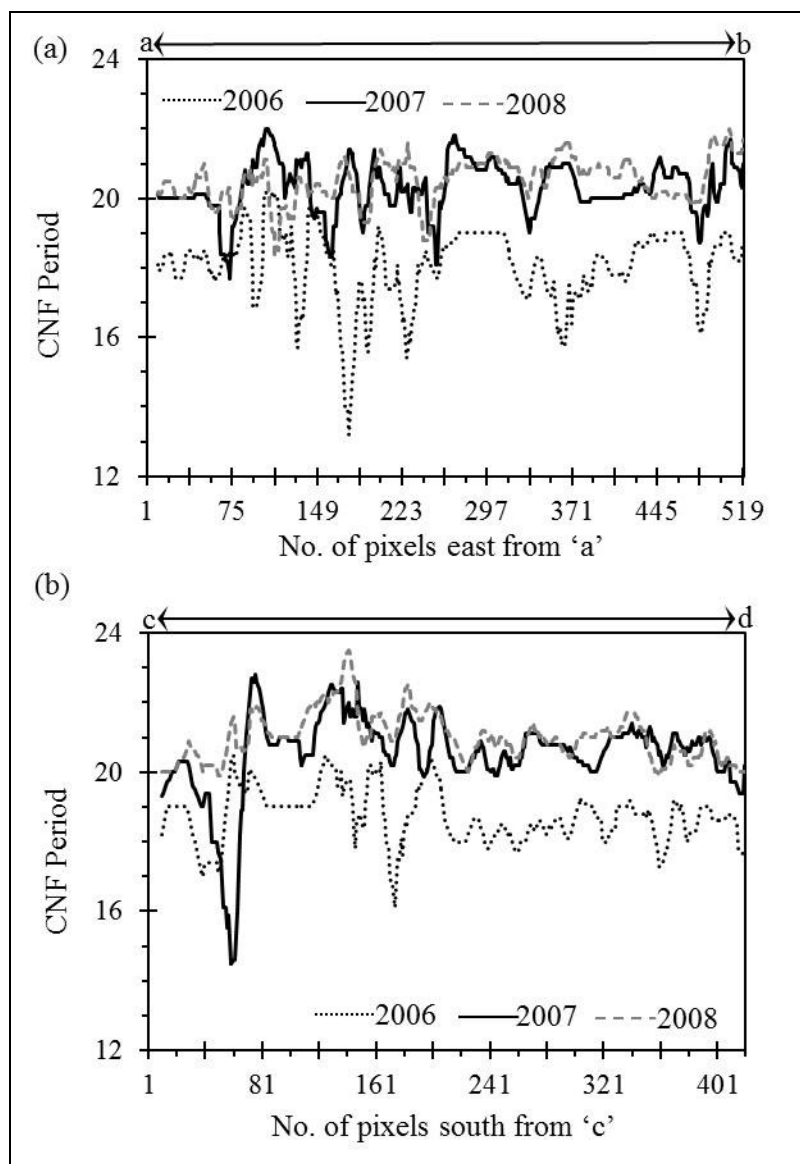


Figure 5.16: The moving average of 10 consecutive pixels of CNF period occurrence and its variations over the years of 2006-08 along the two transects: (a) a-b (east to west); and (b) c-d (north to south).



The relatively earlier CNF occurrences (≤ 152 DOY, i.e., before 01 June 2008) were observed mainly in the natural sub-regions of dry mixedwood, lower foothills, and portion of central mixedwood in the south. These are related to the fact that these regions experience relatively warm temperature regimes (Dowing and Pettapiece, 2006).

On the other hand, the relatively delayed CNF occurrences (≥ 177 DOY, i.e., after 24 June in 2008) were found to be in the high elevation regions (i.e., >750 m above the mean sea level), such as, Rocky Mountains, Caribou mountain, and Birch mountain (see Figure 5.13-5.15). These delayed CNF occurrences are expected as high elevations experience relatively cooler temperature regimes and longer snow cover periods (Hassan et al., 2007a; refer SGN Maps).

In general, the timing of the CNF occurrences was found to be increasing towards north direction. It is consistent with decreasing tendency of the temperature and snow-melt regimes in the northern hemisphere in the same direction (Hassan et al., 2007a; Akther and Hassan, 2011).

During the period 2006-2008, the periods of CNF occurrence along the two transects (see Figure 5.16), revealed that the CNF occurrence periods were variable. The moving average trends revealed that the CNF occurrence was getting late for each year; from about 19th period in 2006 to 22th period in 2008. These changes might be as a function of climate change, however it requires more investigation to confirm which is beyond the scope of this Thesis.

CHAPTER 6: CONCLUSIONS

6.1 Summary

In this Thesis, the methods to delineate two of the boreal spring phenological stages were developed by integrating: (i) ground-based measurements, (ii) phenological modeling, and (iii) remote sensing-based techniques. More detailed descriptions associated with these developments are summarized as follows:

Objective 1: “develop methods for determining SGN, and implement over Alberta in generating the spatial dynamics”. In this phase of this research, the potential of four MODIS-based indices (*i.e.*, EVI, NDWI_{1.64 μ m}, NDWI_{2.13 μ m}, and NDSI) were evaluated for determining SGN stages in Alberta. Initially, a qualitative evaluation over two forest fire prone natural sub-regions were conducted and found that both of the NDWI’s had better capabilities with compare to EVI and NDSI. Further investigation on NDWI’s, it revealed that NDWI_{2.13 μ m} could predict better (*i.e.* on an average ~66% of times within ± 1 period of deviation during the period 2006-2008) the SGN stages in comparison with NDWI_{1.64 μ m} (*i.e.* ~51% of times within ± 1 period of deviation). Thus, the temporal dynamics of NDWI_{2.13 μ m} were used to map SGN with spatial resolution of 500m at landscape levels.

Objective 2: “develop methods for determining CNF, and implement over the conifer dominant boreal forest stands in Alberta”. In this phase of study, the potential of mapping CNF stage using MODIS-based two predictors (*i.e.*, GDD and NDWI_{2.13 μ m}) was

evaluated over boreal-dominant regions in the Canadian province of Alberta. As a first step, the implementation of an existing GDD-mapping method was explored with appropriate calibration and validation procedures. This analysis showed reasonable agreements (*i.e.*, $r^2 \approx 0.67$) between the MODIS-derived values and the ground-based estimates of the air temperature. It was then used to generate GDD-maps for the entire province. The next step was to determine study-area specific thresholds for both AGDD and $NDWI_{2.13\mu m}$ -values individually for CNF predictions. It was found that thresholds of 200 degree days AGDD-values and 0.525 $NDWI_{2.13\mu m}$ -values were the best ones. Additionally, both of these individual thresholds were integrated using logical ‘OR’ and ‘AND’ combinations. Hence, it was demonstrated that the logical ‘OR’ produced the best agreements (*i.e.* ~69% of times within ± 1 period of deviation) in comparison to the ground-based observations. These logical ‘OR’ were then used to map CNF with spatial resolution of 500m at landscape levels.

6.2 Contribution to Science

The development(s) in this Thesis are primarily proof of concepts in determining two phenological stages (*i.e.*, SGN and CNF). Thus, the MODIS-based $NDWI_{2.13\mu m}$ and GDD could be employed in predicting the variability of SGN and CNF stage at landscape level. It would certainly be useful in the remote areas where the lookout towers are not available. Specific contributions are as follows:

- (i) It determines the best SWIR band in the NDWI formulation, and its applicability’s in understanding the dynamics of both SGN and CNF over boreal-dominant forest regions.

- (ii) The implementation of remote sensing-based techniques is unique in mapping CNF stages.
- (iii) The study of vegetation phenology using remote sensing is a topical. However, the application of remote sensing-based GDD is implemented so far for the first time.

6.3 Recommendations for Future Work

The developed techniques of this Thesis and their potential can be explored for further enhancement in several ways; some of such recommendations are as follows:

- (i) *Usage:* The developed techniques of SGN and CNF mapping may potentially be incorporated in the framework of forest fire management as both of the phenomenon of fire danger and fire behavior are highly related with the vegetation phenological stages. These also may be useful to reconstruct historical datasets of the phenological occurrences. Such datasets would largely assist in associating the changes in the phenological stages due to changing regimes of climate. However, in such scenarios it may be required to recalibrate the various thresholds to accommodate the adaptation of the vegetation.
- (ii) *Temporal resolution:* The temporal resolution of current MODIS-based products used in the study was the standard 8-day. The usage of developed techniques could be explored at finer resolutions of temporal coverage, such as 2 to 4 days intervals.
- (iii) *Spatial resolution:* The spatial resolution of the remote sensing-based GDD used was at 1 Km. The usage potential of enhanced GDD [previously downscaled to

the spatial resolutions of 250m and 27.5 m in some studies (Hassan et al., 2007a; Hassan et al., 2007b)] could potentially be explored.

- (iv) *Ground-based observations*: The potential of the developed techniques may be furthered enhanced using ground based observation datasets; as of: (a) detailed snow course data; and (b) diverse CNF records addressing entire range of conifer species. However, that may require recalibration of the species specific CNF occurrence thresholds.
- (v) *Specific thresholds*: The global threshold level of NDWI and GDD for the CNF occurrence over the entire province was used in this study. The potential of regional (and further stand specific) thresholds may be explored to delineate the CNF occurrence.
- (vi) *Climatic regimes*: The various climatic factors (mainly, water regimes and photoperiod) were assumed to be ignorable for the phenological modeling in this study. Their inclusion and usage of complex phenological models may be explored.
- (vii) *Base temperature*: In this study 5°C was used as the base temperature in GDD calculations, as it was assumed to be the temperature triggering the plant physiology. However, the assumption might be requiring further and thorough investigation, in particular to the northern forests.
- (viii) *Other biomes*: The developed techniques could be useful for other biomes across the world; however, it requires prior investigation and further validation before such implementations.

REFERENCES

- Agee, J. K., Wright, C. S., Williamson, N., & Huff, M. H. (2002). Foliar moisture content of pacific northwest vegetation and its relation to wildland fire behaviour. *Forest ecology and Management*, 167, 57-66.
- Agren, G. I., McMurtrie, R. E., Parton, W. J., Pastor, J., & Shugart, H. H. (1991). State-of-the-Art of models of production-decomposition linkages in Conifer and Grassland Ecosystems. *Ecological Applications*, 1, 118–138.
- Ahl, D. E., Gower, S. T., Burrows, S. N., Shabanov, N.V., Myneni, R. B., & Knyazikhin, Y. (2006). Monitoring spring canopy phenology of a deciduous broadleaf forest using MODIS. *Remote Sensing of Environment* 101, 88-95.
- Akhter, M. S., & Hassan, Q. K (2011). Mapping of climate driven variables over boreal environment. *Boreal Environment Research*. (In Press)
- Bailey, J. D., & Harrington, C. A. (2006). Temperature regulation of bud-burst phenology within and among years in a young Douglas-fir (*Pseudotsuga menziesii*) plantation in western Washington, USA. *Tree Physiology*, 26, 421-430.
- Beaubien, E. G., & Freeland, H. J. (2000). Spring phenology trends in Alberta, Canada: Links to ocean temperature. *International Journal of Biometeorology*, 44, 53-59.
- Burgan, R. E. (1979). *Estimating live fuel moisture for the 1978 national fire danger rating system*. USDA Forest Service: Research paper INT-226, pp. 16.
- Campbell, R. K., & Sugano, A. I. (1979). Genecology of bud-burst phenology in douglas-fir: response to flushing temperature and chilling. *Botanical Gazette*, 140, 223-231.

- Canadian Council of Forest Ministries (CCFM)* (2011). Canada's Boreal Forest, 3pp.,
URL: http://www.sfmcanada.org/english/bp_overview.asp (last accessed 30 June, 2011).
- Carlson, M., Wells, J., & Roberts, D. (2009). *The carbon the world forgot: Conserving the capacity of Canada's boreal forest region to mitigate and adapt to climate change*. Boreal Songbird Initiative, Seattle, WA, and Ottawa. pp. 33. URL: <http://www.borealbirds.org/resources/carbon/report-full.pdf> (last accessed 30 June, 2011).
- Chen, D., Huang, J., & Jackson, T. J. (2005). Vegetation water content estimation for corn and soybeans using spectral indices derived from MODIS near- and short-wave infrared bands. *Remote Sensing of Environment*, 98, 225-236.
- Chiang, J. -M., & Brown, K. J. (2007). Improving the budburst phenology subroutine in forest carbon model PnET. *Ecological Modelling*, 205, 515-526.
- Clark, R. N. (1999). *Spectroscopy of Rocks and Minerals, and Principles of Spectroscopy*. In A. N. Rencz (Ed.), *Manual of Remote Sensing, Volume 3, Remote Sensing for the Earth Sciences* (pp. 3-58), New York: John Willey and Sons.
- Cleland, E. E., Chiune, I., Menzel, A., Mooney, H. A., & Schwartz, M. D. (2007). Shifting plant phenology in response to global change. *Trends in Ecology and Evolution*, 22, 357-365.
- Dankers, R., and De Jong, S. M. (2004). Monitoring snow-cover dynamics in Northern Fennoscandia with SPOT VEGETATION images. *International Journal of Remote Sensing*, 25, 2933-2944.

- Delbart, N., Kergoats, L., Toan, T. L., Lhermitte, J., & Picard, G. (2005). Determination of phenological dates in boreal regions using normalized difference water index. *Remote Sensing of Environment*, 97, 26-38.
- Delbart, N., Toan, T. L., Kergoats, L., & Fedotava, V. (2006). Remote sensing of spring phenology in boreal regions: a free of snow effect method using NOAA-AVHRR and SPOT-VGT data (1982–2004). *Remote Sensing of Environment*, 101, 52-62.
- Delbart, N., Picard, G., Toan, T. L., Kergoat, L., Quengan, S., Woodward, I., Dye, D., & Fedotava, V. (2008). Spring phenology in Boreal Eurasia over a nearly century time scale. *Global Change Biology*, 14, 603-614.
- Dowing, D. J., & Pettapiece, W. W. (2006). *Natural regions and subregions of Alberta*. Natural Regions Committee: Government of Alberta, Alberta, Canada. Publication No. T/852.
- Dufour, B., & Morin, H. (2010). Tracheid production phenology of *Picea mariana* and its relationship with climatic fluctuations and bud development using multivariate analysis. *Tree Physiology*, 30, 853-865.
- Forest Fire Management Terms* (FFMT) (1999). Forest Protection Division, Alberta Land and Forest Service: Alberta, Canada, 37-38.
- Fisher, J. I., & Mustard, J. F. (2007). Cross-scalar satellite phenology from ground, Landsat, and MODIS data. *Remote Sensing of Environment*, 109, 261–273.
- Frensholt, R., & Sandholt, I. (2003). Derivation of a shortwave infrared water stress index from MODIS near- and shortwave infrared data in a semiarid environment. *Remote Sensing of Environment*, 87, 111-121.

- Gamache, I., & Payette, S. (2004). Height growth response of tree line black spruce to recent climate warming across the forest-tundra of eastern Canada. *Journal of Ecology*, 92, 835-845.
- Gao, B.C. (1996). NDWI a normalized difference water index for remote sensing of vegetation liquid water from space. *Remote Sensing of Environment*, 58, 257-266.
- Gu, Y., Brown, J. F., Miura, T., Leeuwen, W. J. D. V., & Reed, B. C. (2010). Phenological classification of the United States: a geographical framework for extending multi-sensor time series data. *Remote Sensing*, 2, 526-544.
- Gu, Y., Brown, J. F., Verdin, J. P., & Wardlow, B. (2007). A five-year analysis of MODIS NDVI and NDWI for grassland drought assessment over the central Great Plains of the United States. *Geophysics Research Letters*, 34, doi:10.1029/2006GL029127.
- Gunter S., Stimm B., Cabrera, M., Diaz, M. L., Lojan, M., Ordonez, E., Richter, M., & Weber M. (2008). Tree phenology in montane forests of southern Ecuador can be explained by precipitation, radiation and photoperiodic control. *Journal of Tropical Ecology*, 24, 247-258.
- Gyllenstrand, N., Clapham, D., Källman, T., & Lagercrantz, U. (2007). Norway spruce flowering Locus T Homolog is implicated in control of growth in conifers. *Plant Physiology*, 144, 248-257.
- Hall, D. K., Riggs, G. A., Salomonson, V. V., DiGirolamo, N. E., & Bayr, K. J. (2002). MODIS snow-cover products. *Remote Sensing of Environment* 83, 181-194.
- Hannerz, M. (1999). Evaluation of temperature models for predicting bud burst in Norway spruce. *Canadian Journal of Forest Research*, 29, 9-19.

- Hart, S. A., & Chen, H. Y. H. (2006). Understory vegetation dynamics of North American boreal forests. *Critical Reviews in Plant Sciences*, 25, 381-397.
- Hassan, Q. K., Bourque, C. P. -A., & Meng, F. -R. (2006). Estimation of daytime net ecosystem CO₂ exchange over balsam fir forests in eastern Canada: Combining averaged tower-based flux measurements with remotely sensed MODIS data. *Canadian Journal of Remote Sensing*, 32, 405-416
- Hassan, Q. K., Bourque, C. P. -A., Meng, F. -R., & Richards, W. (2007a). Spatial mapping of growing degree days: an application of MODIS-based surface temperatures and enhanced vegetation index. *Journal of Applied Remote Sensing*, 1, 013511:1-013511:12.
- Hassan, Q. K., Bourque, C. P. -A., & Meng, F. -R. (2007b). Application of Landsat-7 ETM+ and MODIS products in mapping seasonal accumulation of growing degree days at enhanced resolution. *Journal of Applied Remote Sensing*, 1, 013539:1-013539:10.
- Hassan, Q. K., & Bourque, C. P. -A. (2009). Potential species distribution of balsam fir based on the integration of biophysical variables derived with remote sensing and process-based methods. *Remote Sensing*, 1, 393-407.
- Hassan, Q. K., & Bourque, C. P. -A. (2010). Spatial enhancement of MODIS-based images of leaf area index: Application to the boreal forest region of northern Alberta, Canada. *Remote Sensing*, 2, 278-289.
- Huete, A., Didan, K., Miura, T., Rodriguez, E. P., Gao, X., & Ferreira, L. G. (2002). Overview of the radiometric and biophysical performance of the MODIS vegetation indices. *Remote Sensing of Environment*, 83, 195-213.

- Jackson, T. J., Chen, D., Cosh, M., Li, F., Anderson, M., Walthall, C., Doriaswamy, P., & Hunt, E. R. (2004). Vegetation water content mapping using Landsat data derived normalized difference water index for corn and soybeans. *Remote Sensing of Environment*, 92, 475-482.
- Jenkins, J. P., Braswell, B. H., Frokling, S. E., & Aber, J. D. (2002). Detecting and predicting spatial and inter annual patterns of temperate forest spring time phenology in eastern US. *Geophysics Research Letters*, 29, doi:10.1029/2001GL014008.
- Johnson, E. A. (1992). *Fire and Vegetation Dynamics: Studies from the North American boreal forest* (pp. 45-57). Cambridge: Cambridge University Press.
- Jones, G. E., & Cregg, B. M. (2006). Screening exotic firs for the Midwestern United States: interspecific variation in adaptive traits. *HortScience*, 41, 323-328.
- Jönsson, A. M., Eklundh, L., Helström, M., Barring, L., & Jönsson, P. (2010). Annual changes in MODIS vegetation indices of Swedish coniferous forests in relation to snow dynamics and tree phenology. *Remote Sensing of Environment*, 114, 2719-2730.
- Julien, Y., & Sobrino, J. A. (2009). Global land surface phenology trends from GIMMS database. *International Journal of Remote Sensing*, 30, 3495-3513.
- Klien, A. G., Hall, D. K., & Riggs, G. A. (1998). Improving snow cover mapping in forests through the use of canopy reflectance model. *Hydrological Process.*, 12, 1723-1744.

- Lawson, B. D., & Armitage, O. B. (2008). *Weather guide for the Canadian Forest Fire Danger Rating System*. Northern Forestry Centre, Canadian Forest Service, Natural Resources Canada: Edmonton, Alberta, Canada. pp. 73.
- Leinonen, I., & Kramer, K. (2002). Applications of phenological models to predict the future carbon sequestration potential of boreal forests. *Climatic Change*, 5, 99-113.
- Liang, L., & Schwartz, M., 2009. Landscape phenology: an integrative approach to seasonal vegetation dynamics. *Landscape Ecology*, 24, 465-472.
- Liang, L., Schwartz, M. D., & Fei, S. (2011). Validating satellite phenology through intensive ground observations and landscape scaling in a mixed seasonal forest. *Remote Sensing of Environment*, 115, 143-157.
- Man, R., Kayahara, G. J., Dang, Q. L., & Rice, J. A. (2009). A case of severe frost damage prior to bud break in young conifers in Northeastern Ontario: Consequence of climate change? *Forestry Chronicle*, 85, 453-462.
- Man, R., & Lu, P. (2010). Effects of thermal model and base temperature on estimates of thermal time to bud break in white spruce seedlings. *Canadian Journal of Forest Research*, 40, 1815-1820.
- McCloy, Keith R. (2010). Development and Evaluation of Phenological Change Indices Derived from Time Series of Image Data. *Remote Sensing*, 2, 2442-2473.
- Morisette, J. T., Richardson, A. D., Knapp, A. K., Fisher, J. I., Graham, E. A., Abatzoglou, J., Wilson, B. E., Breshears, D. D., Henebry, G. M., Hanes, J. M., & Liang, L., 2009. Tracking the rhythm of the seasons in the face of global change: phenological research in 21st century. *Front Ecological Environment*, 7, 253-260.

- Moulin, S., Kerogat, L., Viovy, N., & Dedieu, G. (1997). Global-Scale Assessment of vegetation phenology using NOAA/AVHRR satellite measurements. *Journal of Climate*, 10, 1154-1170.
- O`Reilly, C., & Parker, W. H. (1982). Vegetative phenology in a clonal seed orchard of *Picea glauca* and *Picea Marianna* in northwestern Ontario. *Canadian Journal of Forestry Research*, 12, 408-413.
- Penulas, J., Fillela, I., Zhang, X., Llornes, L., Ogaya, R., Lloret, F., Comas, P., Estiarte, M., & Terradas, J. (2004). Complex spatiotemporal phenological shifts as a response to rainfall changes. *New Phytologist*, 161, 837-846.
- Picard, G., Quegan, S., Delbart, N., Lomes, M. R., Toan, T. L., & Woodward, F.I. (2005). Bud-burst modelling in Siberia and its impact on quantifying the carbon budget. *Global Change Biology*, 11, 2164-2176.
- Power, K., & Gillis, M. (2006). *Canada's Forest Inventory 2001*. Natural Resource Canada, Canadian Forest Service, Information Report BC-X-408.
- Prescott, J. A., & Collins, J. A. (1951). The lag of temperature behind solar radiation. *Quarterly Journal of the Royal Meteorological Society*, 77, 121-126.
- Quiring, D. T. (1994). Influence of inter-tree variation in time of budburst of white spruce on herbivory and the behaviour and survivorship of *Zeiraphera Canadensis*. *Ecological Entomology*, 19, 17-25.
- Reed, B. C., Schwartz, M. D., & Xiao, X. (2009). Remote sensing phenology: status and the way forward. In A. Noormets (Ed.), *Phenology of ecosystem Processes* (pp. 231-246), New York: Springer Science+ Business Media.

- Richardson, A. D., Hollinger, D. Y., Dail, D. B., Lee, J. T., Munger, J. W., & O'Keefe, J. (2009). Influence of spring phenology on seasonal and annual carbon balance in two contrasting New England forests. *Tree Physiology*, 29, 321-331.
- Rinne, J., Aurela, M., & Manninen, T. (2009). A simple method to determine the timing of snow melt by remote sensing with application to the CO₂ balances of northern Mire and Heath ecosystems. *Remote Sensing*, 1, 1097-1107.
- Rossi, S., Deslauriers, A., Anfodillo, T., & Carraro, V. (2007). Evidence of threshold temperature for xylogenesis in conifers at high altitudes. *Oecologia*, 152, 1-12.
- Royce, E. B., & Barbour, M. G. (2001). Mediterranean climate effects. II. Conifer growth phenology across a Sierra Nevada ecotone. *American Journal of Botany*, 88, 919-932.
- Simpson, I. J., Akagi, S. K., Barletta, B., Blake, N. J., Choi, Y., Diskin, G. S., Fried, A., Fuelberg, H. E., Meinardi, S., Rowland, F. S., Vay, S. A., Weinheimer, A. J., Wennberg, P. O., Wieberg, P., Wisthaler, A., Yang, M., Yokelson, R. J., & Blake, D. R. (2011). Boreal forest fire emissions in fresh Canadian smoke plumes: C₁-C₁₀ volatile organic compounds (VOCs), CO₂, CO, NO₂, NO, HCN and CH₃CN. *Atmospheric Chemistry and Physics Discussion*, 11, 9515-9566.
- Tanja, S., Berninger, F., Vesala, T., Markkanen, T., Hari, P., Makella, A., Ilvesniemi, H., Hanninen, H., Nikinmaa, E., Huttula, T., Laurila, T., Aurela, M., Grelle, A., Lindorth, A., Arneth, A., Shibistova, O., & Lloyd, J. (2003). Air temperature triggers the recovery of evergreen boreal forest photosynthesis in spring. *Global Change Biology*, 9, 1410-1426.

- Thayn, J. B., & Price, K. P. (2008). Julian dates and introduced temporal error in remote sensing vegetation phenology studies. *International Journal of Remote Sensing*, 29, 6045-6049.
- Trombetti, M., Riaño, D., Rubio, M. A., Cheng, Y. B., & Ustin, S. L. (2008). Multi-temporal vegetation canopy water content retrieval and interpretation using artificial neural networks for the continental USA. *Remote Sensing of Environment*, 112, 203-215.
- Van -Wagner, C. E. (1977). Conditions for start and spread of crown fire. *Canadian journal of Forestry Research*, 7, 23-34.
- Wang, Y., & Zwiazek, J. J. (1999). Spring changes in water relations, gas exchange, and carbohydrates of white spruce (*Picea glauca*) seedlings. *Canadian journal of Forestry Research*, 29, 332-338.
- Weilgolaski, F. -E. (1999). Starting dates and basic temperatures in phenological observations of plants. *International Journal of Biometeorology*, 42, 158-168.
- Westerling, A. L.; Hidalgo, H. G.; Cayan, D. R.; Swetnam, T. W. (2006). Warming and earlier spring increase western U.S. forest wildfire activity. *Science*, 313, 940-943.
- White, M. A., De Beurs, K. M., Didan, K., Inouye, D. W., Richardson, A. D., Jensen, O. P., O'Keefe, J., Zhang, G., Nemani, R. R., Van Leeuwen, W. J. D., Brown, J. F., De Wit, A., Schaepman, M., Lin, X., Dettinger, M., Bailey, A. S., Kimball, J., Schwartz, M. D., Baldocchi, D. D., Lee, J. T., & Lauenroth, W. K. (2009). Intercomparison, interpretation, and assessment of spring phenology in North America estimated from remote sensing for 1982–2006. *Global Change Biology*, 15, 2335–2359.

- Wilson, E. H., & Sader, S. A. (2002). Detection of forest harvest type using multiple dates of Landsat TM imagery. *Remote Sensing of Environment*, 80, 385-396.
- Xiao, X., Boles, S., Liu, J., Zhuang, D., & Liu, M. (2002). Characterization of forest types in north eastern China, using multi-temporal SPOT-4 VEGETATION sensor data. *Remote Sensing of Environment*, 82, 335-348.
- Xiao, X., Zhang, J., Yan, H., Wu, W., & Biradar, C. (2009). Land surface phenology: Convergence of satellite and CO₂ eddy flux observations. In A. Noormets (Ed.), *Phenology of ecosystem Processes* (pp. 247-270), New York: Springer Science+ Business Media.
- Yi, Y., Yang, D., Huang, J., & Chen, D. (2008). Evaluation of MODIS surface reflectance products for wheat leaf area index (LAI) retrieval. *ISPRS Journal of Photogrammetry and Remote Sensing*, 63, 661-677.
- Yilmaz, M. T., Hunt, E. R., Jr., & Jackson, T. J. (2008) Remote sensing of vegetation water content from equivalent water thickness using satellite imagery. *Remote Sensing of Environment*, 112, 2514-2522.
- Zarco-Tejada, P. J., Rueda, C. A., & Ustin, S. L. (2003) Water content estimation in vegetation with MODIS reflectance data and model inversion methods. *Remote Sensing of Environment*, 85, 19-124.
- Zhang, X., Friedl, M. A., Schaaf, C. B., Strahler, A. H., Hodges, J. C. F., Gao, F., Reed, B. C., & Huete, A. (2003). Monitoring vegetation phenology using MODIS. *Remote Sensing of Environment*, 84, 471-475.

Zhang X., Friedl M. A., Schaff, C. B., & Strahler, A. H. (2004). Climate controls on vegetation phenological patterns in northern mid- and high latitudes inferred from MODIS data. *Global Change Biology*, 10, 1133-1145.

Web-References

- Earth Observing System Data and Information System (EOSDIS)*. (2009). *Earth Observing System ClearingHouse (ECHO) / Warehouse Inventory Search Tool (WIST) Version 10.X [online application]*. Greenbelt, MD: EOSDIS, Goddard Space Flight Center (GSFC), National Aeronautics and Space Administration (NASA). URL: <https://wist.echo.nasa.gov/api/> (last accessed on 30 June 2011).
- National Aeronautics and Space Administration (NASA)*. (2011). URL: <http://modis.gsfc.nasa.gov/about/> (last accessed on 30 June 2011).
- MODIS Reprojection Tool (MRT) (2008).Version 4.0*. USGS: Sioux Falls, SD, USA. URL: https://lpdaac.usgs.gov/lpdaac/tools/modis_reprojection_tool (last accessed on 30 June 2011).

APPENDIX

A.1 Copyright Permissions

The appendix provides the certificates for permissions/licences to use the copyrighted material from various sources; organized as follows:

- *Certificate from a Co-author*: Dr. Robert Sleep, a co-author in two publications; permission obtained through personal communication.
- *Certificate(s) for Published Journal Articles*: Obtained through Copyright Clearance Center of Elsevier Publishers, as agreements of usage for three articles (figures from which were used after modifications) namely:
 1. Zarco-Tejada et al., 2003;
 2. Zhang et al., 2003; and
 3. Delbart et al., 2005
- *Certificate for a Book Chapter*: Title page of the book chapter, Clark (1999), showing that content is not copyrighted and is in the public domain.
- *Certificate from Publication*: Parts of a published journal paper (Title: Evaluating Potential of MODIS-based Indices in Determining “Snow Gone” Stage over Forest-dominant Regions in Alberta, Canada.); showing that the copyrights are owned by authors.

A.1.1 Certificate from a Co-author

From: "Bob Sleep" <Bob.Sleep@gov.ab.ca>
 Subject: RE: Copyright Permission
 Date: Mon, July 18, 2011 9:37 am
 To: nsekhon@ucalgary.ca
 Cc: qhassan@ucalgary.ca

Navdeep

I give permission to use these articles in your thesis.
 I thank you for your kind words. Would you please provide to me a copy of your thesis once it is available.
 I wish you all the best in your future endeavors wherever they may take you.

Bob Bob Sleep
 Remote/Sensing GIS Analyst
 Geomatics Section Wildfire Air Operations Branch
 Forestry Division Department of Sustainable Resource Development
 Government of Alberta
 9th Floor Great West Life Building 9920 - 108th Street Edmonton, Alberta T5K 2M4
 email: bob.sleep@gov.ab.ca
 Tel: 1-780-422-0218
 Fax: 1-780-415-1509
 Bob Sleep Tel 780/422-0218; Fax 780/415-1509 bob.sleep@gov.ab.ca

-----Original Message-----

From: nsekhon@ucalgary.ca [<mailto:nsekhon@ucalgary.ca>]

Sent: Monday, July 18, 2011 9:27 AM
 To: Bob Sleep Cc: qhassan@ucalgary.ca
 Subject: Copyright Permission

Dear Dr. Robert Sleep,

You may remember that we jointly published articles with Dr. Quazi K Hassan. The citation of articles are as follows:

1. Sekhon, N. S., Hassan, Q. K., & Sleep, R. W. (2010). Evaluating Potential of MODIS-based Indices in Determining "Snow Gone" Stage over Forest-dominant Regions. *Remote Sensing*, 2, 1348-1363; and
2. Sekhon, N. S., Hassan, Q. K., & Sleep, R. W. (2010). Use of Remote Sensing in Understanding Spring Phenology over the Forest Dominant Natural Subregions of Alberta. *Canadian Geomatics Conference*, June 14-18, 2010, Calgary AB, Canada, 10-05-Paper-115, 5 pp.

As per our previous verbal discussions, I am intending to use above articles in my Thesis (Title: Remote sensing-based determination of boreal spring phenology); Being primary investigator of the presented work. The Thesis would be published in both 'Print' and 'Electronic' versions.

I request to you a written permission for usage of the articles in my Thesis. It would be my pleasure to address any of your concerns.

I will always be indebted for your vital inputs into our joint work.

Thank You.

Sincerely,

Navdeep S. Sekhon

A.1.2 Certificate for Published Journal Articles

(a) Zarco-Tejada et al. (2003)

ELSEVIER LICENSE TERMS AND CONDITIONS	
Jul 17, 2011	
<p>This is a License Agreement between Navdeep S Sekhon ("You") and Elsevier ("Elsevier") provided by Copyright Clearance Center ("CCC"). The license consists of your order details, the terms and conditions provided by Elsevier, and the payment terms and conditions.</p>	
<p>All payments must be made in full to CCC. For payment instructions, please see information listed at the bottom of this form.</p>	
Supplier	Elsevier Limited The Boulevard, Langford Lane Kidlington, Oxford, OX5 1GB, UK
Registered Company Number	1982084
Customer name	Navdeep S Sekhon
Customer address	Department of Geomatics Engineering, Calgary, AB T2N 1N4
License number	2711650718889
License date	Jul 17, 2011
Licensed content publisher	Elsevier
Licensed content publication	Remote Sensing of Environment
Licensed content title	Water content estimation in vegetation with MODIS reflectance data and model inversion methods
Licensed content author	P. J. Zarco-Tejada, C. A. Rueda, S. L. Ustin
Licensed content date	25 April 2003
Licensed content volume number	85
Licensed content issue number	1
Number of pages	16
Start Page	109
End Page	124
Type of Use	reuse in a thesis/dissertation
Intended publisher of new work	other
Portion	figures/tables/illustrations
Number of figures/tables/illustrations	1
Format	both print and electronic

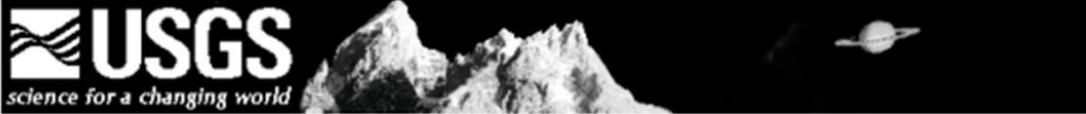
(b) Zhang et al. (2003)

ELSEVIER LICENSE TERMS AND CONDITIONS	
	Jul 17, 2011
<p>This is a License Agreement between Navdeep S Sekhon ("You") and Elsevier ("Elsevier") provided by Copyright Clearance Center ("CCC"). The license consists of your order details, the terms and conditions provided by Elsevier, and the payment terms and conditions.</p>	
<p>All payments must be made in full to CCC. For payment instructions, please see information listed at the bottom of this form.</p>	
Supplier	Elsevier Limited The Boulevard, Langford Lane Kidlington, Oxford, OX5 1GB, UK
Registered Company Number	1982084
Customer name	Navdeep S Sekhon
Customer address	Department of Geomatics Engineering, Calgary, AB T2N 1N4
License number	2711650576095
License date	Jul 17, 2011
Licensed content publisher	Elsevier
Licensed content publication	Remote Sensing of Environment
Licensed content title	Monitoring vegetation phenology using MODIS
Licensed content author	Xiaoyang Zhang, Mark A. Friedl, Crystal B. Schaaf, Alan H. Strahler, John C. F. Hodges, Feng Gao, Bradley C. Reed, Alfredo Huete
Licensed content date	March 2003
Licensed content volume number	84
Licensed content issue number	3
Number of pages	5
Start Page	471
End Page	475
Type of Use	reuse in a thesis/dissertation
Portion	figures/tables/illustrations
Number of figures/tables/illustrations	1
Format	both print and electronic

(c) Delbart et al. (2005)

ELSEVIER LICENSE TERMS AND CONDITIONS	
	Jul 17, 2011
<p>This is a License Agreement between Navdeep S Sekhon ("You") and Elsevier ("Elsevier") provided by Copyright Clearance Center ("CCC"). The license consists of your order details, the terms and conditions provided by Elsevier, and the payment terms and conditions.</p>	
<p>All payments must be made in full to CCC. For payment instructions, please see information listed at the bottom of this form.</p>	
Supplier	Elsevier Limited The Boulevard, Langford Lane Kidlington, Oxford, OX5 1GB, UK
Registered Company Number	1982084
Customer name	Navdeep S Sekhon
Customer address	Department of Geomatics Engineering, Calgary, AB T2N 1N4
License number	2711650807388
License date	Jul 17, 2011
Licensed content publisher	Elsevier
Licensed content publication	Remote Sensing of Environment
Licensed content title	Determination of phenological dates in boreal regions using normalized difference water index
Licensed content author	Nicolas Delbart, Laurent Kergoat, Thuy Le Toan, Julien Lhermitte, Ghislain Picard
Licensed content date	15 July 2005
Licensed content volume number	97
Licensed content issue number	1
Number of pages	13
Start Page	26
End Page	38
Type of Use	reuse in a thesis/dissertation
Intended publisher of new work	other
Portion	figures/tables/illustrations
Number of figures/tables/illustrations	1
Format	both print and electronic

A.1.3 Certificate for a Book Chapter



**Spectroscopy of Rocks and Minerals, and
Principles of Spectroscopy**

by
Roger N. Clark

U.S. Geological Survey, MS 964
Box 25046 Federal Center
Denver, CO 80225-0046

(303) 236-1332
(303) 236-1371 FAX

<http://speclab.cr.usgs.gov>

rclark@speclab.cr.usgs.gov

Derived from Chapter 1 in:
Manual of Remote Sensing

John Wiley and Sons, Inc
A. Rencz, Editor
New York
1999

This book chapter was produced by personnel of the US Government
therefore it can not be copyrighted and is in the public domain

This Web Page last revised June 25, 1999

How to Reference:
Clark, R. N., Chapter 1: Spectroscopy of Rocks and Minerals, and Principles of Spectroscopy, in
Manual of Remote Sensing, Volume 3, Remote Sensing for the Earth Sciences, (A.N. Rencz, ed.) John
Wiley and Sons, New York, p 3- 58, 1999.

A.1.4 Certificate from Publication

Remote Sens. **2010**, *2*, 1348-1363; doi:10.3390/rs2051348

OPEN ACCESS

Remote Sensing

ISSN 2072-4292

www.mdpi.com/journal/remotesensing

Article

Evaluating Potential of MODIS-based Indices in Determining “Snow Gone” Stage over Forest-dominant Regions

Navdeep S. Sekhon ¹, Quazi K. Hassan ^{1,*} and Robert W. Sleep ²

¹ Department of Geomatics Engineering, Schulich School of Engineering, University of Calgary, 2500 University Dr. NW Calgary, Alberta, T2N 1N4, Canada; E-Mail: nsekhon@ucalgary.ca

² Forestry Division, Alberta Department of Sustainable Resource Development, 9th Floor, 9920-108 Street, Edmonton, Alberta, T5K 2M4, Canada; E-Mail: Bob.Sleep@gov.ab.ca

* Author to whom correspondence should be addressed; E-Mail: qhassan@ucalgary.ca; Tel.: +1-403-210-9494; Fax: +1-403-284-1980.

Received: 25 February 2010; in revised form: 28 April 2010 / Accepted: 6 May 2010 /

Published: 11 May 2010

Abstract: “Snow gone” (SGN) stage is one of the critical variables that describe the start of the official forest fire season in the Canadian Province of Alberta. In this paper, our objective is to evaluate the potential of MODIS-based indices for determining the SGN stage. Those included: (i) enhanced vegetation index (EVI), (ii) normalized difference water index (NDWI) using the shortwave infrared (SWIR) spectral bands centered at 1.64 μm ($\text{NDWI}_{1.64\mu\text{m}}$) and at 2.13 μm ($\text{NDWI}_{2.13\mu\text{m}}$), and (iii) normalized difference snow index (NDSI). These were calculated using the 500 m 8-day gridded MODIS-based composites of surface reflectance data (*i.e.*, MOD09A1 v.005) for the period 2006–08. We performed a qualitative evaluation of these indices over two forest fire prone natural subregions in Alberta (*i.e.*, central mixedwood and lower boreal highlands). In the process, we generated and compared the natural subregion-specific lookout tower sites average: (i) temporal trends for each of the indices, and (ii) SGN stage using the ground-based observations available from Alberta Sustainable Resource Development. The EVI-values were found to have large uncertainty at the onset of the spring and unable to predict the SGN stages precisely. In terms of NDSI, it showed earlier prediction capabilities. On the contrary, both of the NDWI’s showed distinct pattern (*i.e.*, reached a minimum value before started to increase again during the spring) in relation to observed SGN stages. Thus further analysis was carried out to determine the best predictor by comparing the NDWI’s predicted SGN stages with the ground-based observations at all of the individual lookout tower sites

32. *Natural Regions and Subregions of Alberta*; Downing, D.J., Pettapiece, W.W., Eds.; Pub. No. T/852; Natural Regions Committee: Government of Alberta, Alberta, Canada, 2006. Available online: http://tpr.alberta.ca/parks/heritageinfocentre/docs/NRSRcomplete%20May_06.pdf (accessed on 11 April 2010).
33. *MODIS Reprojection Tool*; Version 4.0. USGS: Sioux Falls, SD, USA, February 2008. Available online: https://lpdaac.usgs.gov/lpdaac/tools/modis_reprojection_tool (accessed on 7 September 2009).
34. Huete, A.; Didan, K.; Miura, T.; Rodriguez, E.P.; Gao, X.; Ferreira, L.G. Overview of the radiometric and biophysical performance of the MODIS vegetation indices. *Remote Sens. Environ.* **2002**, *83*, 195-213.
35. Klien, A.G.; Hall, D.K.; Riggs, G.A. Improving snow cover mapping in forests through the use of canopy reflectance model. *Hydrol. Process.* **1998**, *12*, 1723-1744.

© 2010 by the authors; licensee MDPI, Basel, Switzerland. This article is an Open Access article distributed under the terms and conditions of the Creative Commons Attribution license (<http://creativecommons.org/licenses/by/3.0/>).